From the Department of Cell and Molecular Biology
Karolinska Institutet, Stockholm, Sweden

IDENTIFICATION AND FUNCTIONAL CHARACTERIZATION OF EPSTEIN-BARR VIRUS ENCODED DECONJUGASES

Sebastian Hildebrand

Karolinska Institutet

Stockholm 2011

Cover: Ribbon models of BPLF1-N binding to NEDD8

Published by Karolinska Institutet.

ISBN 978-91-7457-263-6

Printed by: US-AB Solna
Nanna Svartz väg 4
SE 171 77 Solna

"The Way is the Goal." *Mahatma Gandhi*

ABSTRACT

The post-translational conjugation or deconjugation of proteins by ubiquitin (Ub) or ubiquitin-like molecules (UbLs: e.g. SUMO, NEDD8, ISG15) has emerged as a major regulatory mechanism of various cellular activities. The controlled processes include protein transcription, translation, trafficking and degradation, signal transduction, replication and apoptosis. All modifier get covalently linked to their substrates via the cascade activity of three enzymes (E1, E2, E3). After execution of the modification mediated signaling, deconjuagases, belonging to the class of deubiquitinating enzymes (DUBs) or Ubl-specific proteases (ULPs), cleave the modifier of its substrate for possible recycling. Given the central role of the conjugation and deconjugation pathway in all aspects of cellular physiology, it is understandable that viruses have developed mechanisms to exploit those pathways for their own benefit. RNA and DNA viruses express their own E3 ligases or manipulate cellular E3 ligases to facilitate the modification of mostly cellular proteins, which, in the case of ubiquitination, often leads to their degradation. Also several viral encoded DUBs or ULPs have been described, e.g. facilitating the suppression of ubiquitination and ISGylation mediated antiviral effects.

Epstein-Barr virus (EBV) is a large double-stranded DNA tumor virus encoding ~100 open reading frames (ORFs). EBV belongs to the human herpes virus (HHV) family. The virus establishes latent infections in 90% of the human population worldwide and like other herpesviruses has a latent and lytic life cycle. EBV is associated with a variety of malignancies of lymphoid cells, like Burkitt´s lymphoma and Hodgkin´s lymphoma as also of epithelial cells, like nasopharyngeal carcinoma and gastric carcinoma.

The overall aim of this study was to identify and functional characterize EBV encoded deconjugases. We developed a bacterial screening assay based on the usage of Ub/Ubl-GFP reporter constructs. We screened an EBV-ORFeome library for their activity against Ub-, NEDD8-, SUMO-1,-2,-3 and ISG15-GFP reporter. As a result we discovered that the BSLF1- and BXLF1-ORF comprised deubiquitinating activity. We were further able to confirm the earlier described deubiquitinating function of the BPLF1-ORF. BPLF1 is a large tegumental protein, comprising DUB activity in its N-terminus, which was described for all of its HVV-family homologues. In our screening assay we could also detect that BPLF1-N cleaves the NEDD8-GFP reporter with similar efficiency as the Ub-GFP reporter. Following this observation we could show that BPLF1-N was able to process Ub- and NEDD8-linked functional probes with similar efficiency suggesting equal affinities towards ubiquitinated and neddylated substrates. We could show that BPLF1-N binds to and deneddylates cullins, which are assembled in cullin-RING ligases (CRLs). This CRL deneddylation facilitated the stabilization of their substrates involved in cell cycle regulation. Those accumulated BPLF1-N controlled CRL substrates were essential for an S-phase like cellular environment and endoreduplication in BPLF1-N expressing cells. We further demonstrated that the impact of BPLF1-N expression on viral genome replication was dependent on stabilization of the DNA licensing factor CDT1.

LIST OF PUBLICATIONS

This thesis is based on the following publications that will be referred to in the text by their roman numerals:

I Sompallae R, Gastaldello S, **Hildebrand S**, Zinin N, Hassink G, Lindsten K, Haas J, Persson B, Masucci MG. Epstein-barr virus encodes three bona fide ubiquitin-specific proteases. Journal of Virology 2008 Nov;82(21):10477-86.

II Gastaldello S, **Hildebrand S**, Faridani O, Callegari S, Palmkvist M, Di Guglielmo C, Masucci MG. A deneddylase encoded by Epstein-Barr virus promotes viral DNA replication by regulating the activity of cullin-RING ligases. Nature Cell Biology 2010 Apr;12(4):351-61.

ABBREVIATIONS

APC	Anaphase-promoting complex
BCR	B cell receptor
CDT	Chromatin licensing and DNA replication factor
CRL	Cullin-ring ligase
Cul	Cullin
CYLD	Cylindromatosis
DUB	Deubiquitinating enzyme
E1	Ubiquitin activating enzyme
E2	Ubiquitin conjugating enzyme
E3	Ubiquitin ligase
EBNA	EBV nuclear antigen
EBV	Epstein-Barr virus
EGFR	Epidermal growth factor receptor
GST	Glutathione S-transferase
HCMV	Human cytomegalovirus
HCV	Hepatitis C virus
HHV	Human herpes virus
HMM	Hidden Markov Model
HIV	Human immunodeficiency virus
HPV	Human papilloma virus
HSV	Herpes simplex virus
ICP0	Infected cell protein 0
IFN	Interferon
IRF	Interferon regulatory factor
ISG15	Interferon stimulated gene 15
JAMM	Jab1/MPN domain metalloenzyme
JAK	Janus kinase
KSHV	Kaposis sarcoma herpes virus
LMP	Latent membrane protein
K	Lysin
MCMV	Murine cytomegalovirus
MHCI	Major histocompatibility complex class 1
MJD	Machado-Joseph disease proteases
NEDD8	Neuronal-precursor cell-expressed developmentally down-regulated protein 8
ORF	Open reading frame
OUT	Ovarian tumor
PCA	Polymerase chain reaction
PCNA	Proliferating cell nuclear antigen
PML	Probable transcription factor
PLpro	Papain-like protease
RanGAP1	Ran GTPase-activating protein
RING	Really interesting new gene
SARS-CoV	Severe acute respiratory syndrome corona virus
SCF	Skp, Cullin, F-box containing complex
SENP	Sentrin specific peptidase
SUMO	Small Ubiquitin-like Modifier
STAT	Signal transducers and activators of transcription
SV40	Simian Virus 40
Ub	Ubiquitin
UbL	Ubiquitin like modifier
Ub-AMC	Ubiquitin aminomethylcoumarin
Ub-VME	Ubiquitin vinyl methyl ester
Ub-VS	Ubiquitin vinylsulfon
UCH	Ubiquitin carboxy-terminal hydrolase
ULP	Ubiquitin like specific protease
UPS	Ubiquitin poteasome system
USP	Ubiquitin specific protease
VHL	Von Hippel–Lindau

TABLE OF CONTENTS

1. INTRODUCTION ……...1
1.1.1 The ubiquitin and ubiquitin-like modification system ……..1
1.1.2 Ubiquitin modification ……2
1.1.3 SUMO modification ……2
1.1.4 NEDD8 modification ……3
1.1.5 ISG15 modification ……..4
1.1.6 Human DUBs and ULPs and examples of their function ……5
1.1.7 USPs ……5
1.1.8 UCHLs ……6
1.1.9 OTUs ……6
1.1.10 MJDs ……6
1.1.11 JAMMs ……7
1.1.12 ULPs ……7
1.2 Human virus encoded DUBs and their described function ……...7
1.3 The role of Ubiquitin and UbL-modifier in the life cycle of human viruses ...8
1.3.1 Viral entry ……9
1.3.2 Viral replication ……....9
1.3.3 Immune response ……10
1.3.4 Viral budding ……..11
1.4 Introduction to EBV ……...11
1.5 The role of ubiquitin and UbL-modifier in the EBV life cycle ……..12
2. AIMS OF THE STUDY ……15
3. METHODS, RESULTS AND DISCUSSION ……..16
3.1 Paper I ……16
3.2 Paper II ……....18
4. ONGOING RESEARCH AND FUTURE PERSPECTIVES ……...22
5. ACKNOWLEDGEMENTS ……...23
6. REFERENCES ……..24
7. PAPER I
8. PAPER II

1. INTRODUCTION

1.1.1 The ubiquitin and ubiquitin-like modification system

The post-translational modification of proteins by Ub (ubiquitin) or UbLs (ubiquitin-like molecules: e.g. SUMO, NEDD8, ISG15) has emerged as a major regulatory mechanism of various cellular activities. Those controlled processes include protein transcription, translation, trafficking and degradation, signal transduction, replication and apoptosis (1, 2, 3, 4, 5). So far 13 UbLs are described in human. All of them have a size between 8-18 kDa and they all show a high secondary structure homology to ubiquitin (2). Conjugation of Ub and UbLs to their targets requires the sequential action of three enzymes: a modifier-activating enzyme (E1), one of several modifier conjugating enzymes (E2s), and one member of a large and diverse group of modifier-target ligases (E3s) that mainly determines target specificity (1). This enzyme cascade mediates the conjugation of the C-terminal glycine of Ub or UbL to the epsilon-NH2 group of a lysine residue (K) of the target protein. Ub and UbLs are produced as precursor proteins (Ub also as a polypeptide), and carboxy-terminal processing by specific proteases is required to generate an active modifier. Those specific deconjugating enzymes, called DUBs (deubiquitinating enzymes) and ULPs (Ubl-specific proteases), also cleave the modifier from its target protein by hydrolyzing the covalent bondage between substrate and modifier. The purpose of this reaction is to establish a sufficient pool of free Ub/Ubls and to determine certain signaling or functional alteration caused by the modification (6). An overview of the ubiquitin and ubiquitin-like modification system with examples for the non-proteolytic and proteolytic outcomes are visualized in figure 1.

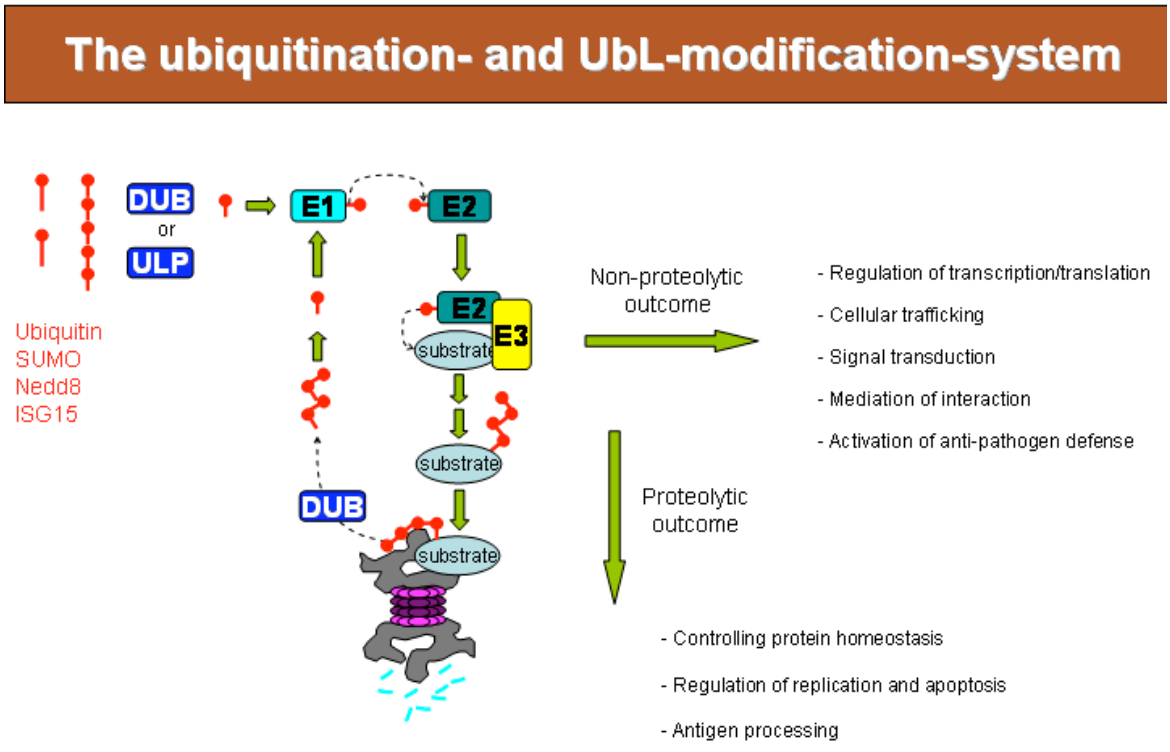

Figure 1. Ub polypeptides or UbL pro-peptides need to be processed from DUBs or ULPs to make their terminal Glycin accessible for conjugation. Via an enzymatic cascade of activating enzyme (E1), conjugating enzyme (E2) and substrate ligase (E3) the modifier gets covalently linked to its substrate. This modification can either have a non-proteolytic or a proteolytic outcome. After signaling the modifier gets deconjugated from its substrate by DUBs or ULPs for possible recycling into the system.

1.1.2 Ubiquitin modification

Ubiquitin, a small globular protein composed of 76 amino acids, is highly conserved during evolution. The first discovered function of ubiquitin is its involvement in the UPS (ubiquitin-proteasome system). This pathway is a major intracellular system for protein degradation. The connection of at least four K48 linked Ub molecules to a protein serves as localization signal to the proteasome where the labeled protein gets degraded (1). This pathway plays a crucial role in a wide variety of cellular function, including degradation of damaged or unneeded proteins, cellular trafficking, antigen processing, cell cycle regulation and apoptosis (7). Apart from the described K48 Ub chain mediated protein degradation several other Ub mediated function have been described. Ubiquitin contains seven lysine residues K6, K11, K27, K29, K33, K48, and K63. Formation of the ubiquitin chain can occur by linking the ubiquitin polymer to any of these lysine residues in homogeneous or mixed form. The length and the linkage construction of the created Ub chain determine the faith of the modified protein. Apart from modification via K48 Ub chains, monoubiquitination and K63 Ub chain conjugation are the best characterised Ub modifications. Many membrane receptors are monoubiquitinated, which serves in most cases as endocytosis signal and in many circumstances as signal for lysosomal degradation. Also histones are monoubiquitinated, which serves as signal for histone-mediated transcriptional regulation. Monoubiquitination has also been described to alter sub-cellular location or determine cellular interaction of the modified substrate (8, 9). For instance PCNA (proliferating cell nuclear antigen) is a homotrimeric replication sliding clamp that encircles DNA and provides a platform to recruit other proteins involved in DNA replication and repair. Monoubiquitinated PCNA recruits TLS (translation synthesis) polymerases, which display low processivity and reduced fidelity allowing DNA lesion bypass, to replace the high-fidelity polymerases. The monoubiquitination of PCNA can be further extended to K63-linked polyubiquitin chains. This polyubiquitination activates an alternative lesion bypass pathway called template switch, which recruits the undamaged strand of the DNA duplex as a template to direct DNA synthesis (10). Further described protein-protein interactions mediated via K63-linked polyubiquitination are important for kinase signalling activation (e.g. leading to NF-κB activation), receptor endocytosis and protein trafficking (11). The best characterized UbL-modifier in human are SUMO, NEDD8 and ISG15.

1.1.3 SUMO modification

The mammalian SUMO (Small ubiquitin-like modifier) family is comprised of three members with described physiological function. SUMOs have a size of about 95 amino acids and constitute a highly conserved protein family found in all eukaryotes. SUMO-1 share ~50% sequence identity with SUMO-2 and -3. SUMO-2 and SUMO-3 share ~95% sequence identity. SUMO-2 and -3 are able to form monomeric and heteromeric poly-SUMO chains like Ubiquitin. SUMO-1 in contrast, is not able to form poly-SUMO chains but may bind covalently to SUMO-2 and -3 conjugated chains and terminate them. Most SUMO-modified proteins, which have been characterized in human, are involved in transcription. The transcriptional effects of SUMO can be divided into two groups, those that involve PML nuclear bodies and those that involve sumoylated transcription factors bound to DNA promoters. PML nuclear bodies are matrix-associated domains that recruit an ever-growing variety of proteins. The PML-protein is the key organizer of these domains, which up on sumoylation facilitates the formation of PML nuclear bodies, recruiting among others transcription factors, which get activated via this association. Sumoylation occurring direct on the transcription factor facilitates in most cases transcriptional repression.

This occurs either by altering the stability of a DNA bound transcription factor or by the recruitment of a transcriptional repressor. In general most sumoylated substrates are localized in the nucleus and many of those substrates require their NLS (nuclear localization sequence) for sumoylation. The most abundant SUMO-1 conjugate in vertebrate cells is RanGAP1. This protein is the GTPase activating protein for the small GTPase Ran, which plays a central role in nuclear transport. SUMO-1 modification of RanGAP1 facilitates binding of the modified protein to the nuclear pore complex. This tightly bound RanGAP1 was shown to be crucial in nuclear import assays *in vitro* and soluble RanGAP1 could not substitute for it. One way SUMO affects the function of its substrates is sumoylation on otherwise ubiquitination specific lysine residues. PCNA or IκBα are examples for this phenomena. In the case of PCNA sumoylation and ubiquitination compete for the same site whereas sumoylation was shown to alter PCNAs function by inhibiting ubiquitination dependent post-replication DNA repair. Also the sumoylation of ubiquitination sites of particular high molecular weight proteins after various cellular stress conditions with SUMO-2 and-3 chains was reported. This sumoylation pattern was reversed after normalization of the cellular stress stimuli, suggesting a role of sumoylation to inhibit those sites for ubiquitination mediated proteasomal degradation (12).

1.1.4 NEDD8 modification

The UbL-modifier NEDD8 (Neuronal-precursor cell-expressed developmentally down-regulated protein 8) was originally discovered as a down regulated protein in neural precursor cells during the development of murine brain. The 76 amino acid big modifier is very similar to Ubiquitin in size, structure and charge distribution. Both modifiers share an almost 60% sequence identity. The most prominent neddylated substrates are the cullin family, which comprise in human six members (Cul-1,-2,-3,-4a,-4b,-5). Cullins serve as scaffold/bridge proteins in multi subunit ubiquitin ligase complexes also called CRLs (cullin-RING ligases). The C-terminus of a cullin integrated in such a complex serves as binding site for Roc1 or Roc2, which are E2 binding adaptors. Roc1 or Roc2 attract and bind an E2 conjugating enzyme, which brings ubiquitin to the complex required for CRL-substrate ubiquitination. The N- terminus of a CRL integrated cullin serves in most cases as binding site for a variable adaptor protein. On this adaptor protein (or direct to the cullin N-terminus) binds a substrate-targeting module, which determines the pool of substrates connecting to the specific CRLs. Via the different composition of mainly those substrate recognition modules, ~400 different CRLs have been described in human. It is believed, that ~20% of all proteins targeted for proteasomal degradation are polyubiquitinated by CRLs. The C-terminal neddylation of cullins assembled in CRLs was shown to enable a sufficient polyubiquitination of the CRL substrate protein (13, 14). Also other neddylated substrates have been described. The E3 ligase MDM2, which ubiquitinates p53, may also neddylate p53, which inhibits its transcriptional activity (15). The VHL (von Hippel–Lindau) tumour suppressor protein is the cause of the familial VHL disease (cancer syndrome) and most sporadic RCC (renal clear-cell) carcinomas. Needylation of VHL has been reported to be important for VHL binding to fibronectin and to promote its matrix assembly. A non-neddylateable VHL mutant failed to bind to and promote the assembly of fibronectin. Deregulated ECM, as well as abnormal cell-matrix interactions are hallmarks of solid tumors. Alterations in the fibronectin component of the ECM have been correlated with cellular transformation, like VHL-associated tumorigenesis (16). Also BCA3 (breast cancer associated protein 3) was shown to be a NEDD8 substrate and to function as a tumor suppressor upon modification. When NEDD8 is removed from BCA3, oncogenes are no longer suppressed, resulting in resistance to apoptosis and excessive cell proliferation.

Neddylation of BCA3 suppresses NFκB-dependent transcription through its ability to bind to p65 and the cyclin D1 promoter (17). The EGFR (epidermal growth factor receptor) functions as a tyrosine kinase upon activation by its ligands, which triggers DNA synthesis and cell proliferation. It was shown, that EGFR neddylation enhances its subsequent ubiquitination, resulting in its endocytosis and sorting for lysosomal degradation (18).

1.1.5 ISG15 modification

Human ISG15 (IFN-stimulated gene 15) has a size of 157 amino acids and consist of two domains, where each domain is structurally similar to ubiquitin. ISG15, like other ISGs, is an interferon-inducible gene product, which is strongly upregulated upon viral or bacterial infection. It was further described to be upregulated after LPS (Lipopolysaccharide) and double stranded RNA stimuli. The first discovered substrate of this modifier was Spi2a (serin protease inhibitor 2a), which regulates intracellular proteases in antigen-presenting cells. In general ISG15 is considered as a broad-spectrum inhibitor of virus production upon viral infection. Antiviral activity associated with viral or host protein ISGylation has been reported for DNA and RNA viruses, like HCMV (human cytomegalovirus), HSV (herpes simplex virus), SV (Sindbis virus) and HCV (hepatitis C virus). Mass spectrometric analysis has led to the identification of at least 200 putative ISG15 target proteins. Many of them have crucial functions in the type I IFN response, including JAK1 and STAT1. ISGylation of those signalling proteins was shown to increase their activity to enhance the cellular response to interferons (19). This was achieved by e.g. induction of the antiviral effector enzymes PKR and RNase L. Those protein activations trigger a global inhibition of protein synthesis and virus replication. This is achieved through the phosphorylation of eIF-2α (for PKR) and breakdown of RNA (for RNase L). It was also shown that up on activation of PKR and RNase L an upregulation of ISG15 mRNA levels was achieved (20, 21). Upon viral infection, ISG induction occurs in two intervals: first an IFN-independent induction of a subset of ISGs is induced and second an IFN-dependent induction via the production of IFN-α/β follows. In many viral infections, IFN-independent ISG induction is mediated by IRF-3 phosphorylation, homodimerization, and nuclear translocation. Activated IRF3, in turn, induces the expression of type I IFN genes, whose products trigger strong induction of a subsets of ISGs, including IFN-β which after its release and ligand-binding to its receptor initiates IFN-dependent ISG induction via the IFN receptor and JAK/STAT signalling pathways. ISG15 has been reported in HBV (hepatitis B virus) to prevent virus-mediated degradation of IRF3 (interferon regulatory factor 3), thereby increasing the induction of IFNβ expression (22). ISG15 can also be secreted from stimulated cells by a yet not described mechanism and is believed to function as a cytokine to modulate the immune response. In this manner ISG15 was shown to stimulate interferon γ secretion by monocytes and macrophages, proliferation of natural killer cells, and chemotactic responses in neutrophils (23). Some viruses have developed specific strategies to counteract the activity of ISGs. The influenza B virus protein NS1B is able to bind to ISG15 and by doing so inhibits protein ISGylation (24). ISG15 overexpression in cell culture was shown to hinder efficient budding of Ebola VP40 virus like particles. The Ebola virus matrix protein VP40 is a major viral structural protein and plays a central role in virus assembly and budding at the plasma membrane of infected cells. VP40 needs to be ubiquitinated to facilitate efficient viral budding. It has been reported, that the cellular E3 ligase Nedd4, which ubiquitinates VP40, gets ISGylated, which inhibits its enzymatic activity hindering efficient Ebola VP40 virus like particle budding (25).

1.1.6 Human DUBs and ULPs and examples of their function

All DUBs and ULPs are Cystein proteases, with the exception of the JAMM metalloproteases, which cleave the modifier from the substrates in a Zn^{2+}- and ATP-dependent manner. So far approx. 100 human DUBs have been identified, and based on the sequence similarities, they have been classified into five distinct subfamilies: USPs (Ubiquitin-specific proteases), UCHLs (Ubiquitin carboxyl-terminal hydrolases), OTUs (Otubain proteases), MJDs (Machado-Joseph disease proteases) and JAMMs (Jab1/MPN domain metalloenzymes) (6). The human ULPs are represented by the SENP (sentrin specific peptidase) family (12).

1.1.7 USPs

USPs (Ubiquitin-specific proteases) belong to the largest and most diverse DUB family. Those enzymes have specific substrates and can regulate distinct signaling pathways at various levels. Examples include USP7, which stabilizes p53 and MDM2 (E3 ligase of p53) in cells (26). CYLD is a K63-linked Ub chain specific USP in the NF-κB pathway that inhibits the activation of the IKK kinase complex (27). USP28 stabilizes the transcription factor c-myc (28), while USP8/UBPY affects endosomal trafficking (29). USP14 is associated with the proteasome and is required for ubiquitin recycling by removing K48-linked Ub chains from proteasomal substrates (30). Beside the main characteristic of USPs, to cleave ubiquitin linkages, members of this family have also been described to have dual activities towards UbL-modifier. For example USP2, USP5 and USP14 are able to hydrolyze ISG15 conjugates. Those activities were previously elucidated by the ability of those USPs to bind to the suicidal probe ISG15-VS (31). Those chemical probes are widely used to characterize catalytic active cysteine deconjugases. Those probes contain besides Ub or a specific UbL a reactive compound, which binds and inhibits in most cases the catalytic site of the targeted enzyme (32). Several USPs have been described to comprise a dual specificity to Ub and NEDD8 (33). For instance USP21 has been described to recognize NEDD8 and to be able to deneddylate cellular substrates (34). Several USPs have been implicated in malignant transformation including for example the product of the cylindromatosis or turban tumor syndrome gene CYLD, which was identified as a regulator of the NF-kB pathway (2). Some USPs exert distinct growth regulatory activities by acting as oncoproteins or tumor suppressor proteins (3). The size of USPs ranges between 330 and 3500 amino acids and their catalytic domain comprising conserved cysteine and histidine boxes has a size between 300 and 850 amino acids. The N- and C-terminal extension domains of USPs determine their substrate specificity and are involved in protein-protein interaction and determination of cellular localization (35). Structural studies have defined the USP domain fold, and 5 crystal structures of mammalian USP domains have been published (36-40). USP domains share a common fold, which is conserved in almost all USPs. This structure was defined from the crystal structure of USP7. This USP domain resembles a three-domain architecture comparable to an open hand formation containing Thumb, Palm and Fingers. The Thumb consists of eight α helices, while the Palm contains eight central β strands and two helices. The fingers are comprised of four β strands in the center and two at the tip. The catalytic triad residues are located between the Thumb (Cys) and Palm subdomains (His/Asp) (37).

1.1.8 UCHLs

The UCHL (Ubiquitin carboxyl-terminal hydrolase) family is comprised of 4 members (UCHL1, UCHL3, UCHL37 and Bab1), which have generally small sizes (20-30 kDa). Their sequences are conserved among species with approximately 40% homology. UCHL1 is highly expressed in neurons and reduced levels have been observed in various neurodegenerative diseases. Mutations in the UCHL1 gene have been reported to be linked to Parkinson's disease and expression of UCHL1 was shown to rescue synaptic dysfunction in Alzheimer's disease model mice (41, 42). Abnormal overexpression of UCHL1 has been reported to relate to several forms of cancer (43). UCHL3 is expressed in various tissues and cleaves beside Ub also neddylated substrates. Studies using UCHL3 deficient mice have suggested a role in growth and cell survival (44, 45). UCHL37 specifically cleaves K48-linked Ub chains and is associated with the 19S regulatory subunit of the 26S proteasome (46).

1.1.9 OTUs

OTUs (Otubain proteases) are a recently identified DUB family with so far approximately 15 members. They belong to the ovarian tumor superfamily of proteins with more then 100 members. OTU homologues in different species show a high degree of homology. Also their enzymatic cores are highly conserved but their substrate specificities appear to be quite diverse. Otu1 (otubain 1) has been shown *in vitro* to cleave K48-linked Ub chains and to decrease global Ub conjugate level after overexpression *in vivo* (47), (48). Otu2 (otubain 2) was shown to be inactive *in vitro* against ubiquitin peptide/isopeptide-linked substrates (49), but was able to cleave the flurogenic probe Ub-AMC (50). Other human OTU proteins known to have DUB activity are A20, Cezanne, TRABID, DUBA and VCIP135. A20 is a dual active enzyme comprising DUB and E3 ligase activities, which are required for termination of TLR (Toll-like receptor) signalling resulting in NF-κB activation and inactivation of TNF (tumour necrosis factor) induced cytotoxicity and apoptosis (51, 52). Similar to A20, Cezanne has been shown to inhibit NF-κB through modulation of the ubiquitination state of two of its positive regulators, TRAF6 and RIP-1 (53, 54). Cezanne was shown accumulate in acute lymphoblastic leukemia and Burkitt lymphoma (55). While the precise role of Cezanne in cancer is unknown, its inhibition of NF-κB suggests that Cezanne may act as a tumor suppressor. VCIP135´s DUB function was described to be required for Golgi membrane fusion (56) and DUBA1 was reported to deubiquitinate the E3 ligase TRAF3 resulting in negative regulation of IFN-1 signalling and down regulation of the innate immune response (57).

1.1.10 MJDs

MJDs (Machado-Joseph disease proteases) are conserved cysteine proteases that include four human DUBs (Ataxin-3, ATXN3L, Josephin-1 and Josephin-2). MJDs are conserved throughout eukaryotes and share a common cysteine protease domain (Josephin domain) of approximately 180 amino acids. The first discovered and best characterized MJD is Ataxin-3. Insertion of a polyglutamine repeat in Ataxin-3 was shown to cause the neurodegenerative Machado-Joseph disease giving this DUB class its name. In contrast to ataxin-3, much less is known about the other three human MJDs (58). NMR and crystallization based structural analysis has been published for Ataxin-3 but for no other MJDs (59). ATXN3L, Josephin-1 and -2 have been shown to possess DUB activity but no substrates are described so far (58).

1.1.11 JAMMs

JAMMs (Jab1/MPN domain metalloenzymes) comprise 5 members with described DUB activity. With a big exception to all other DUBs, JAMMs are lacking a catalytic cysteine. Instead, they are metalloproteases, which coordinate a catalytically essential zinc ion within their active sites. The three best known JAMMs are Poh1, Jab1 and Brcc36. Poh1 is a subunit of the 19 S subcomplex which releases K48-linked polyUb chains from substrates targeted to the proteasome for degradation. It has been suggested that Poh1 functions as a proteasomal "proofreading" device that determines the fate of incoming substrates as to whether they will be rescued or degraded (60). Jab1 is a component of the CSN (COP9 signalosome), a multisubunit complex very similar to the 19S proteasome lid complex, which cleaves NEDD8 of the cullins assembled in CRLs (61). Brcc36 was shown to recognize and cleave particular K63-linked ubiquitin chains. Among others Brcc36 is a component of the BRCA1-A complex, which specifically recognizes K63-linked ubiquitinated histones H2A and H2AX at DNA lesions sites, leading to target the BRCA1-BARD1 heterodimer to sites of DNA damage at double-strand breaks (62).

1.1.12 ULPs

Human ULPs (Ubl-specific proteases) comprised the SENP (sentrin specific peptidase) family, which consist of eight members. They are all homologues of the earlier discovered yeast ULP1 homologue. ULP1 and SENPs are classified as a large group of cysteine proteases, which catalyze cleavage of the peptide bond after the C-terminal glycine to activate the modifier as well as deconjugate them from their substrate. ULP1 and SENPs are comprised of a ~200 amino acid long catalytic domain containing the active residue triad Cys, His and Asp. Their N- terminal domain has a variable length and sequence and is responsible for localisation, target interaction and specificity. One member, SENP8, also called NEDP1 or DEN1, is specific for NEDD8 activation and substrate deconjugation. SENPs have been shown to have distinct sub-cellular localizations controlled by their non-conserved N-terminal regions. SENP1 and SENP3 are predominantly localized into the nucleus. SENP2 isoforms are found in the cytoplasm, binding to the nucleoplasmic side of the nuclear pore complex ore localize to PML nuclear bodies. SENP6 is localized in the cytoplasm (12).

1.2 Human virus encoded DUBs and their described function

Nairoviruses and Arteriviruses, two unrelated RNA virus families, have been shown to express OTU domain-containing proteases. The L-protein of Nairoviruses, e.g. from the highly pathogenic CCHFV (Crimean-Congo Haemorrhagic Fever Virus) has been shown to process Ub and ISG15 conjugates and pro-ISG15 and pro-NEDD8 *in vitro*. CCHFV was also able to cleave Ub and ISG15 conjugates in cells. ISGylation and ubiquitination mediate antiviral effects. The NF-κB immune pathway is regulated by ubiquitination. CCHFV-L was described to inhibit NF-κB activation by the inhibition of endogenous p65 nuclear translocation upon TNFα stimulation (63). The SARS corona virus encoded PLpro protein was described to show deubiqitinase and isgylase activity *in vitro*. It is an enzyme with dual function first described to carry out N-terminal processing of the viral replicase polyprotein and then later also to cleave K48-linked polyubiquitin chains and ISG15 pro-peptides *in vitro*. Crystallization of PLpro revealed that it belongs to the USP family but its function as a DUB in the course of infection has not been demonstrated (64). Also the human corona virus NL63 was reported to encode the PLP2 protein, an enzyme with dual function.

PLP2 was also first described to be involved in viral replicase polyprotein processing and later on found to posses DUB activity. PLP2 was able to cleave K48-linked Ub chains and bind to the Ub-VS suicidal probe *in vitro* (65). Also the adenovirus encoded protease adenain has been described as an enzyme with dual function. Adenain is a nuclear and cytosolic protein. It was first described to be involved in virion maturation by cleaving e.g. viral capsid precursor and to be involved in cell lysis and release of the virions by cleaving cytoskeletal proteins (66). Adenain was described to cleave K48-linked Ub chains and ISG15 pro-peptides *in vitro*. During adenoviral infection the overall levels of ubiquitinated proteins (especially in the nucleus) decreased with increased adenain expression levels. The involvement of the adenain comprised DUB activity in the viral life cycle is not elucidated and no substrates are described yet (67). The HHV (human herpesvirus) family comprises eight members, which are subcategorized in α-, β- and γ- herpesviruses according to their site of latency. All human herpesviruses encode for a large tegumental protein. The N-termini of all of these proteins have been shown to contain a conserved region with comprised DUB activity (68). The first discovered member was UL36 of HSV1, which was detected by usage of the suicidal probe Ub-VME in HSV-1 infected cell lysates. The crystal structure of a mouse herpesvirus homologue, MCMV (murine cytomegalovirus) suggests that the herpesviral DUBs represent a new family of deubiquitinating enzymes, which is called "herpesvirus tegument USPs". Among the best characterized UL36 homologues in human are BPLF1 from Epstein-Barr virus, UL48 from human cytomegalovirus and ORF64 from Karposi Sarcoma virus. UL36 was shown in further investigation to cleave K48-linked Ub-chains *in vitro* (69). In earlier work a null mutant was generated in the UL36 gene to elucidate its role in the virus life cycle. Absence of UL36 lead to failure in targeting capsids to the correct maturation pathway resulting in accumulation of DNA-filled capsids in the cytosol not maturing into enveloped viruses (70). It remains unclear if this detected phenotype is due to elimination of UL36´s DUB activity because the UL36 null mutation, containing an internal deletion of amino acid 362-1555, does not eliminate the active site residues but may interfere with folding and enzymatic activity. Also UL48 was shown to bind to the DUB probe Ub-VME and cleave K48-linked Ub-chains *in vitro* as described for UL36. Its catalytic active Cys- and His-residues were characterized via mutation analysis (71). Orf64 from KSHV was shown to be capable of deubiquitinating cellular proteins *in vitro* and *in vivo*. Orf64´s DUB activity was detectable against K48- and K63-linked Ub chains *in vitro*. Also the catalytic active cysteine was characterized via mutation analysis. Cell fractionation studies revealed that Orf64 is localized in the cytosol and nucleus. To test the function of ORF64, siRNA (short interfering RNA) knockdown studies on latently infected cell, which were induced into lytic replication, were conducted. The depletion of Orf64 by siRNA resulted in decreased lytic viral transcription and decreased lytic protein expression (72).

1.3 The role of Ubiquitin and UbL-modifiers in the life cycle of human viruses

Given the central role of Ub- and UbL-modifications it is not surprising that many pathogens have devoted a considerable part of their genetic information to the production of proteins that mimic, block or redirect the activities of their host conjugating/deconjugating machineries. Modulation of those pathways is involved in virtually every step of the virus life cycle including virus entry, replication and assembly of new virus particles, immunity avoidance and virus exit.

1.3.1 Viral entry

Viral entry can be broadly defined as all events, leading to the arrival of the uncoated virus genome into the nucleus. HSV (Herpes simplex virus) entry into cells is a multistep process that engages the host cell machinery. In experiments, were the proteasome was blocked by usage of proteasomeal inhibitors, viral entry was disabled at an early step, after capsid penetration into the cytosol but prior to capsid arrival at the nuclear periphery. In addition, HSV successfully entered cells in the absence of a functional host ubiquitin-activating enzyme, suggesting that viral entry is ubiquitin independent. It was proposed, that proteasomal degradation of virion and/or host proteins is required for efficient delivery of incoming HSV capsids to the nucleus. The candidate proteins remain to be elucidated (73).

1.3.2 Viral replication

In the case of host replication interference, generally DNA tumor viruses modulate the cell cycle to enhance their own replication. A common mechanism shared by these viruses, is to target cell cycle regulator proteins for degradation, which often results in cell transformation. A classical example is the viral mediated down regulation of the tumor suppressor p53. The HPV (human papillomavirus) -16 and -18, E6 proteins redirect the cellular single protein E3 ligase E6AP to mediate proteasomal degradation of p53, which contributes to their oncogenicity by allowing uncontrolled cellular proliferation without induced apoptosis (74). A more common mechanism to control the turn over of particular cellular proteins is the manipulation of CRLs (cullin-RING-ligases). Examples for viral targeting of CRLs are the HPV-16 and -18, E7 proteins, which function as a substrate-binding module in a cullin 2 based CRL. This assembled complex targets the Retinoblastoma protein (pRb), a tumor suppressor controlling G1-S-phase transition, for proteasomal degradation, shutting of this cell cycle arrest point (75). The Adenovirus proteins E1B55K and E4orf6 form a dimer, which functions as a substrate binding module in a cullin 5 based CRL, targeting the tumor suppressor p53 and the MRN- (Mre11, Rad50, Nbs1) complex, which is involve in DNA double strand break repair, for proteasomal degradation (76). E1B55K also contains a consensus site for sumoylation responsible for its nuclear localization. A sumoylation site mutant (K104R) showed altered localization and reduced ability to bind to p53, which also resulted in reduced cell transformation rates (77). The adenovirus E4orf4 and the HPV encoded E2 proteins were shown to inhibit the cell cycle by interfering with the APC (anaphase-promoting complex). APC is a cellular E3 ubiquitin ligase, which is essential for progression through the M-phase. Both viral proteins were additional described to inhibit the degradation of cyclin B resulting in a G2/M phase arrest (78). SV40 (Simian-Virus 40) expresses its LT (large T antigen), which binds to the SCF (Skp1, Cullin1, F-box)-complex (cullin1 based CRL) by inhibiting the substrate binding module F-box protein Fbw7. Most of the Fbw7 targeted substrates are potential cell cycle regulator or oncogenes like cyclin E, c-Myc, c-Jun and Notch, which up on inhibition of Fbw7 get stabilized (79). The HPV encoded E2 protein and the adenovirus E4orf4 were shown to inhibit the cell cycle by interfering with the APC. Both viral proteins were additional shown to inhibit the degradation of cyclin B resulting to a G2/M phase arrest (80). Cytidine is a component of RNA, which is formed when cytosine is attached to a ribose ring. After infection of RNA retroviruses, host cells are trying to diminish cytidine to disturb viral replication. The cellular APOBEC- (apolipoprotein B mRNA editing enzyme catalytic polypeptide-like) family are mRNA editing enzymes, which edit cytosine to uracil essential for RNA synthesis.

It has been shown that APOBEC3G was able to diminish the non-coding strand of the HIV genome by converting deoxycytosin to deoxyuracil resulting in guanin to adenin hypermutations in the viral coding strand, restricting its propagation. To prohibit this pathway HIV encodes for the Vif protein, which functions as a substrate-targeting module in two described Cul5 based CRLs that target APOBEC3G for polyubiquitination and proteasomal degradation (81, 82). Instead of hijacking cellular E3 ubiquitin ligases several viruses have been described to encode their own E3 ubiquitin ligases within their genome. HSV-1 encodes for the ICP0 (infected cell protein 0), an E3 ubiquitin ligase, which has been shown to induce polyubiquitination and degradation of a variety of proteins, including the PML protein, G1/S-phase specific cyclin D3, p53 and the DUB USP7. ICP0 contains two E3 ligase sites. One of those sites recruits the cellular E2 ubiquitin conjugating enzyme UbcH5a as well as the DUB USP7. ICP0 has also been shown to undergo autoubiquitination, which was reversed by the recruited USP7. ICP0 was also shown to facilitate polyubiquitination and proteasomal degradation of USP4. When cells were infected with an ICP0 null mutant an enhanced viral replication was detected. Among all known targeted proteins of ICP0, the polyubiquitination and degradation of PML was suggested for the detected replication phenotype (83). Also KSHV (Kaposi sarcoma herpesvirus) was shown to encode a protein with E3 ubiquitin ligase function, called RTA (replication and transcription activator). RTA was earlier described to serves as transactivator protein, which is essential for activation of viral DNA replication upon initial infection and reactivation from latency. This viral multifunctional protein was shown to target several RTA repressor, like K-RBP (KSHV-RTA binding protein) and Hey1, a cellular transcriptional repressor, for polyubiquitination and proteasomal degradation. This RTA mediated repression of those two transcriptional repressors was shown to be essential for the reactivation of lytic DNA replication (84, 85)

1.3.3 Immune response

In addition to altering the cell cycle, viruses manipulate CRLs to interfere with the immune response of the host cells. HIV-1 (Human immunodeficiency virus 1) encodes the Vpu-protein, which functions as a substrate-binding module in the SCF complex. The Vpu modified CRL induces the polyubiquitination of the CD4 receptor in the ER-membrane, which causes its cytosolic translocation and proteasomal degradation. CD4 functions as a co-receptor for the TCR (T-cell receptor). Both receptors together mediate adaptive immunity by binding to MHC class I (86). Viruses often activate the antiviral interferon response during infection. The JAK-STAT pathway is an interferon induced cytokine signaling pathway in mammals and a key player in antiviral defense. STAT (signal transducer and activator of transcription) proteins comprise a family of transcription factors important in cell growth, survival and differentiation, which get activated after pathway induction. The rubulavirus encoded V protein serves as a substrate-targeting module in a Cul4a based CRL. It also binds directly to STAT2 (for human parainfluenza virus type 2) or STAT2 can be used to recruit STAT1 (for simian virus 5 and mumps virus). STAT2 or the heterodimer STAT1/STAT2 get connected to the CRL via the V protein and in following polyubiquitinated as signal for proteasomal degradation (87). The mumps virus encoded V protein was shown to target STAT3 directly via this above described composition, also as mechanism to diminish the antiviral response (88). There are also viral proteins known, which dislocate unwanted proteins from the ER. The HCMV (human cytomegalovirus) encoded US11 and US2 proteins dislocate MHC-I from the ER to the cytosol, were it becomes polyubiquitinated and proteasomal degraded (89). Also the KSHV (Kaposi's sarcoma herpes virus) encoded proteins K3 and K5 have been shown to down-regulate MHC-I mainly on the cell surface.

K3 and K5 are membrane proteins containing an N-terminal located E3-ligase domain, which adds K63- linked Ub chains to MHC-I, mediating its endosomal sorting and lysosomal degradation (90). The destruction of MHC-I decreases antigen presentation to T cells, avoiding immune recognition. The CD4 receptor is a co-receptor, which assists the TCR (T cell receptor) of helper T-cells by antigen-presenting cell recognition essential for innate immunity activation. After cellular CD4 synthesis, the protein gets located within the ER-membrane and sorted to the cell outer membrane. The HIV encoded Vpu protein is a transmembrane protein, which is also integrated into the ER-membrane. It binds to CD4 and βTRCP, a substrate targeting module in the Cul1 based SCF complex. This CRL interaction modulates CD4 polyubiquitination and proteasomal degradation, resulting in inefficient antigen-presenting cell recognition of helper T-cells (91). As described above, induction of ISG15 expression upon viral infection appears to be a broad-spectrum inhibitor of virus production. Influenza B virus infection causes strong induction of ISG15 expression. Its viral encoded NS1 protein was found to bind to ISG15, preventing it from binding to its E1 activating enzyme UBE1L, causing inhibition of cellular ISGylation (92).

1.3.4 Viral budding

RNA viruses, like HIV-1 and RSV (Rous sarcoma virus) complete their replication cycle by forming vesicles that bud from the plasma membrane. The Gag polyprotein has been reported to be necessary and sufficient for the assembly and budding of virus-like particle. A central located Gag protein domain, called L (late) domain, was reported to bind to cellular proteins involved in the host VPS (vacuolar protein sorting) pathway, a cellular budding process that formats multivesicular bodies, very similar to virus budding. Among those recruited cellular proteins are Nedd4-family E3 ligases, which have been shown to facilitate ubiquitination of the viral Gag-protein. Gag ubiquitination is correlated with successful virus release, also facilitating its own sorting into viral vesicles as they bud from the plasma membrane (93). Tsg101 (tumor supressor gene 101) is involved in vascular protein sorting and multivesicular body biogenesis by binding to monoubiquitinated proteins. Also Tsg101 was shown to bind to the ubiquitinated Gag protein by binding to Gag and ubiquitin. This interaction was shown to be essential for viral budding and release of HIV and Ebola virus (94).

These above described findings emphasize the pivotal role of Ub/UbL conjugation/deconjugation in modulating critical aspects of the virus-host cell interaction.

1.4 Introduction to EBV

EBV is a 172 kb long double-stranded DNA tumor virus, which establishes latent infections in 90% of the human population worldwide. Infection occurs in most cases during childhood with no or mild symptoms. Infection occurring in adulthood is known to cause a benign lymphoproliferative disease called “infectious mononucleosis”. This viral illness is characterized by moderate symptoms like fever, sore throat and swollen lymph glands. EBV is associated with a variety of malignancies of lymphoid cells, like Burkitt´s lymphoma, Hodgkin´s lymphoma and NK- and T-cell- lymphomas as also of epithelial cells, like nasopharyngeal carcinoma and gastric carcinoma. Like other herpesviruses EBV has a latent and a lytic life cycle. Epithelial cells of the oropharynx are the site of primary infection and are also believed to be the major site for viral replication. B-lymphocytes have been shown to serve as sites for the viral latent cycle and life long persistence. The EBV-genome does not normally integrate into the cellular DNA but persists as circular episome in the host cell.

The viral latency comprehends the expression of a subset of latent proteins and an array of transcribed non-coding RNAs (EBERs) and microRNAs depending of the type of latency (Type I, II, III). Those nine latent proteins are comprised of six “EBV nuclear antigens”, called EBNA-1, -2, -3A, -3B, -3C and LP and three “latent membrane proteins”, called LMP-1, -2, and -3. The viral latency is well studied and understood to a higher degree then the regulation of the viral lytic phase (95, 96). Upon induction of the lytic phase the first detectable expressed proteins are the two immediate-early gene products BZLF1 and BRLF1. Both proteins transactivate viral promoters, which leads to an ordered cascade of viral early and late gene expression. Early gene products include proteins involved in viral DNA replication and DNA metabolism. The lytic phase of DNA replication is dependent on seven viral replication proteins: BZLF1, binding to the oriLyt (origin of lytic phase); BALF5, a DNA polymerase; BMRF1, a polymerase processivity factor; BALF2, a single-stranded DNA-binding protein and BSLF1, BBLF4, BBLF2/3 proteins comprising a primase-helicase complex. Viral lytic replication occurs in discrete nuclear sites, named replication compartments, in which viral replication proteins are assembled. Induction of the EBV lytic program results in inhibition of cellular DNA replication as well as explosive replication of viral DNA (97).

1.5 The role of ubiquitin and UbL-modifiers in the EBV life cycle

Nedd4 ubiquitin ligase family members have been reported to have a function in the maintenance of EBV latency in B lymphocytes. The BCR (B cell receptor) is known to mediate reactivation of the lytic cycle from the latent state. This is achieved by BCR cross-linking resulting in activation of signaling pathways, which initiates the viral transactivator BZLF1. Among others Lyn and Syk are two cytoplasmic tyrosine kinases, which upon binding to activated BCR mediate activation of BZLF1. The viral latent protein LMP2A contains two PPPY motifs, which were shown to recruit Nedd4 family members. After LMP2A binding to Lyn and Syc the recruited Nedd4 E3 ligases facilitate the polyubiquitination of those two tyrosine kinases, which causes their proteasomal degradation. The depletion of Lyn and Syk prevents signaling of activated BCR resulting in the maintenance of the latent cycle (98). The lytic switch gene BZLF1 was found to be modified by SUMO-1. Unconjugated SUMO-1 level in cells are quite low. It has been shown, that BZLF1 competes with the PML-protein for SUMO-1 required for their both modification. By doing so BZLF1 degreases PML-protein sumoylation, causing the inhibition of PML body formation. Among others PML body formation is induced by type I and II interferons, induced upon viral infection, suggesting a function with an antiviral capacity. The disruption of PML bodies, which was demonstrated by all classes of herpesviruses, suggests that this function is important for efficient lytic replication. It has also been shown, that sumoylation of BZLF1 decreases its transactivating ability (99). BZLF1 was also shown to serve as a substrate binding module in a Cul2 and Cul5 based CRL. Those assembled CRLs were reported to target p53 for polyubiquitination and proteasomal degradation (100) as described already for other viruses above. EBNA3C is a critical component for EBV immortalization of infected B lymphocytes. EBNA3C was found to be modified with SUMO-1 and upon this modification co-localized with PML nuclear bodies. This co localisation was shown to decrease the effect of PML body formation, possibly due to competition among PML and EBNA3C for limited free SUMO-1 resources. The site of sumoylation was elucidated by usage of an EBNA3C truncated form. An EBNA3CΔ343-545 was not able to undergo sumoylation and did not co localize with PML nuclear bodies.

Since EBNA3C transcriptional activation is mediated by amino acids 365 to 545, which are required for binding to SUMO, EBNA3C modification with SUMO could be important for EBNA3C described transcriptional effects (101). EBNA3C was also shown to interact with the Rb protein and to facilitate its proteasomal degradation via the SCF-Skp2 complex. Overexpressed EBNA3C into EBV negative epithelial and lymphoid cell lines resulted in decreased Rb protein level. It has been shown, that the ability of EBNA3C to facilitate the degradation of Rb was down regulated by expression of a dominant negative SCF-Skp2 complex. No down regulation of Rb was detected in the absence of EBNA3C (102). Most intracellular proteins are destroyed via polyubiquitination mediated degradation in the proteasome. Resulting peptide fragments of degraded antigens are presented at the cell surface in association with MHC-I for immune recognition (103). EBNA1 is the most prominent latent protein of EBV with the broadest array of function. It is known to be essential for the maintenance of the viral genome, transcription and translation of the viral DNA, viral host persistence and cellular transformation. It has been demonstrated, that the internal Gly-Ala repeat domain of EBNA1 was able to interfere with the proteasome resulting in its protection from degradation. As a result, no EBNA1 peptide fragments are assessable for MHC-I binding and presentation on the cell surface, impairing immune recognition (104). EBNA1 has also been shown to interact with the DUB USP7, which has also been described to deubiquitinate p53 and its E3 ligase Mdm2. EBNA1 and p53 compete for the same interaction site on USP7. EBNA1 was shown to have a ~10 fold higher affinity to the USP7 binding site then p53, being able to control p53 binding and deubiquitination. Functional studies were able to show, that binding of EBNA1 to USP7 was able to protect cells to undergo apoptosis by lowering p53 levels (105). Most substrates are ubiquitinated on lysine residues, although ubiquitination on Cysteine and Serine residues as the ubiquitination of N-termini has also been reported. A database search identified several lysine free viral proteins, with lysine rich cellular and viral homologues. It is believed, that the comprehension of Lysine less proteins could be advantageous to viruses to protect them from polyubiquitination mediated degradation. The EBV encoded BHRF1 protein is a lysine less protein and a Bcl2 (B-cell lymphoma 2) family member. Bcl2 as BHRF1 are responsible for the release of mitochondrial cytochrome C, controlling cellular apoptosis (106, 107). It was shown in apoptotic cells, that Bcl2 was polyubiquitinated and degraded. To elucidate the impact of the lysine residues within Bcl2 concerning its described function, all lysines were removed via site-directed mutagenesis. It was demonstrated, that this lysine less Bcl2 mutant was resistance to degradation and was able to inhibit cell apoptosis (108). It could be speculated, that the lysine less BHRF1 is also able to escape ubiquitination and degradation with resulting pro-apoptotic conditions. LMP1 is one of the EBV gene products, which are essential for B-cell transformation. It is also the only EBV protein that has oncogenic potential in non-B cells. The family of IRFs (Interferon regulatory factors) comprise transcription factors, which are predicted to contribute to EBV oncogenesis through regulation of a spectrum of oncogenes or apoptosis related genes. IRF7 is a central regulator of type 1 IFN-mediated innate and adaptive immune responses. It has been shown that IRF7 is modified from TRAF6 with K63-linked polyubiquitin, which protects the protein from proteasomal degradation and also causes its transcriptional activation. TRAF6 is a member of the TRAF protein family, which are involved in signal transduction controlling both innate and adaptive immune responses. TRAF6 has also been shown to comprise E3 ubiquitin ligase activity. TRAF6 and its E3 ligase activity are required for LMP1 stimulated IRF7 ubiquitination. A20 is an enzyme with dual function, comprising DUB and E3 ubiquitin ligase activity in one protein. Further it has been shown that LMP1 induces A20, which upon induction negatively regulates IRF7 transcriptional activity by deubiquitinating IRF7.

A DUB deficient truncation or point mutation reduced the ability of A20 to inhibit IRF7, a ligase mutant didn't show any effect. Knockdown of A20 resulted in an increase in endogenous IRF7 K63-linked polyubiquitination and transcriptional activation (109, 110). Upon EBV infection, several cellular DUBs are known to increase in activity including USP-5, -7, -13, -15 and -22. Those DUBs recruited by EBV may stabilize β-catenin in latently infected B-cells. β-catenine is a key component of the Wnt signaling pathway that regulates growth and differentiation of cells. Wnt signaling deregulation has been implicated in cancer development and could also play a role in EBV associated cancer development (111). An overview of all the interactions of EBV with the cellular ubiquitin and ubiquitin like-modification system introduced above, are visualized in figure 2.

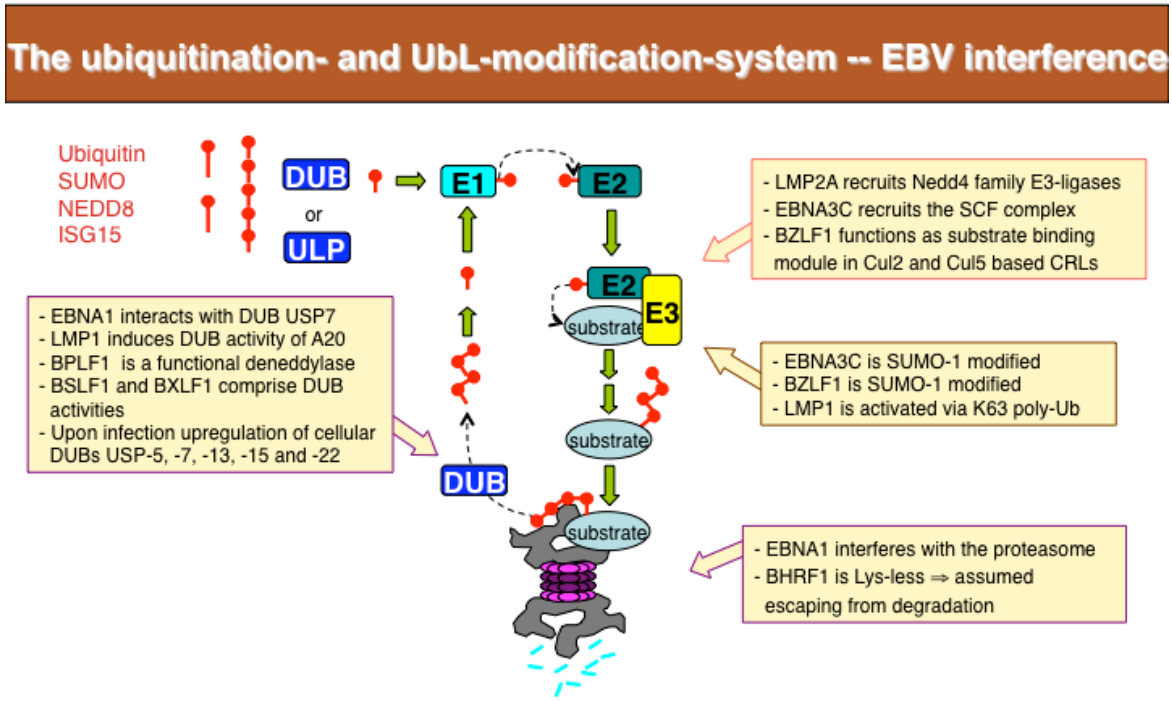

Figure 2. EBV encoded ORFs interfere with the ubiquitination and UbL-modification system at different sites.

2. AIMS OF THIS STUDY

The general aim of the work presented in this thesis, was to elucidate and characterize novel deubiquitinating enzymes (DUBs) or ubiquitin-like proteases (ULPs) encoded within the genome of Epstein-Barr virus (EBV).

More specifically, we wanted to:

- develop a bacterial screening assay based on usage of Ub/UbL-modifier reporter constructs, to test the EBV-ORFeome for encoded functional DUBs and ULPs

- characterize the discovered DUBs and ULPs via mutation analysis and usage of functional reporter and probes

- elucidate the functional role of EBV encoded DUBs or ULPs in the viral life cycle, including detection of interaction partners

3. METHODS, RESULTS AND DISCUSSION

3.1 Publication I

"Epstein-Barr Virus encodes three bona fide ubiquitin-specific proteases"

This publication was divided into a bioinformatics part and a biochemical orientated experimental part. The overall aim was it to predict *in silico* EBV encoded ORFs with distant functional homologues of human DUBs using sequence analysis methods. Candidate ORFs were further characterized by detecting their functional ability to process an ubiquitin conjugated reporter and probe construct. In following the *in silico* detected catalytic active cysteines were confirmed via mutation analysis.

Bioinformatics approach:

EBV encodes approximately 100 ORFs were most of them remain to be functional characterized. Given the essential role of DUBs within a cell, as described in previous chapters, a bioinformatics orientated strategy was developed with the aim to predict viral DUBs with distant functional human homologues. Four search strategies based on sequence analysis were used to identify putative DUBs encoded in the EBV genome.
(i) Sequence alignment with the conserved C- and H-boxes of known DUB families. As mentioned before, all DUBs contain conserved regions within their catalytic domains, which are for most of them located around the catalytic active cysteine and histidine, also called C- and H-boxes. In the case of the JAMM DUB family, which are metalloproteases, only H-boxes are present. A data set containing the sequences of human DUBs was aligned to the EBV ORF-eome by using the program CLUSTAL W. This widely used multiple sequence alignment program starts by doing a pair wise sequence alignment. Afterwards it generates a phylogenetic tree, a branching diagram showing the evolutionary relationships among species. Thereafter the program uses the phylogenetic tree to carry out a multiple alignment. Subsequently, sequence alignment with the BLAST (Basic Local Alignment Search Tool) program was performed. BLAST belongs to the most used sequence analysis methods and enables homology detection using pair wise sequence comparison. The characteristics of this program are short running times with a minimal sacrifice to distant sequence relationships. The resulting scores from a BLAST search have a well-defined statistical interpretation, making it possible to discriminate real matches from background hits (112).
(ii) Pattern search of conserved catalytic domains is a family based method, which uses as search criteria the conserved sequence information assembled in a set of homologue proteins (113). Patterns are the occurrence of distinct amino acids, which are conserved throughout members of a certain protein family. In our study, family based search pattern were derived from the aligned C- and H-box sequences of the known human DUBs. Pattern search with those conserved boxes accomplishes a more stringed assessment of the possibility that identified domains might be true C- or H-box homologues.
(iii) Hidden Markov Model (HMM)-based searches involve two steps. At first a statistical model from the sets of aligned sequences has to be build and second that model has to be compared to query sequences. HMM is a profile-based model, which is in general more sensitive than pair wise methods like described above.

HMMs are “trained” to make use of position specific scoring matrices, which represent the distribution of amino acids at each position in the conserved domains of particular protein families (114). In our studies family specific HMMs were trained from the aligned C- and H-boxes of the different human DUB families.
(iv) Identification of Cys and His residues that are conserved in homologues encoded by other members of the HHV (human herpes virus) family, followed by an HMM search was the last step of investigation. This analysis was based on the assumption that amino acid residues, which are critical for protein function, like enzymatic activity, may be conserved in the HHV-family. In our studies we were able to locate conserved Cys and His residues in identified HHV-family ORF homologues by sequence comparison. In following the patches surrounded by the detected conserved Cys and His residues were searched for known DUB, C- and H-box patterns by using the DUB family specific trained HMMs.
Via the above described search strategies several viral candidate ORFs were identified to comprehend possible DUB function. To select the most potential ORFs for following functional studies, scoring criteria were devised for each search, which were compiled in a global DUB score (see publication I for details). In total 16 EBV ORFs, which achieved the highest global DUB score, were selected for following functional studies.

Biochemical approach:

In order to evaluate the possible DUB function of the viral candidate ORFs we developed a bacterial screening assay. We cloned the candidate ORFs or ORF-domains in GST bacterial expression vectors and designed a reporter construct, which is comprised of Ubiquitin C-terminal covalently linked with the N-terminus of GFP. Afterwards the Ub-GFP reporter construct and one of the GST-tagged EBV-ORFs at the time were transformed into E.Coli. The enzymatic activity of the candidate ORF was assayed by co-expression of the Ub-GFP reporter construct. Cleavage of the Ub-GFP reporter was detected via SDS-Page and Western blotting by usage of a specific antibody against an epitope located on the GST protein. To check the positive cleavage of the reporter during each assay, a GST fused USP19 (human DUB) was used. Via this method three EBV candidate ORFs could be identified, which were able to cleave the Ub-GFP reporter significantly above background. The N-terminal fragment of BPLF1, a large tegumental protein with earlier described DUB activity conserved amongst the HHV-family (68) was able to cleave the Ub-GFP reporter to the highest degree. The EBV ORFs BSLF1, known to function as an EBV primase, and BXLF1, known to function as an EBV thymidine kinase, were also able to cleave the reporter.
In order to further characterize their DUB activity, those three proteins were overexpressed in bacteria and in following purified. The purified proteins were assayed by detection of cleavage of the flurogenic substrate Ub-AMC. This substrate contains the flurophore AMC, which upon 380 nm wavelength excitation and cleavage of the conjugated Ubiquitin starts to emit fluorescence with a wavelength of 460 nm (115). The whole *in vitro* assay was performed in a fluorometer, which detects the intensity of the cleaved substrate emission. All three EBV ORFs hydrolyzed Ub-AMC with different kinetics suggesting different affinities for the substrate. The ability of BSLF1 and BXLF1 to cleave Ub-AMC was significantly improved when equal amounts of immunoprecipitated proteins expressed in mammalian cells were taken for the assay. This circumstance may be explained by the impact of possible posttranslational modifications in increasing the activity of BSLF1 and BXLF1, which are not achieved in bacteria.
In order to further characterize the DUB activity of BPLF1-N, BSLF1 and BXLF1, the predicted catalytic active cysteine residues were mutated to alanine residues to achieve catalytic inactive proteins.

These mutations were achieved by PCR mediated site-directed mutagenesis. For applying this technique complement DNA primer were designed, which were able to anneal to a patch containing the predicted active cysteine. The base triplet coding for cysteine were changed to the base triplet coding for alanine. The mutated plasmids were amplified by PCR. The mutated plasmids were separated from the pool of non-mutated plasmids by digestion of the metylated DNA of the unmutated DNA by the endonuclese DpnI. The unmutated DNA, multiplied and metylated by bacteria, is cleaved by DpnI. After transforming the remaining mutated DNA plasmid into bacteria, the linear plasmids is ligated to circular DNA, which is ready for amplification and protein expression. Via this method the catalytic inactive protein mutants BPLF1_C61A, BSLF1_C819A_C824A and BXLF1_C491A were generated. Their loss of catalytic inactivity was demonstrated by their inability to process the flurogenic probe Ub-AMC. The active cysteine of BPLF1 and BSLF1 were shown to be conserved throughout the HHV-family but just conserved among human γ-herpes viruses for BXLF1.
Those three characterised EBV encoded DUBs, BPLF1, BSLF1 and BXLF1 are expressed in the nucleus during the early phase of the productive virus cycle. According to their annotated functions, they are involved in DNA replication and nucleotide metabolism pathways that are known to be regulated by posttranslational modifications like Ub and UbLs. The following publication (II) will discuss the essential role of BPLF1_N in virus replication. The DUB functions of BSLF1 and BXLF1 within the virus life cycle need to be investigated in further studies.

3.2 Publication II

“A deneddylase encoded by Epstein–Barr virus promotes viral DNA replication by regulating the activity of cullin-RING ligases”

The overall aim of this work was it to elucidate the functional purpose of the discovered deneddylase activity comprised in the N-terminal fragment of the viral encoded BPLF1 ORF. We were able to confirm the deneddylase activity of BPLF1-N in different assays with different NEDD8 conjugated functional probes. We were also able to identify members of the cullin family as substrates of BPLF1-N´s deneddylase activity. We further elucidated the consequence of BPLF1-N binding and deneddylating cullins assembled in CRLs, which was the stabilization of CRL substrates involved in cell cycle regulation. We could show that this BPLF1-N controlled accumulation of replication regulating proteins was essential for an S-phase like cellular environment and endoreduplication in BPLF1-N expressing cells. We further could demonstrate that the impact of BPLF1-N expression on viral genome replication was controlled by one stabilized CRL substrate, the DNA licensing factor CDT1.

In order to extend the scope of the bacterial screening assay we designed new reporter constructs. Apart from the Ub-GFP reporter, we further constructed NEDD8-GFP, SUMO1-GFP, SUMO2-GFP, SUMO3-GFP and ISG15-GFP reporter by linking the C-terminus of the UbL-modifier covalently to the N-terminus of GFP. We used an EBV-ORF library, were the entire ORF or ORF-domains were cloned into GST-bacterial expression vectors. The assay was performed by expressing the particular Ub/UbL-reporter construct together with one of the GST-tagged EBV-ORFs in E.Coli bacteria. The possible cleavage of the Ub/UbL-GFP reporter was detected via SDS-PAGE and Western blotting by usage of a specific antibody against an epitope located on the GST protein.

To check the positive cleavage of the Ub/UbL-reporter during each assay, GST-fused human DUBs or ULPs were used. The most striking result of this assay was it, that the N-terminal fragment of BPLF1 was able to process the NEDD8-GFP reporter with similar efficiency as the Ub-GFP reporter.
In order to characterize further the novel discovered deneedylase activity of BPLF1, we performed functional assays. We detected an equal efficiency of bacterial expressed and purified GST-BPLF1-N processing the flurogenic substrates Ub-AMC and NEDD8-AMC (see for method explanation in publication I introduction and reference 115).
We compared the ability of eukaryotic expressed BPLF1-N to bind to the Ub-VS and NEDD8-VS functional probes. Those probes are widely used to characterize catalytic active cysteine deconjugases. They contain besides Ub or a specific UbL a reactive compound, which binds and inhibits in most cases the catalytic site of the targeted cysteine deconjugase (32). The resulting interaction of the probe towards the enzyme can be visualized by a shifted enzyme protein band in Western Blot. For the assay we used an equal amount of eukaryotic expressed flag-BPLF1 and titrated different amounts of the Ub-VS and NEDD8-VS probes to the reaction. As a result we also detected here, that BPLF1-N was able to bind both probes with comparable efficiency.
Taken together all three functional assays with the functional reporter and probes Ub/NEDD8-GFP, Ub/NEDD8-AMC and Ub/NEDD8-VS suggest similar affinities for BPLF1-N towards ubiquitinated and neddylated substrates. Ubiquitin and NEDD8 have the same size and share a similar structure and surface charge distribution. Given the high degree of homology between both modifiers the detected dual specificity for BPLF1-N is not surprising and is also shared by other USPs (116).
Next we addressed the question, if BPLF1-N is able to deneddylate cellular proteins *in vitro* and *in vivo*. We expressed V5-tagged NEDD8 in eukaryotic cells and captured neddylated conjugates on anti-V5-conjugated sepharose beads. Those beads were incubated *in vitro* with purified GST-BPLF1-N, resulting in hydrolysis of cellular NEDD8 conjugates, which was detected in Western blots by usage of an anti-V5 antibody. The same experiment was repeated with the difference, that Flag-BPLF1 was co-expressed in the V5-NEDD8 expressing eukaryotic cells. After lysing the cells and detecting the V5-NEDD8 conjugates in a Western blot, we observed that BPLF1-N was able to hydrolyse the neddylated cellular conjugates. Thus, BPLF1-N appears to be a true deneddylase.
After this indication we were wondering which cellular neddylated substrates are targeted by BPLF1-N. The best characterized neddylated cellular proteins are the cullin family, which comprise in human six members: Cul-1,-2,-3,-4a,-4b,-5. The C-terminal neddylation of Cullins assembled in CRLs was shown to enable a sufficient polyubiquitination of the particular CRL substrate protein (13, 14). In our studies we could show, that BPLF1-N is able to deneddylate Cul1 and Cul4a *in vivo*. We co-expressed in eukaryotic cells Flag-BPLF1-N with V5-NEDD8 and Myc tagged Cul1 and Cul4a, which are two representative members of the cullin family. After lysing the cells and running their lysate on a SDS-PAGE, we were able to detect BPLF1-N´s ability to hydrolyze V5-NEDD8 conjugated Cul1 and Cul4a.
After showing this effect we wanted to investigate, if the enzyme also binds to those two cullins. We transfected eukaryotic cells with Flag-BPLF1-N and Myc-Cul1 or Myc-Cul4a and performed co-immunoprecipitations (Co-IPs). Cell lysates were separated and the Co-IPs were conducted in both ways, using the Flag- and Myc- antibody. Both cullins were shown to bind to BPLF1-N, which was detected in following Western blots of the anti-Flag and anti-Myc Co-IP fractions. After showing this interaction for overexpressed Cul1 and Cul4a, we repeated this Co-IP experiment performed with endogenously expressed Cul4a. We transfected eukaryotic cells with Flag-BPLF1-N and separated again the cell lysates, for Co-IP experiments in both ways, with an anti-Cul4a and an anti-Flag antibody. Endogenous Cul4a was able to bind Flag-BPLF1-N, detected in the anti-Cul4a and anti-Flag Co-IP.

Neddylation of cullins integrated in CRLs enables the E3-ligase complex to polyubiquitinate its specific substrate, which leads to its proteasomal degradation. We were wondering, if we were able to stabilize known CRL substrates by overexpressing BPLF-1-N. By knowing that BPLF1 is a nuclear protein expressed in the early phase of the productive virus cycle, we assumed an involvement of the protein in DNA replication. Several CRL regulated substrates are involved in cell cycle control, like the licensing factor CDT1, the tumor suppressor p21 and p27 and the cyclin phosphatase cdc 25c. All those proteins are targeted by Cul1 and/or Cul4 based CRLs. Expression of those CRL substrates together with BPLF1-N lead to their stabilisation detected via Western blot. The accumulation of those cell cycle regulators was reversed in a dose dependent manner by overexpression of V5-NEDD8, whereas a mutant V5-NEDD8-VV, lacking the C-terminal Gly residue required for conjugation, and HA-ubiquitin had minor or no effects. As described in earlier chapters, viral modulation of CRLs is a common mechanism to control pathways essential for the virus life cycle, like viral replication or hiding from the immune surveillance. Several DNA viruses, like HPV (75), Adenovirus (76), SV40 (79) and now also due to our studies EBV, have been described to manipulate CRLs to insure their undisturbed genome replication.

After overexpression of BPLF1-N in various eukaryotic cell types it could be shown, that the enzyme localises predominately to the nucleus, detected via immunofluorescence. The effect of this nuclear accumulation of BPLF1-N was an increased size of the nucleus and on prolonged expression, extensive cell death. Those detected effects were not due its overexpression but due its catalytic activity, because a catalytic inactive mutant, BPLF1-N C61A missed to establish this phenotype. To investigate the cause of the nuclear enlargement, BPLF1-N transfected cells were stained with propidium iodide, a fluorescent agent, which binds to DNA. After this treatment the cell cycle profile and DNA content was assessed of those cells. Taken together the compiled results of those experiments indicated a deregulation of the S-phase and an ongoing re-replication of cellular DNA without mitosis (endoreduplication). Almost all BPLF1-N expressing cells died within 4-5 days. This phenotype was reversed in a dose-dependent manner by overexpression of NEDD8 but not by overexpression of ubiquitin. This result suggests that BPLF1-N´s deneddylase activity rather then its DUB activity seems to be responsible for this phenotype.

Further BPLF1-N overexpression experiments in different eukaryotic cell lines elucidated the stabilisation of several CRL substrates or activation of certain regulator proteins, essential for DNA synthesis and cell cycle progressing. To summarize, the composition of those activated or stabilised proteins also represents our earlier detected cell cycle milieu of an S-phase like environment and endoreduplication in BPLF1-N expressing cells (see for details publication II). Among those stabilised proteins was the DNA licensing factor CDT1 (chromatin licensing and DNA replication factor 1). CDT1 functions as a regulatory protein of the pre-RC (pre-replication complex), which is essential for the initiation of DNA replication. The pre-RC binds to the oriP (origin of replication) and “licenses” the initiation of replication during the S-phase. Cdt1 is tightly regulated through ubiquitin-dependent proteolysis facilitated by Cul1 and Cul4 based CRLs. The involvement of the cellular DNA replication machinery in replication of the viral genome is poorly understood for the HHV-family.

To elucidate whether the detected S-phase like environment and endoreduplication in BPLF1-N expressing cells has an impact of viral replication we used the Akata-Bx1 cell line. This B-cell lymphoma cell line carries a recombinant EBV genome within, which can be induced to start its lytic cycle by crosslinking of cell surface immunoglobulins. Entrance into the viral replication state can be visualised by the expression of a viral early protein substituted with GFP (green fluorescent protein). EBV replication in those cells causes the same phenotype as in BPLF1-N overexpressed cell lines, an S-phase like environment and endoreduplication, detected via cell cycle diagram assays.

Also in those EBV reactivated cells the same milieu of activated or CRL stabilised proteins essential for DNA synthesis and cell cycle progressing was detected as in BPLF1-N expressing cells. Among them also the stabilised Cul1 and Cul4 based CRL target CDT1. Upon silencing BPLF1 expression in those induced Akata cells via the transduction of shRNA (short hairpin RNA) against BPLF1 mRNA, the normal cell cycle diagram could be reconstituted. After overexpression of CDT1 in those BPLF1 knock downed cells, the BPLF1-N detected S-phase like phenotype could be reconstituted to a certain extend. This result demonstrates the big impact of the BPLF1-N stabilized CRL substrate CDT1. It also indicates the essential involvement of probably other stabilized CRL substrates to reconstitute the BPLF1-N overexpression phenotype.
In order to investigate the impact of BPLF1 expression towards viral genome replication, we assayed the viral DNA contend in BPLF1 knock down induced Akata cells via RTq-PCR (real time quantitative-PCR). The knock down of BPLF1 resulted in an almost complete inhibition of virus DNA replication. Thereafter, we also wanted to investigate the impact of overexpressed CDT1 in BPLF1 knock downed, induced Akata cells. Overexpression of CDT1 in those cells let to reactivation of viral replication to an almost full degree. To summaries this data demonstrates that stabilisation of CDT1 is critical for the introduction of an S-phase-like cellular environment, and the driving factor for viral replication.

To investigate whether BPLF1-N´s deneddylase activity and caused induction of cellular DNA re-replication are conserved among the HHV-family, we tested the BPLF1 homologues UL36 of HSV and M48 of MCMV. GST fusions of the N-termini of UL36 and M48 cleaved the Ub-GFP and NEDD8-GFP reporter constructs with comparable efficiency in the above explained bacterial screening assay. Also Flag tagged UL36-N and M48-N reacted with the Ub-VS and NEDD8-VS suicidal probes as described earlier for Flag-BPLF1-N. Overexpression of Flag-UL36-N and Flag-M48-N also introduced an S-phase cellular environment and endoreduplication, as seen after Flag-BPLF1-N expression. Taken together, those results suggest that the function of BPLF1 is conserved among members of the HHV-family.

4. ONGOING RESEARCH AND FUTURE PERSPECTIVES

In previous experiments we could show, that BPLF1-N was able to bind to Cul1 and Cul4a. In order to address the question, if BPLF1-N was able to bind to the whole cullin family, we overexpressed all Myc-tagged cullins (Cul-1,-2,-3,-4a,-4b,-5) together with Flag-BPLF1-N in eukaryotic cells. In following we performed Co-IP experiments with Flag- and Myc-antibodies and were able to Co-IP Flag-BPLF1 with all Myc-cullins and also all Myc-cullins with Flag-BPLF1. These results indicate that CRLs comprised of the entire cullin family may be target of BPLF1-N.
We were also interested to investigate on which cullin domain BPLF1-N binding occurs and if the binding is direct or if cellular adaptors are involved. To address this question we generated different GST tagged Cul4a domains. In following pull-down assays with eukaryotic cell lysates containing overexpressed Flag-BPLF1-N, we could identify its site of interaction towards the cullin C-terminus, closely located to the neddylation site. In order to investigate, if cellular adaptors are involved in this binding, the experiment was repeated with bacterial expressed and purified His-BPLF1-N. Also this attempt resulted in binding of BPLF1-N to the same C-terminal located Cul4a domain, showing that this interaction is direct and no cellular adaptors are involved.
In order to elucidate the BPLF1-N residues involved in binding towards cullins, *in silico* sequence alignments among all human virus homologues of BPLF1_N were conducted. The alignment result revealed a conserved α-helical structure located on the enzymes surface. A high degree on conservation was detected on two charged residues Asp86 and Asp90 pointing outwards of this α-helix. After mutating those two residues into opposite charged residues Asp86Arg and Asp90Arg the interaction of Flag-BPLF1_D86R_D90R towards Myc-Cul1 and Myc-Cul4a could be reduced to ~90%, detected via Co-IP experiments. To insure that this degrease in binding was not due possible structural changes caused by the mutation, the conserved α- helical structure containing Asp86 and Asp90 were cloned into a bacterial His-expression vector. In following the same mutations D86R_D90R were applied on this BPLF1-N helical fragment and pull down assays were conducted with GST-Cul4a. The result was showing again a ~90% reduction in binding compared to the wild type BPLF1-N helical fragment. The outcome of those binding experiments strongly suggests that the two conserved residues Asp86 and Asp90 located within the conserved α- helical structure are the essential residues involved in the interaction towards Cul1 and Cul4a and possibly to all cullins.

As in publication II shown, overexpression of BPLF1-N induces a cellular S-phase like environment and leads to endoreduplication. As we could show, this phenotype was caused by BPLF1`s ability to bind to cullins and its impact to stabilize CRL substrates. In future experiments the cell cycle analysis will be repeated with the binding mutant BPLF1_D86R_D90R. If we would detect a strong degrease or an absence of the described BPLF1-N phenotype, we would have an additional strong argument for the capacity of BPLF1 to bind to cullins and its ability to stabilise CRL substrates.

5. ACKNOWLEDGEMENTS

I would like to express my sincere gratitude to everyone who has supported me in accomplishing this thesis. Special thanks to:

My supervisors:

Maria Masucci, who took me in as a graduate student and introduced me to the world of science. Maria, thank you for the time in you lab it was really an experience. I admire your ambition and dedication to your work and wish you all the best!

Kristina Lindsten, who was my co-supervisor. Also to you many thanks for everything! I could always come to you, when I had a scientific question and you always took your time. I wish you all the best, especially for the exciting life in front of you with your three handsome sons and the new house.

My mentor:

Teresa Frisan, who is always "fresh like a rose". Teresa, we had so much fun in the lab, especially because our benches were next to each other. With your catching positive and lively character you are an essential column of this group.

People, who I worked close together with:

I would like to thank Thorsten Pfirmann and Stefano Gastaldello. Working together with you on a project was a pleasure and increased my ability to work and think in a team. I wish you for your future all the best!

All former and present members of the group:

An old German adage says that the character of a person is formed by the interaction with other persons. That's why my friends, thank you for creating me! It was a pleasure to work with you and I will always remember you. Thank you Bin, Christian, Claudia, Deborah, Diego, Dimath, Eliana, Eugenie, Gerco, Gerry, Helena, Javier, Kelly, Lina, Linda, Mia, Micke, Natalia, Nouman, Pino, Omid, Roberta, Riccardo, Rikard, Simone, Stefan, Ulrika, Vanessa, Vaya, Ximena, Xinsong and Yvonne.

6. REFERENCES

1. Hershko, A., Ciechanover, A. (1998) The ubiquitin system. Annu. Rev. Biochem. 67:425-n79.

2. Kirkin, V., Dikic, I. (2007) Role of ubiquitin- and Ubl-binding proteins in cell signaling. Curr Opin Cell Biol. 19(2):199-205.

3. Herrmann, J., Lerman, L.O., Lerman, A. (2007) Ubiquitin and Ubiquitin-Like Protein Regulation. Circ. Res. 100(9):1276-91.

4. Johnson, E.S. (2004) Protein modification by SUMO. Annu Rev Biochem. 73:355-82.

5. Xirodimas, D.P. (2008) Novel substrates and functions for the ubiquitin-like molecule NEDD8. Biochem Soc Trans. 36(5):802-6.

6. Amerik, A.Y., Hochstrasser, M. (2004) Mechanism and function of deubiquitinating enzymes. Biochim Biophys Acta. 1695(1-3):189-207.

7. Ciechanover A.(1994) The ubiquitin-proteasome proteolytic pathway. Cell. 79(1):13-21.

8. Hoeller, D., Crosetto, N., Blagoev, B., Raiborg, C., Tikkanen, R., Wagner, S., Kowanetz, K., Breitling, R., Mann, M., Stenmark, H., Dikic, I. (2006) Regulation of ubiquitin-binding proteins by monoubiquitination. Nat Cell Biol. 8(2):163-9.

9. Hicke L. (2001) Protein regulation by monoubiquitin. Nat Rev Mol Cell Biol. 2(3):195-201.

10. Chen, Z.J., Sun, L.J. (2009) Nonproteolytic functions of ubiquitin in cell signaling. Mol Cell. 33(3):275-86.

11. Yang, W.L., Zhang, X., Lin, H.K. (2010) Emerging role of Lys-63 ubiquitination in protein kinase and phosphatase activation and cancer development. Oncogene. 29(32):4493-503.

12. Johnson, E.S. (2004) Protein modification by SUMO. Annu Rev Biochem. 73:355-82.

13. Pan, Z.Q., Kentsis, A., Dias, D.C., Yamoah, K., Wu, K. (2004) Nedd8 on cullin: building an expressway to protein destruction. Oncogene. 23(11):1985-97.

14. Jackson S, Xiong Y. (2009) CRL4s: the CUL4-RING E3 ubiquitin ligases. Trends Biochem Sci. 34(11):562-70.

15. Wade, J., Harper, J. (2004) Neddylating the Guardian. Cell 1:2-4.

16. Stickle, N.H., Chung, J., Klco, J.M., Hill, R.P., Kaelin, W.G. Jr., Ohh, M. (2004) pVHL modification by NEDD8 is required for fibronectin matrix assembly and suppression of tumor development. Mol Cell Biol. 24(8):3251-61.

17. Gao, F., Cheng, J., Shi, T., Yeh, E.T. (2006) Neddylation of a breast cancer-associated protein recruits a class III histone deacetylase that represses NFB-dependent transcription. Nature Cell Biology 8:1171 – 1177.

18. Oved, S., Mosesson, Y., Zwang, Y., Santonico, E., Shtiegman, K., Marmor, M.D., Kochupurakkal, B.S., Katz, M., Lavi, S., Cesareni, G., Yarden, Y. (2006) Conjugation to Nedd8 instigates ubiquitylation and down-regulation of activated receptor tyrosine kinases. J Biol Chem. 281(31):21640-51.

19. Skaug, B., Chen, Z.J. (2010) Emerging role of ISG15 in antiviral immunity. Cell 143(2):187-90.

20. Guerra, S., Lopez-Fernandez, L.A., Garcia, M.A., Zaballos, A., Esteban, M. (2006) Human gene profiling in response to the active protein kinase, interferon-induced serine/threonine protein kinase (PKR), in infected cells. Involvement of the transcription factor ATF-3 IN PKR-induced apoptosis. J Biol Chem 281:18734–18745.

21. Malathi, K., Paranjape, J.M., Bulanova, E., Shim, M., Guenther-Johnson, J.M. et al. (2005) A transcriptional signalling pathway in the IFN system mediated by 2'–5'-oligoadenylate activation of RNase L. Proc Natl Acad Sci U S A 102:14533–14538.

22. Meng, Z., Xu, Y., Wu, J., Tian, Y., Kemper, T., Bleekmann, B., Roggendorf, M., Yang, D., Lu, M. (2008) Inhibition of hepatitis B virus gene expression and replication by endoribonuclease-prepared siRNA. J Virol Methods. 150(1-2):27-33.
23. D'Cunha, J., Ramanujam, S., Wagner, R.J., Witt, P.L., Knight, E. Jr., Borden, E.C. (1996) In vitro and in vivo secretion of human ISG15, an IFN-induced immunomodulatory cytokine. J Immunol. 157(9):4100-8.
24. Yuan, W., Krug, R.M. (2001) Influenza B virus NS1 protein inhibits conjugation of the interferon (IFN)-induced ubiquitin-like ISG15 protein. Embo J. 20:362–371.
25. Okumura A, Pitha PM, Harty RN. (2008) ISG15 inhibits Ebola VP40 VLP budding in an L-domain-dependent manner by blocking Nedd4 ligase activity. Proc Natl Acad Sci U S A. 105(10):3974-9.
26. Christopher, L. B., Wei, G. (2006) p53 Ubiquitination: Mdm2 and Beyond. Review. Molecular Cell 21, 307–315.
27. Sun, S.C. (2008) Deubiquitylation and regulation of the immune response. Nat Rev Immunol. 8(7):501-11.
28. Popov, N., Wanzel, M., Madiredjo, M., Zhang, D., Beijersbergen, R., Bernards, R., Moll, R., Elledge, S.J., Eilers, M. (2007) The ubiquitin-specific protease USP28 is required for MYC stability. Nat Cell Biol. 9(7):765-74.
29. Clague, M.J., Urbé, S. (2006) Endocytosis: the DUB version. Trends Cell Biol. 16(11):551-9.
30. Guterman, A., Glickman, M.H. (2004) Deubiquitinating enzymes are IN/(trinsic to proteasome function). Curr Protein Pept Sci. 5(3):201-11.
31. Catic, A., Fiebiger, E., Korbel, G.A., Blom, D., Galardy, P.J., Ploegh, H.L. Screen for ISG15-crossreactive deubiquitinases. PLoS One. 2(7):e679.
32. Borodovsky, A., Kessler, B.M., Casagrande, R., Overkleeft, H.S., Wilkinson, K.D., Ploegh, H.L. (2001) A novel active site-directed probe specific for deubiquitylating enzymes reveals proteasome association of USP14. EMBO J. 20(18): 5187–5196.
33. Reyes-Turcu, F.E., Ventii, K.H., Wilkinson, K.D. (2009) Regulation and cellular roles of ubiquitin-specific deubiquitinating enzymes. Annu Rev Biochem. 78:363-97.
34. Gong, L., Kamitani, T., Millas, S., Yeh, E.T. (2000) Identification of a novel isopeptidase with dual specificity for ubiquitin- and NEDD8-conjugated proteins. J Biol Chem. 275(19):14212-6.
35. Nijman, S. M., Luna-Vargas, M. P. Velds, A. Brummelkamp, T. R. Dirac, A. M. Sixma T. K. and Bernards, R. (2005) A genomic and functional inventory of deubiquitinating enzymes. Cell 123, 773–786.
36. Komander, D., Lord, C.J., Scheel, H., Swift, S., Hofmann. K., Ashworth. A., Barford. D. (2008) The structure of the CYLD USP domain explains its specificity for Lys63-linked polyubiquitin and reveals a B box module. Mol Cell. 29(4):451-64.
37. Hu, M., Li, P., Li, M., Li, W., Yao, T., Wu, J.W., Gu.W., Cohen, R.E., Shi, Y., (2002) Crystal structure of a UBP-family deubiquitinating enzyme in isolation and in complex with ubiquitin aldehyde. Cell 111(7):1041-54.
38. Hu, M., L,i P., Song, L., Jeffrey, P.D., Chenova, T.A., Wilkinson, K.D., Cohen, R.E., Shi, Y. (2005) Structure and mechanisms of the proteasome-associated deubiquitinating enzyme USP14. EMBO J. 24, 3747-3756.
39. Avvakumov, G.V., Walker, J.R., Xue, S., Finerty, P.J. Jr., Mackenzie, F., Newman, E.M., Dhe-Paganon, S. . (2006) Amino-terminal dimerization, NRDP1-rhodanese interaction, and inhibited catalytic domain conformation of the ubiquitin-specific protease 8 (USP8).
J Biol Chem 281(49):38061-70.
40. Renatus, M., Parrado, S.G., D'Arcy, A., Eidhoff, U., Gerhartz, B., Hassiepen, U., Pierrat, B., Riedl, R., Vinzenz, D., Worpenberg, S., Kroemer, M. (2006) Structural basis of ubiquitin recognition by the deubiquitinating protease USP2. Structure 14(8):1293-302.

41. Healy, D.G., Abou-Sleiman, P.M., Wood, N.W. (2004) Genetic causes of Parkinson's disease: UCHL-1. Cell and Tissue Research 318(1):189-194.
42. Setsuie, R., Wada, K. (2007) The functions of UCH-L1 and its relation to neurodegenerative diseases. Neurochem Int. 51(2-4):105-11.
43. Sacco, J.J., Coulson, J.M., Clague, M.J., Urbé, S., (2010) Emerging roles of deubiquitinases in cancer-associated pathways. IUBMB Life. 62(2):140-57.
44. Sano, Y., Furuta, A., Setsuie, R., Kikuchi, H., Wang, Y.L., Sakurai, M., Kwon, J., Noda, M., Wada, K. (2006) Photoreceptor cell apoptosis in the retinal degeneration of Uchl3-deficient mice. Am J Pathol 169:132–141.
45. Kwon, J., Wang, Y.L., Setsuie, R., Sekiguchi, S., Sato, Y., Sakurai, M., Noda, M., Aoki, S., Yoshikawa, Y., Wada, K. (2004) Two closely related ubiquitin C-terminal hydrolase isozymes function as reciprocal modulators of germ cell apoptosis in cryptorchid testis. Am J Pathol 165:1367–1374.
46. Lee, M.J., Lee, B.H., Hanna, J. King, R.W., Finley, D. (2010) Trimming of ubiquitin chains by proteasome-associated deubiquitinating enzymes. Mol Cell Proteomics. [ahead of print].
47. Wang, T., Yin, L., Cooper, E.M. et al. (2009) Evidence for bidantate substrate binding as the basis for the K48 linkage specificity of otubain1. J Mol Biol. 386(4):1011-23.
48. Soares, L., Seroogy, C., Skrenta, H., Anandasabapathy, N., Lovelace, P., Chung, C.D., Engleman, E., Fathman, C.G. (2004) Two isoforms of otubain 1 regulate T cell anergy via GRAIL. Nat Immunol. 5:45–54.
49. Balakirev, M.Y., Tcherniuk, S.O., Jaquinod, M., Chroboczek, J. (2003) Otubains: A new family of cysteine proteases in the ubiquitin pathway, EMBO Rep. 4(5):517-22.
50. Nanao, M.H., Tcherniuk, S.O., Chroboczek, J., Dideberg, O., Dessen, A., Balakirev, M.Y. (2004) Crystal structure of human otubain 2. EMBO Rep. 5:783–8.
51. Boone, D. L., Turer, E. G., Lee, R. C., Ahmad, M. T., Wheeler, C., Tsui, P., Hurley, M., Chien, S., Chai, O., Hitotsumatsu, E., McNally, C., Pickart, A. (2004). The ubiquitin-modifying enzyme A20 is required for termination of Toll-like receptor responses. Nat. Immunol. 5:1052-1060.
52. Wertz, I. E., O'Rourke, K. M., Zhou, Z., Eby, M. et al. (2004) De-ubiquitination and ubiquitin ligase domains of A20 downregulate NF-kappaB signalling. Nature 430:694-699.
53. Enesa, K., Zakkar, M., Chaudhury, H., Luong le, A., Rawlinson, L., Mason, J. C., Haskard, D. O., Dean, J. L., Evans, P. C. (2008) NF-kappaB suppression by the deubiquitinating enzyme Cezanne: a novel negative feedback loop in pro-inflammatory signaling. Journal of biological chemistry 283, 7036-7045.
54. Evans, P. C., Smith, T. S., Lai, M. J., Williams, M. G., Burke, D. F., Heyninck, K., Kreike, M. M., Beyaert, R., Blundell, T. L., and Kilshaw, P. J. (2003) A novel type of deubiquitinating enzyme. The Journal of biological chemistry 278, 23180-23186.
55. La Starza, R., Crescenzi, B., Pierini, V., Romoli, S., Gorello, P., Brandimarte, L., Matteucci, C., Kropp, M. G., Barba, G., Martelli, M. F., and Mecucci, C. (2007) A common 93-kb duplicated DNA sequence at 1q21.2 in acute lymphoblastic leukemia and Burkitt lymphoma. Cancer genetics and cytogenetics 175, 73-76.
56. Wang, Y., Satoh, A., Warren, G., Meyer H.H. (2004) VCIP135 acts as a deubiquitinating enzyme during p97–p47-mediated reassembly of mitotic Golgi fragments. J Cell Biol. 164(7): 973–978.
57. Kayagaki, N., Phung, Q., Salina Chan, A., Chaudhari, R. et al. (2007) DUBA: a deubiquitinase that regulates type I interferon production. Science 5856:1628-1632.
58. Weeks, S.D.,Stephen, D., Grast, K.C., Hernandez-Cuebas L., Loll, P.J. (2010) Crystal structure of a Josephin-ubiquitin complex: evolutionary restraints on ATAXIN-3 deubiquitinating activity. J Biol Chem. [ahead of print].

59. Mao, Y., Senic-Matuglia. F., Di Fiore, P.P., Polo, S., Hodsdon, M.E., De Camilli, P., (2005) Deubiquitinating function of ataxin-3: insights from the solution structure of the Josephin domain. Proc Natl Acad Sci U S A. 102(36):12700-5.
60. Verma, R., Aravind, L., Oania, R., McDonald, W.H., Yates, J.R. et al. (2002) Role of Rpn11 metalloprotease in deubiquitination and degradation by the 26S proteasome. Science 298(5593):611-5.
61. Schmaler, T., Dubiel, W., (2010) Control of Deneddylation by the COP9 Signalosome. Subcell Biochem. 54:57-68.
62. Wang, B., Elledge, S.J. Ubc13/Rnf8 ubiquitin ligases control foci formation of the Rap80/Abraxas/Brca1/Brcc36 complex in response to DNA damage. Proc Natl Acad Sci U S A. 104(52):20759-63.
63. Frias-Staheli, N., Giannakopoulos, N.V., Kikkert, M., Taylor, S.L. (2007) Ovarian tumor domain-containing viral proteases evade ubiquitin- and ISG15-dependent innate immune responses. Cell Host Microbe. 2(6):404-16.
64. Lindner, H.A., Lytvyn, V., Qi, H., Lachance, P., Ziomek, E., Ménard, R. (2007) Selectivity in ISG15 and ubiquitin recognition by the SARS coronavirus papain-like protease. Arch Biochem Biophys. 466(1):8-14.
65. Chen, Z., Wang, Y., Ratia, K., Mesecar, A.D., Wilkinson, K.D., Baker, S.C. (2007) Proteolytic processing and deubiquitinating activity of papain-like proteases of human coronavirus NL63. J Virol. 81(11):6007-18.
66. Ruzindana-Umunyana, A., Imbeault, L., Weber, J.M. (2002) Substrate specificity of adenovirus protease. Virus Res. 89(1):41-52.
67. Balakirev. M.Y., Jaquinod, M., Haas, A.L., Chroboczek, J. (2002) Deubiquitinating function of adenovirus proteinase. J Virol. 76(12):6323-31.
68. Schlieker, C., Korbel, G.A., Kattenhorn, L.M., Ploegh, H.L. (2005) A deubiquitinating activity is conserved in the large tegument protein of the herpesviridae. J Virol. 79(24):15582-5.
69. Kattenhorn, L.M., Korbel, G.A., Kessler, B.M., Spooner, E., Ploegh, H.L. (2005) A deubiquitinating enzyme encoded by HSV-1 belongs to a family of cysteine proteases that is conserved across the family Herpesviridae. Mol. Cell 19(4):547-57.
70. Desai, P.J. (2000) A null mutation in the UL36 gene of herpes simplex virus type 1 results in accumulation of unenveloped DNA-filled capsids in the cytoplasm of infected cells. J. Virol. 74(24):11608-18.
71. Gredmark, S., Schlieker, C., Quesada, V., Spooner, E., Ploegh, H.L. (2007) A functional ubiquitin-specific protease embedded in the large tegument protein (ORF64) of murine gammaherpesvirus 68 is active during the course of infection. J Virol. 81(19):10300-9.
72. González, C.M., Wang, L., Damania, B. (2009) Kaposi's sarcoma-associated herpesvirus encodes a viral deubiquitinase. J Virol. 83(19):10224-33.
73. Delboy, M.G., Roller, D.G., Nicola, A.V. J (2008) Cellular proteasome activity facilitates herpes simplex virus entry at a postpenetration step. Virol. 82(7):3381-90.
74. Mammas, I.N., Sourvinos, G., Giannoudis, A., Spandidos, D.A. (2008) Human papilloma virus (HPV) and host cellular interactions. Pathol. Oncol. Res. 14(4):345-54.
75. Huh, K.W., Zhou, X., Hayakawa, H., Cho, J.H., Libermann, T.A., Jin, J., Wade Harper, J., Munger, K. (2007) Human Papillomavirus Type 16 E7 Oncoprotein Associates with the Cullin 2 Ubiquitin Ligase Complex, Which Contributes to Degradation of the Retinoblastoma Tumor Suppressor. Journal of Virology 81(18):9737-47.
76. Querido, E., Morrison, M.R., Chu-Pham-Dang, H., Thirlwell, S.W., Boivin, D., Branton, P.E. (2001) Identification of three functions of the adenovirus e4orf6 protein that mediate p53 degradation by the E4orf6-E1B55K complex. J Virol. 75(2):699-709.

77. Endter, C., Kzhyshkowska, J., Stauber, R., Dobner, T. (2001) SUMO-1 modification required for transformation by adenovirus type 5 early region 1B 55-kDa oncoprotein. Proc Natl Acad Sci U S A 98(20):11312-7.
78. Blanchette, P., Branton, P.E. (2008) Manipulation of the ubiquitin-proteasome pathway by small DNA tumor viruses. Virology 384(2):317-23.
79. Welcker, M., Clurman, B.E. (2005) The SV40 Large T Antigen Contains a Decoy Phosphodegron That Mediates Its Interactions with Fbw7/hCdc4, The Journal of Biological Chemistry 280, 7654-7658.
80. Heilman, D.W., Green, M.R., Teodoro, J.G. (2005) The anaphase promoting complex: a critical target for viral proteins and anti-cancer drugs. Cell Cycle. 4(4):560-3.
81. Yu, X., Yu, Y., Liu, B., Luo, K., Kong, W., Mao, P., Yu, X.F. (2003) Induction of APOBEC3G ubiquitination and degradation by an HIV-1 Vif-Cul5-SCF complex. Science 302(5647):1056-60.
82. Liu, B., Sarkis, P.T., Luo, K., Yu, Y., Yu, X.F. (2005) Regulation of Apobec3F and human immunodeficiency virus type 1 Vif by Vif-Cul5-ElonB/C E3 ubiquitin ligase.
J Virol. 79(15):9579-87.
83. Everett, R.D., Young, D.F., Randall, R.E., Orr, A. (2008) STAT-1- and IRF-3-dependent pathways are not essential for repression of ICP0-null mutant herpes simplex virus type 1 in human fibroblasts. J Virol. 82(17):8871-81.
84. Gould, F., Harrison, S.M., Hewitt, E.W., Whitehouse, A. (2009) Kaposi's sarcoma-associated herpesvirus RTA promotes degradation of the Hey1 repressor protein through the ubiquitin proteasome pathway. J Virol. 83(13):6727-38.
85. Yang, Z., Yan, Z., Wood, C. (2008) Kaposi's sarcoma-associated herpesvirus transactivator RTA promotes degradation of the repressors to regulate viral lytic replication. J Virol. 82(7):3590-603.
86. Nomaguchi, M., Fujita, M., Adachi, A. (2008) Role of HIV-1 Vpu protein for virus spread and pathogenesis. Microbes Infect. 10(9):960-7.
87. Precious, B., Childs, K., Fitzpatrick-Swallow, V., Goodbourn, S. R., Randall, R.E.
(2005) Simian Virus 5 V Protein Acts as an Adaptor, Linking DDB1 to STAT2, To Facilitate the Ubiquitination of STAT1. J Virol. 79 (21):13434–13441.
88. Ulane, C.M., Rodriguez, J.J., Parisien, J.P., Horvath, C.M. (2003) STAT3 Ubiquitylation and Degradation by Mumps Virus Suppress Cytokine and Oncogene Signaling. J Virol. 77(11): 6385-93.
89. Barel, M.T., Hassink, G.C., van Voorden, S., Wiertz, E.J. (2006) Human cytomegalovirus-encoded US2 and US11 target unassembled MHC class I heavy chains for degradation. Mol Immunol. 43(8):1258-66.
90. Lidia, M., Duncan, L., Piper, S., Dodd, R., Saville, M. et al. (2006) Lysine-63-linked ubiquitination is required for endolysosomal degradation of class I molecules. EMBO J. 25(8):1635–1645.
91. Binette, J., Dubé, M., Mercier, J., Halawani, D., Latterich, M., Cohen, E.A. (2007) Requirements for the selective degradation of CD4 receptor molecules by the human immunodeficiency virus type 1 Vpu protein in the endoplasmic reticulum. Retrovirology. 4:75.
92. Yuan, W., Krug, R.M. (2001) Influenza B virus NS1 protein inhibits conjugation of the interferon (IFN)-induced ubiquitin-like ISG15 protein. EMBO J. 20(3):362-71.
93. Zhadina, M., Bieniasz, P.D. (2010) Functional interchangeability of late domains, late domain cofactors and ubiquitin in viral budding. PLoS Pathog. 21;6(10):e1001153.
94. Garrus, J.E. et al. (2001) Tsg101 and the vacuolar protein sorting pathway are essential for HIV-1 budding. Cell 107, 55–65.
95. Masucci, M.G. (2004) Epstein-Barr virus oncogenesis and the ubiquitin-proteasome system. Oncogene 23(11):2107-15.

96. Gandhi, M.K. (2006) Epstein-Barr virus-associated lymphomas. Expert Rev Anti Infect Ther. 4(1):77-89.
97. Kudoh, A., Fujita, M., Kiyono, T., Kuzushima, K., Sugaya, Y., Izuta, S., Nishiyama, Y., Tsurumi, T. (2003) Reactivation of lytic replication from B cells latently infected with Epstein-Barr virus occurs with high S-phase cyclin-dependent kinase activity while inhibiting cellular DNA replication. J Virol. 77(2):851-61.
98. Winberg, G., Matskova, L., Chen, F., Plant, P., Rotin, D., Ernberg I., Pawson, T. (2000) Latent membrane protein 2A of Epstein-Barr virus binds WW domain E3 protein-ubiquitin ligases that ubiquitinate B-cell tyrosine kinases. Mol Cell Biol. 20(22): 8526–8535.
99. Adamson, A.L., Kenney, S. (2001) Epstein-barr virus immediate-early protein BZLF1 is SUMO-1 modified and disrupts promyelocytic leukemia bodies. J Virol. 75(5):2388-99.
100. Sato, Y., Kamura, T., Shirata, N., Murata, T., Kudoh, A. et al. (2009) Degradation of Phosphorylated p53 by Viral Protein-ECS E3 Ligase Complex. PLoS Pathog. 5(7): e1000530.
101. Rosendorff, A., Illanes, D., David, G., Lin, J., Kieff, E., Johannsen, E. (2004) EBNA3C coactivation with EBNA2 requires a SUMO homology domain. J Virol. 78(1):367-377.
102. Knight, J.S., Sharma, N., Robertson, E.S. (2005) Epstein-Barr virus latent antigen 3C can mediate the degradation of the retinoblastoma protein through an SCF cellular ubiquitin ligase. Proc Natl Acad Sci U S A 102(51):18562-6.
103. Ciechanover A. (1994) The ubiquitin-proteasome proteolytic pathway. Cell 79(1):13-21.
104. Levitskaya, J., Sharipo, A., Ainars Leonchiks, A., Ciechanover, A., Masucci, M.G., (1997) Inhibition of ubiquitin/proteasome-dependent protein degradation by the Gly-Ala repeat domain of the Epstein–Barr virus nuclear antigen 1. Proc Natl Acad Sci U S A. 94(23): 12616–12621.
105. Saridakis, V., Sheng, Y., Sarkari, F., Holowaty, M.N., Shire, K., Nguyen, T., Zhang, R.G., Liao, J., Lee, W., Edwards, A.M., Arrowsmith, C.H., Frappier, L. Structure of the p53 binding domain of HAUSP/USP7 bound to Epstein-Barr nuclear antigen 1 implications for EBV-mediated immortalization. Mol Cell 18(1):25-36.
106. Kvansakul, M., Wei, A.H., Fletcher, J.I., Willis, S.N., Chen, L., Roberts, A.W., Huang, D.C., Colman, P.M. (2010) Structural basis for apoptosis inhibition by Epstein-Barr virus BHRF1. PLoS Pathog. 6(12):e1001236.
107. Desbien, A.L., Kappler, J.W., Marrack, P. (2009) The Epstein-Barr virus Bcl-2 homolog, BHRF1, blocks apoptosis by binding to a limited amount of Bim. Proc Natl Acad Sci U S A 106(14):5663-8.
108. Dimmeler, S., Breitschopf, K., Haendeler, J., Zeiher, A.M. (1999) Dephosphorylation Targets Bcl-2 for Ubiquitin-dependent Degradation: A Link between the Apoptosome and the Proteasome Pathway. J Exp Med. 189(11):1815–1822.
109. Ning, S., Alex, D. Campos, A.D., Bryant, G., Darnay, B.G., Gretchen, L., Bentz, G.L., Pagano, J.S. (2008) TRAF6 and the Three C-Terminal Lysine Sites on IRF7 Are Required for Its Ubiquitination-Mediated Activation by the Tumor Necrosis Factor Receptor Family Member Latent Membrane Protein. Mol Cell Biol. 28(20): 6536–6546.
110. Ning, S., Pagano, J.S. (2010) The A20 Deubiquitinase Activity Negatively Regulates LMP1 Activation of IRF7. J Virol. 84(12): 6130–6138.
111. Ovaa, H., Kessler, B.M., Rolén, U., Galardy, P.J., Ploegh, H.L., Masucci, M.G. (2004) Activity-based ubiquitin-specific protease (USP) profiling of virus-infected and malignant human cells. Proc Natl Acad Sci U S A 101(8):2253-8.
112. Altschul, S.F., Gish, W., Miller, W., Myers, E.W., Lipman, D.J. (1990) Basic local alignment search tool. J Mol Biol. 215(3):403-10.
113. Bairoch, A. (1992) PROSITE: a dictionary of sites and patterns in proteins. Nucleic Acids Res. 20 Suppl:2013-8.
114. Eddy, S.R.(1998) Profile hidden Markov models. Bioinformatics 14(9):755-63.

115. Dang, L.C., Melandri, F.D., Stein, R.L., (1998) Kinetic and mechanistic studies on the hydrolysis of ubiquitin C-terminal 7-amido-4-methylcoumarin by deubiquitinating enzymes. Biochemistry 37(7):1868-79.
116. Love, K. R., Catic, A., Schlieker, C. and Ploegh, H. L. (2007) Mechanisms, biology and inhibitors of deubiquitinating enzymes. Nat. Chem. Biol. 3, 697-705.

I

JOURNAL OF VIROLOGY, Nov. 2008, p. 10477–10486 Vol. 82, No. 21
0022-538X/08/$08.00+0 doi:10.1128/JVI.01113-08

Epstein-Barr Virus Encodes Three Bona Fide Ubiquitin-Specific Proteases▽‡

Ramakrishna Sompallae,[1]† Stefano Gastaldello,[1,2]† Sebastian Hildebrand,[1] Nikolay Zinin,[1] Gerco Hassink,[1] Kristina Lindsten,[1] Juergen Haas,[3] Bengt Persson,[1,4] and Maria G. Masucci[1]*

Department of Cell and Molecular Biology, Karolinska Institutet, S-171 77 Stockholm, Sweden[1]; Department of Biomedical Sciences, University of Padua, 35121 Padua, Italy[2]; Division of Pathway Medicine, School of Biomedical Sciences, College of Medicine, University of Edinburgh, Edinburgh, United Kingdom, and Max von Pettenkofer-Institute, LMU-München, Munich, Germany[3]; and IFM Bioinformatics, Linköping University, S-581 83 Linköping, Sweden[4]

Received 27 May 2008/Accepted 8 August 2008

Manipulation of the ubiquitin proteasome system (UPS) is emerging as a common theme in viral pathogenesis. Some viruses have been shown to encode functional homologs of UPS enzymes, suggesting that a systematic identification of these products may provide new insights into virus-host cell interactions. Ubiquitin-specific proteases, collectively known as deubiquitinating enzymes (DUBs), regulate the activity of the UPS by hydrolyzing ubiquitin peptide or isopeptide bonds. The prediction of viral DUBs based on sequence similarity with known enzymes is hampered by the diversity of viral genomes. In this study sequence alignments, pattern searches, and hidden Markov models were developed for the conserved C- and H-boxes of the known DUB families and used to search the open reading frames (ORFs) of Epstein-Barr virus (EBV), a large gammaherpesvirus that has been implicated in the pathogenesis of a broad spectrum of human malignancies of lymphoid and epithelial cell origin. The searches identified a limited number of EBV ORFs that contain putative DUB catalytic domains. DUB activity was confirmed by functional assays and mutation analysis for three high scoring candidates, supporting the usefulness of this bioinformatics approach in predicting distant homologues of cellular enzymes.

The posttranslational modification of proteins by ubiquitin (Ub) and Ub-like molecules (UbLs) and the degradation of polyubiquitinated substrates by the proteasome regulate fundamental cellular processes, including cell growth and differentiation, intracellular signaling, protein trafficking, apoptosis, and the recognition of virus-infected or malignant cells by the host immune response (21, 27, 33, 44, 46). Modulation of the ubiquitin-proteasome system (UPS) is emerging as a central theme in viral pathogenesis, and several examples have been reported of viral proteins that mimic or redirect the activity of the system in order to modify the cellular environment in favor of virus persistence or replication (22, 28, 31, 34, 41, 45). Thus, the identification of viral products that interfere with the UPS may yield new insights on important features of viral pathogenesis and could lead to the development of new means of therapeutic intervention.

Conjugation of Ub or UbLs is achieved through the activity of a cascade of enzymes, including activating enzymes (E1s), conjugating enzymes (E2s), and specific ligases (E3s) that catalyze the covalent linkage of the modifier to Lys residues in the substrate (11). In addition, deconjugating enzymes act as regulators of the system by maintaining the pool of free Ub and UbLs and by determining the rate of turnover of the conjugates (14, 50). In line with this proposed regulatory function, recent evidence points to a critical role of Ub deconjugases (deubiquitinating enzymes [DUBs]) in intracellular signaling, as exemplified by the activation of the transcription factor nuclear factor-κB (NF-κB) by cylindomatosis tumor suppressor, A20, Cezanne, and ubiquitin-specific protease 31 (25, 33) and by the initiation of DNA repair by USP1 (37).

Based on similarity with known family members, the human DUBs have been classified in five subfamilies including: ubiquitin C-terminal hydrolases (UCHs), ubiquitin-specific proteases (USPs), Machado-Joseph disease proteases (MJDs or Josephins), ovarian tumor proteases (otubains, OTUs), and the JAMM (Jab1/MPN/Mov34 metalloenzyme) motif proteases (2, 38). With the exception of JAMMs, the DUBs are cysteine proteases identified by a catalytic triad of Cys, His, and Asp/Asn residues and by the presence of conserved amino acid domains known as Cys- and His-boxes (C- and H-boxes, respectively) that are unique for each family (38). Mutational studies have shown that the Asp/Asn residue is not essential for catalytic activity, although it may contribute to the enzymatic activity by stabilizing the active-site thiolate and imidazolium ion pair (26, 35). The JAMM metalloproteases lack a C-box, while two conserved His residues in the JAMM motif were shown to be essential for activity (49).

Proteins with DUB activity are encoded in the genome of human adenovirus, herpesvirus, coronavirus, and bunyavirus (5, 6, 18, 29, 42). Furthermore, DUB activity was recently demonstrated in proteins encoded by some pathogenic bacteria that lack an intrinsic UPS (40, 52), suggesting that these enzymes play specific roles in the regulation of both viral and bacterial infection. Although these findings make the systematic identification of microbial DUBs a worthy endeavor, the task is complicated by the wide sequence variation of the known enzymes. Moreover, viral and bacterial proteins are often considerably different in sequence and domain organization compared to their mammalian counterparts, which fur-

* Corresponding author. Mailing address: Karolinska Institutet, Box 285, 171 77, Stockholm, Sweden. Phone: 46 8 52486755. Fax: 46 8 337412. E-mail: maria.masucci@ki.se.

† R.S. and S.G. contributed equally to this study.

‡ Supplemental material for this article may be found at http://jvi.asm.org/.

▽ Published ahead of print on 20 August 2008.

TABLE 1. Data sets of DUBs used in this study

Protein family	Characteristic domain	No. of human DUBs	No. of verified DUBs[a]	No. of orthologs	No. of DUBs in pattern search set[b]	No. of DUBs in HMM training set[d]	
						C-box	H-box
USP	Peptidase 19	45	37		45	36	42
UCHL	Peptidase 12	4	4	15	19	10	8
OTU	OTU	8	5	9	17	10	11
MJD	Josephin	3	1	9	12	7	7
JAMM[c]	MPN+	8	2	29	34		21

[a] That is, the number of DUBs with experimentally verified enzymatic activity.
[b] Due to the small number of identified sequences in the human UCH, OTU, JAMM, and MJD subfamilies, orthologs from other species were included in the data set.
[c] The JAMM metalloproteases contain only H-box domains, and sequence homologs with catalytic. His residues were considered for deriving the patterns.
[d] Only C- and H-boxes with <90% sequence identity were used for training the HMMs.

ther hampers the identification of distant functional homologues.

We have used a bioinformatics strategy here to identify putative virus-encoded DUBs. To overcome the difficulty posed by sequence variation, we focused on the conserved C- and H-boxes. Family-specific sequence alignments, pattern searches, and hidden Markov models (HMMs) were generated based on the amino acid sequences of known members of the five DUB subfamilies and then used to search a custom-made database of open reading frames (ORFs) from Epstein-Barr virus (EBV), a human gamma herpesvirus that establishes latent infections and is associated with a broad spectrum of malignancies of lymphoid and epithelial cell origin.

MATERIALS AND METHODS

Data sets. The sequences of DUBs were extracted from the UniProt database version 51.2 (4). The DUB data set consisted of both experimentally verified human enzymes and highly conserved sequence homologs (Table 1). For families with fewer than 10 human sequences, homologues from other species were included. The sequence of the B95.8 EBV genome (3) was obtained from NCBI GenBank (Refseq NC_007605). The sequences of 75 annotated EBV ORFs were retrieved from the Swiss-Prot database. In addition, ORF prediction was carried out with the getORF program available in the EMBOSS package (39), with a length cutoff setting between 150 and 5,000 amino acids (aa), which resulted in 106 predicted ORFs. For ORFs annotated in Swiss-Prot, the progressive number assigned to the predicted ORFs was substituted with the corresponding gene symbol.

DUB searches. (i) Sequence alignment. Sequence comparisons between the human DUBs and the EBV ORFs were carried out by using CLUSTAL W (47) and BLAST (1). CLUSTAL W calculates multiple sequence alignments and was therefore used to investigate whether any of the EBV ORFs clusters with the specific DUB subfamilies. BLAST searches were used to identify putative C- and H-boxes. To this end, members of each DUB family were aligned by using CLUSTAL W, and conserved catalytic domains were extracted with the GoCore program (http://www.helsinki.fi/project/ritvos/GoCore/). The C- and H-box domains of each family were defined on the basis of the conserved regions (UCH, C-box 23aa and H-box 24aa; USP, C-box 16aa and H-Box 21aa; OTU, C-box 19aa and H-box 14aa; MJD, C-box 21aa and H-box 14aa; JAMM domain 25aa), and the sequences were then searched against the EBV ORF database. Hits with arbitrarily chosen E-values of ≤10 and containing Cys or His residues were selected for further analysis.

(ii) Pattern search. C- and H-box specific patterns were constructed to search for putative catalytic domains. The C- and H-boxes of each DUB family were aligned with respect to the conserved Cys and His residues, and search patterns were manually derived from the sequence alignments based on the physicochemical properties.

(iii) HMM search. HMMs were constructed by using the HMMER (17) suite of programs. For each DUB subfamily the HMMs were trained with multiple sequence alignments of C- and H-boxes from a nonredundant set of sequences (Table 1, HMM training set). The HMM results were further categorized based on E-values and raw scores. In every search with subfamily-specific HMMs, matches with E-values of <25 were selected and manually screened for the presence of Cys or His residues in the alignment. Candidates containing putative C- or H-boxes were further categorized based on the HMM scores of the domains. The HMM score is a base 2 log of the probability of alignment to the HMM divided by the probability of random alignment. A score of zero represents 50% likelihood that the sequence is a true match to the model. Since the EBV ORF database contains 106 entries, scores greater than 6.7 correspond to a 99% probability to detect true homologs while a score of −6.6 corresponds to 1% probability. Due to the fact that the genomes of viral and other pathogenic organisms undergo higher mutation rates (16), low thresholds of statistical parameters were used to detect catalytic domains of DUBs.

(iv) Conserved Cys and His residue search. Homologous proteins that are conserved between members of at least one subfamily of human herpesviruses (α-HHVs: herpes simplex virus type 1 [HSV-1], HHV1, HSV-2, HHV2, varicella-zoster virus, and HHV3; β-HHVs: human cytomegalovirus, HHV5, HHV6, HHV7; and γ-HHVs: EBV, HHV4, Kaposi sarcoma herpesvirus, and HHV8) were identified by using BLAST with a cutoff E-value of 0.01, corresponding 99% probability to be a true homolog. Homologous proteins were then aligned by using Vector NTI (32), and the multiple alignments of each cluster were scanned for the presence of conserved Cys and His residues. Sequences flanking the conserved residues were searched for putative C- and H-boxes using the HMMs.

Functional validation of candidate DUBs: cloning of EBV ORFs into prokaryotic expression vector. ORFs derived from the B95-8 virus were transferred from the GATEWAY expression vector pDONR207 (48) to the prokaryotic expression vector pDEST-GST (ampicillin resistance), and *E. coli* DH5α was used for transformation.

Ub-GFP construct. Green fluorescent protein (GFP) was amplified by PCR from pEGFP-N1 vector (Clontech, Palo Alto, CA) with the sense primer 5′-GTTTTCAGATCTAAAGGAGAAGAGCTGTTCACCGGCGTGAGCAAGGGCGAGGAGCTGTTCACC-3′ and the antisense primer 5′-GTTCTCGAGCTTGTACAGCTCGTCCATGCCGAGAGTGAT-3′ and cloned in the BglII and XhoI sites of the pACYCDuet-1 vector (Novagen, Darmstadt, Germany). Ubiquitin was amplified by PCR from an Ub-βGal plasmid with the primer 5′-GTTGAATTCAATGCAAATCTTCGTGAAGACTCTGACTGGTA-3′ and the antisense primer 5′-GTTAGATCTGAACCCACCTCTGAGACGGAGTACCA-3′ and inserted in frame in the EcoRI and BglII sites of the pACYCDuet-1 vector containing GFP. The underlined sequences represent restriction sites.

DUB assays. The GST-ORFs and Ub-GFP reporter plasmids were cotransfected by electroporation in competent BL21(DE3) bacteria that lack endogenous DUBs (9). Antibiotic-resistant colonies were selected in LB agar supplied with 100 μg of ampicillin/ml and 30 mg of chloramphenicol/ml. Exponentially growing bacteria (OD at 600 nm of 0.5) were induced for 5 h at 30°C with 0.5 mM IPTG (isopropyl-β-D-thiogalactopyranoside) and then lysed by sonication in phosphate-buffered saline supplemented with protease inhibitors (Complete Mini protease inhibitor cocktail tablets; Roche, Germany). The lysates were clarified by centrifugation for 10 min at 13,000 rpm, and cleavage of the reporter was analyzed by fractionation in acrylamide bis-Tris 4 to 12% precasted gradient gel (Invitrogen), followed by Western blotting. After transfer to polyvinylidene difluoride membrane (Millipore), the filter was blocked in phosphate-buffered saline supplemented with 5% nonfat milk and 0.1% Tween 20 and incubated for 1 h with anti-rabbit-GFP serum (Abcam, Cambridge, United Kingdom) diluted

1:10,000. After incubation for 1 h with peroxidase-conjugated goat anti-rabbit serum, the complexes were visualized by enhanced chemiluminescence (GE Healthcare, United Kingdom). For the enzyme kinetic assays, GST-USP19, GST-USP19mut, GST-BPLF1-N, GST-BSLF1, and GST-BXLF1 were purified from bacteria lysates (50 mM Tris-Cl [pH 7.5], 150 mM NaCl, 5 mM $MgCl_2$, 1% Triton X-100, 1 mM phenylmethylsulfonyl fluoride, 1 mM dithiothreitol) by incubation for 90 min at 4°C with a solution of 10 mM glutathione in 50 mM Tris-Cl (pH 8.0), and the protein concentrations were determined with a Bio-Rad protein assay. Hydrolysis of the fluorogenic substrate ubiquitin-AMC (Ub-AMC, SE211; Biomol) was assayed at 30°C in 100 μl of assay buffer (50 mM Tris-Cl [pH 7.5], 150 mM NaCl, 2 mM EDTA, 2 mM dithiothreitol) containing 200 nM concentrations of the enzyme, and the V_{max} and K_m of the reactions were calculated by titrating the substrate at concentrations ranging between 0 and 20 mM. The fluorescent product was measured by using a spectrofluorimetry plate reader at 380-nm excitation and 460-nm emission wavelengths. To block the DUB activity, 10 mM *N*-ethylmaleimide (NEM; Sigma) was added to the assay buffer.

Site-directed mutagenesis. Point mutations of the predicted catalytic Cys residues of BPLF1, BSLF1, and BXLF1 genes were engineered by using a QuikChange site-directed mutagenesis kit according to the manufacturer's protocol (Stratagene). Two BPLF1 mutants (C61A and C65A), three single mutants (C462A, C824A, and C819A), and one double mutant (C824/819A) of BSLF1 and two mutants of BXLF1 (C84A and C491A) were constructed. All constructs were then sequenced to verify that only the desired mutations had been introduced.

RESULTS

Four search strategies were used to identify putative DUBs encoded in the EBV genome: (i) sequence alignment with the conserved C- and H-boxes of known DUB families, (ii) pattern search of conserved catalytic domains, (iii) HMM-based searches, and (iv) identification of Cys and His residues that are conserved in homologues encoded by other members of the HHV family, followed by an HMM search.

Sequence alignment searches. A first attempt to identify putative DUBs was performed using CLUSTAL W to align the EBV ORFs with the human DUB data set. Three ORFs clustered with specific DUB subfamilies, BGLF4 and BBLF4 clustered with the OTU subfamily and BcLF1 ORF aligned with JAMMs (not shown), but the homologous regions did not contain Cys or His residues, and these viral ORFs are therefore unlikely to possess enzymatic activity. Since alignment of the entire amino acid sequence may not detect homology restricted to short domains that are critical for enzymatic activity, BLAST was used to identify EBV ORFs containing sequences of homology with the conserved C- and H-boxes of each DUB family using an arbitrary cutoff E-value of ≤10. Twenty-five candidates containing Cys or His residues in homologous regions were found in this search (see Table S1 in the supplemental material), including for example, the BBRF3 ORF that contains a region of strict homology with the USP C-box (E-value = 0.018).

Pattern search. Additional search strategies were conducted to achieve a more stringent assessment of the likelihood that the identified domains might be true C- or H-boxes homologues. Family-specific search patterns were derived from the aligned C- and H-box sequences of the known DUBs. To increase the stringency of the search, when fewer than 10 family members were found in the human data set, homologues from other species were also included in the alignment. The derivation of search patterns for the C- and H-boxes of the UCH family is illustrated in Fig. 1, and the search patterns for USP, OTU, MJD and JAMM families are given in Fig. S1A to D in the supplemental material. In a first attempt, stringent search patterns were derived for each DUB family (UCH, C-box −11/+11 and H-box −7/+16; USP, C-box −8/+7 and H-box −17/+3; OTU, C-box −8/+10 and H-box −8/+5; MJD, C-box −10/+10 and H-box −6/+7; and JAMM motif −7/+17) by including at each position all residues observed in the data set (Fig. 1B, boldface residues) and then used to search the EBV ORF data set, allowing for only a single mismatch. The derived patterns were in all cases able to identify the DUBs belonging to the family but failed to identify any candidate in the EBV ORFs (results not shown), suggesting that they may be too stringent to recognize distant homologues. Less-stringent search patterns were then derived by allowing at each position additional amino acids with similar physicochemical characteristics or, when residues with different physicochemical characteristics were observed, all amino acids (indicated by an "X" in Fig. 1B and in Fig. S1A to D in the supplemental material). Regions of similarity with the C- and/or H-boxes of different DUB families were identified in 30 EBV ORFs (see Table S2 in the supplemental material). Four ORFs contained at least one putative C-box and one H-box, while three ORFs contained only one putative C-box and twenty-three ORFs contained one or more H-box-like domain.

HMM search. Family-specific HMMs were derived for the aligned C- and H-boxes of the different DUB families. In order to increase the probability of identifying distant homologs, only sequences with <90% identity were included in the training set (Table 1). Since the EBV ORF database contains only 106 sequences and the HMMs are based on short C- and H-box domains of 13 to 24 aa, high E-values and low scores were expected. HMM alignments with E-values of ≤25 were therefore considered for further analysis. All hits containing Cys or His residues were further categorized based on the HMM scores (Table 2). Scores of ≥0, corresponding to more than 50% likelihood to be a true match, were considered high. Intermediate scores were between 0 and −6.6 (down to 1% probability to be a true match), while scores less than −6.6 were considered low. Seven EBV ORFs—BALF2, BALF5, BBRF3, BcLF1, BERF3-BERF4, BRLF1, and the predicted ORF88—contained at least one C- or H-box domain with score above 0, suggesting a potential homology with the corresponding DUB domains. Two ORFs—BNRF1 and BPLF1—contained both C- and H-box-like domains with scores ≥−6.6, and eighteen additional ORFs contained either a C- or an H-box-like domain with scores of less than −6.6.

Search for conserved Cys and His residues. A further attempt to identify candidate DUBs was undertaken based on the assumption that amino acid residues that are critical for protein function may be conserved in homologues encoded by different members of the HHV family. Homologous ORFs encoded by the known HHVs were identified by sequence comparison, and the conserved Cys and His residues were located. Twenty-one EBV ORFs contain at least one Cys or His residue that is conserved in homologues encoded by all HHV members, while Cys or His residues conserved only in α- or β-HHVs were detected in two and seven ORFs, respectively; thirteen EBV ORFs shared conserved Cys or His residues only with homologues encoded by the other member of the γ-HHV subfamily, KSHV, that resembles EBV in cell tropism and oncogenic capacity (see Table S3 in the supple-

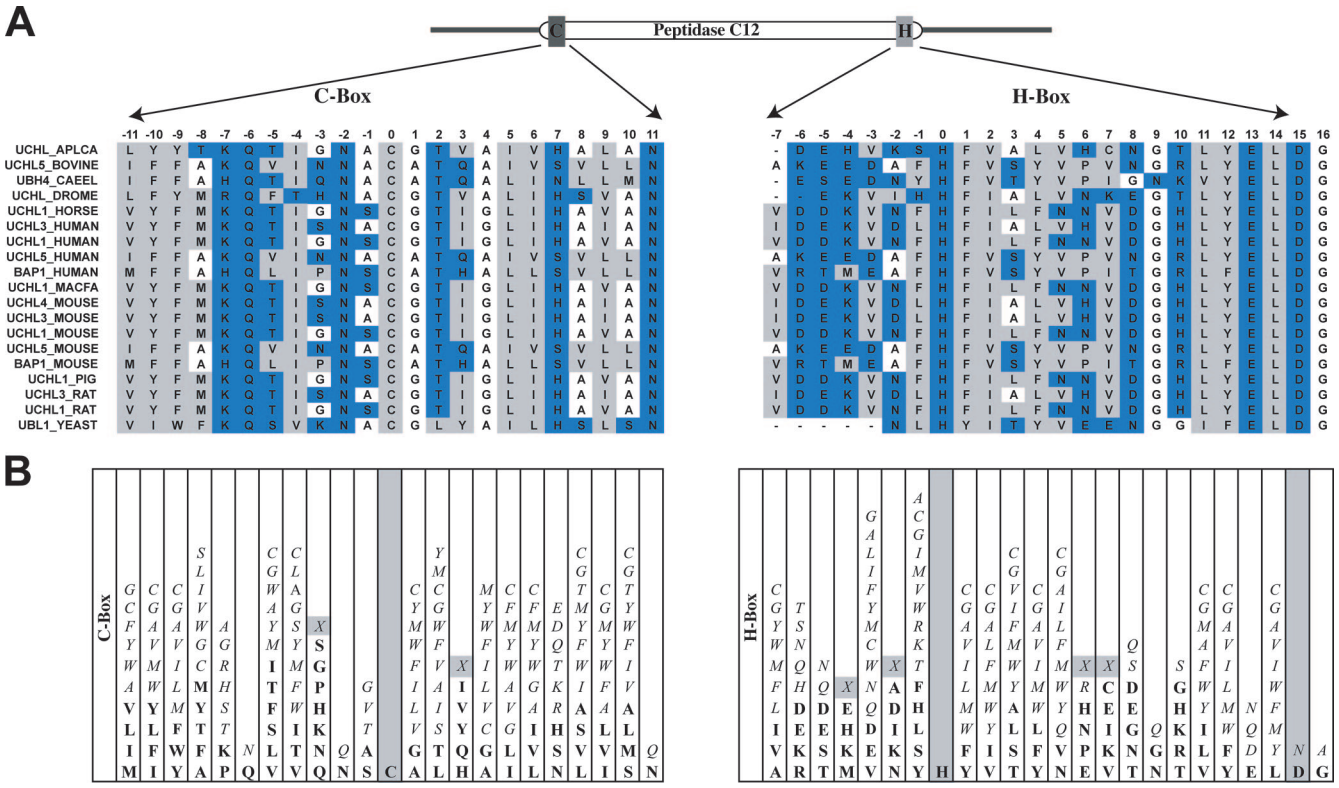

FIG. 1. Derivation of search patterns for the UCH subfamily catalytic domains. (A) The aligned amino acid sequences of the catalytic Cys and His-box regions of UCH (peptidase C12) family members are shown. The numbers above the alignment correspond to the amino acid position relative to the catalytic Cys and His residues. Polar residues are colored blue, hydrophobic residues are gray, and small residues (Gly and Ala) are white. (B) Stringent search patterns were derived by including at each position all amino acids observed in the aligned DUB sequences (indicated in bold). Less-stringent patterns were then obtained by allowing amino acids with similar physicochemical properties (indicated in italics). When different types of amino acids were observed at a given position, all amino acids were allowed in the pattern (indicated by X).

mental material). The sequences adjacent to the conserved residue were searched for putative C- and H-boxes using the DUB family specific HMMs. Nine EBV ORFs were found to contain conserved Cys or His residues located in regions homologous to the DUB C- or H-boxes, and one ORF, BGRF1/BDRF1, contained both C- and H-box homologous domains (see Table S3 in the supplemental material).

DUB score and exclusion criteria. A relatively large number of candidate DUBs were identified by at least one search, and several were identified by more than one. To select the most likely candidates for functional studies, scoring criteria were devised for each search, and these were then compiled in a global DUB score. The scores assigned to each search reflected the likelihood of identifying candidates that possess critical features associated with DUB activity (see Table S4 in the supplemental material). Candidates identified by the BLAST search were given a score of 1, 2, or 3 depending on the degree of similarity with DUB sequences. Candidates identified by the pattern search were scored 1 or 2 based on the presence of C- or H-box-like domains or both, while the score of candidates identified by the HMM considered both the presence of C- and H-box-like domain and their HMM scores (high = >0, intermediate = between 0 and −6.6, or low = <−6.6). The same scoring system was used for candidates identified by the presence of conserved Cys and His residues. The scores of 58 candidates identified by at least one search are shown in Table S4 in the supplemental material. Two ORFs—BGRF1/BDRF1 and BPLF1—were identified by the four searches, nine ORFs were identified by three searches, twenty-two ORFs were identified by two searches, and twenty-five ORFs were found by only one search. All candidates identified in at least three searches and five candidates identified by two searches received scores of ≥4. This group included 16 ORFs, all of which were identified by HMM, and 7 were shown to contain conserved Cys or His residues.

In order to further restrict the number of candidates to be validated by functional studies, ORFs with scores of ≥4 were scrutinized for the presence of structural constraints that could prevent DUB activity. The locations of the putative C- and H-boxes were mapped relative to each other and to other protein domains of known function (Fig. 2). Based on this domain analysis, the BBRF3 and BILF1 ORFs could be excluded since their putative C- and H-boxes are located in transmembrane regions, which would preclude DUB activity. Analysis of the site of expression in EBV-infected cells, expression during different phases of the virus cycle, and functional annotation (Table 3) revealed that some of the high-scoring candidates are structural proteins or glycoproteins associated with the virus capsid and envelope. These proteins are unlikely to possess enzymatic activity, although this cannot be excluded a priori. The remaining candidates include immediate-early, early, late, or latent proteins that are expressed in

TABLE 2. Putative DUB catalytic boxes identified by the HMM search[a]

EBV ORF	C-box		H-box	
	Type	Score	Type	Score
BALF1			OTU	*-0.4*
BALF2	OTU	**1.9**		
	UCH	*–6.4*		
BALF4	OTU	–10.2	UCH	–9.3
BALF5	USP	**0.3**		
BaRF1			UCH	*–1.9*
BBLF2	USP	*–2.9*		
BBLF4	MJD	–15	OTU	*–4.3*
BBRF2	USP	*–3.7*		
BBRF3	USP	**7.8**	OTU	–6.7
	UCH	–9.8		
BcLF1	OTU	**1.3**	OTU	*–4.2*
			USP	–8.4
BcRF1			MJD	–9.5
BDLF2			OTU	–7.6
BERF3-BERF4	USP	**0.69**		
	OTU	–7.9		
	MJD	–8.3		
BFRF2	OTU	–6.8		
BGLF1	OTU	*–1.6*	OTU	–7.7
BGLF2			OTU	*–4.6*
BGLF3			OTU	*–5.3*
BGRF1/BDRF1	MJD	–10.9	MJD	–8.1
BILF1	USP	*–0.6*		
BKRF1	USP	*–3*		
BLLF3			OTU	–7.9
BMLF1	OTU	–6.7		
BMRF2	MJD	–9.2		
BNRF1	USP	*–3.9*	OTU	*–2*
			UCH	–9.1
BORF1	USP	*–4.2*		
BPLF1	USP	*–4.5*	OTU	*–4.3*
BRLF1	USP	**0.9**	OTU	*–6.3*
	OTU	*–4.4*		
BSLF1	OTU	–7.8	OTU	–6.8
BVRF2	USP	*–3.5*	JAMM	–16.2
BXLF1	USP	*–3.4*	USP	–13.2
BXLF2			USP	*–5.2*
			UCH	*–5.5*
			MJD	–7.4
BXRF1			MJD	–8.9
LMP1	MJD	–8.4		
LMP2	USP	*–1*		
ORF101	USP	*–2.5*		
ORF35			OTU	*–5.3*
			MJD	–7.6
ORF42	OTU	–9.6		
ORF86	OTU	*–2.3*		
	USP	*–4.5*		
ORF88	OTU	–11.1	OTU	**2.9**

[a] The type of DUB domain found in each candidate is indicated as follows: USP, ubiquitin-specific protease; OTU, ovarian tumor domain protease; UCH, ubiquitin C-terminal hydrolase; MJD, Josephin domain protease. Boldfacing indicates high scores (>0); italics indicates intermediate scores (between 0 and −6.6); regular typeface indicates low scores (<–6.6)

the nucleus or, in one case, in the cytoplasm of the infected cells or are components of the viral tegument. It is noteworthy that two tegument proteins were found in the group with the highest DUB score and one of them, the protein encoded by the BPLF1 ORF, was previously shown to possess DUB activity (23, 42).

Functional validation of the candidates. In order to validate the DUB score, GST fusions of 11 EBV ORFs with scores of ≥4 and an approximately equal number of ORFs with scores of ≤3 were tested for their capacity to hydrolyze a Ub-GFP reporter plasmid coexpressed in bacteria. The results of a representative assay wherein the ORFs were tested alongside the human USP19 and a catalytic mutant that lacks enzymatic activity are shown in Fig. 3.

The reporter was efficiently cleaved by USP19, as confirmed by the detection of both free GFP (Fig. 3A) and free ubiquitin (data not shown), while cleavage was abolished by mutation of the catalytic Cys residue in the USP19Mut. In line with the reported DUB activity of this ORF, Ub-GFP was cleaved almost completely in bacteria expressing the N terminus of BPLF1 (Fig. 3A and B). The levels of cleavage significantly above background were also detected with BSLF1 and BXLF1, while the activity of BGRF1 and BALF5 was just below the cutoff (3 × the mean percent cleavage in the presence of ORFs with scores ≤3 [Fig. 3B]). The expression of the fusion proteins was in all cases confirmed in Western blots probed with anti-GST antibodies (data not shown). In order to further characterize their DUB activity, bacterially expressed GST-BPLF1-N, GST-BSLF1, and GST-BXLF1 were purified, and their enzyme activity was assayed by cleavage of the fluorogenic substrate Ub-AMC (Fig. 3C). The three EBV ORFs hydrolyzed Ub-AMC with different kinetics and K_m values, suggesting very different affinities for the substrate, but the specificity of the reaction was in all cases confirmed by blocking with the cysteine protease inhibitor NEM. Interestingly, the enzymatic activity of BSLF1 and BXLF1 relative to BPLF1 was significantly improved when equal amounts of immunoprecipitated proteins expressed in mammalian cells were compared for the cleavage of Ub-AMC (compare Fig. 3C and D), suggesting that posttranslational modifications that are not achieved in bacteria cells may be required for optimal activity.

In order to further validate the DUB activity of the candidates, the predicted catalytic Cys residues in BPLF1, BSLF1, and BXLF1 were mutated to Ala by using PCR-mediated site-directed mutagenesis, and the enzymatic activity of recombinant GST tagged proteins was tested against the Ub-AMC substrate (Fig. 4). Two putative C-boxes were predicted in the BSLF1 and BXLF1 ORFs, while a single domain containing two Cys residues was predicted in BPLF1. Alignment of the corresponding sequences in other members of the HHV family revealed that, while BPLF1 Cys61 and BSLF1 Cys819 and Cys824 are conserved in all HHVs, other potentially catalytic Cys residues identified by the bioinformatics search are unique for EBV or shared only by some of the family members. Mutation of the conserved C61 of BPLF1 to Ala abolished the enzymatic activity, while the C65A mutation had no effect, confirming that C61 is the catalytic residue in the C-box (Fig. 4). Single mutation of the nonconserved C462 and conserved C824 of BSLF1 did not affect the enzymatic activity, while the activity of the C819A mutant was significantly reduced. Interestingly, the hydrolysis of Ub-AMC was further decreased in the double mutant C819/824A, suggesting that C824 may partly substitute for the catalytic C819 residue. Homologs of BXLF1 were present only in alpha- and gammaherpesviruses, and the putative catalytic cysteine C491 is conserved only in gammaherpesvirus. Mutation of this residue abolished the enzymatic activity of BXLF1, while mutation of the nonconserved C84 had no effect (Fig. 4). Thus, catalytic Cys residues were iden-

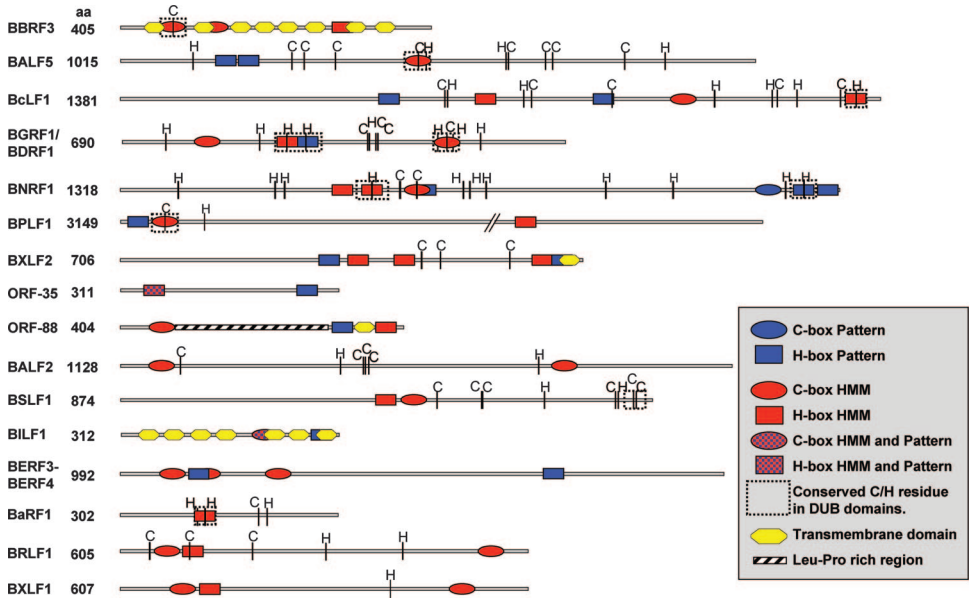

FIG. 2. Mapping of the putative C- and H-box domains in ORFs with high DUB scores. The positions of the putative C- and H boxes identified by the different searches and the Cys and His residues that are conserved in homologues encoded by other HHV family members are indicated. Putative transmembrane domains were identified by a TMHMM search in the candidate ORFs and are indicated as yellow hexagonal regions. In BBFR3, BILF1, and ORF88 the C- and/or B-boxes overlap with or flank transmembrane domains.

tified by mutation analysis in BPLF1, BSLF1, and BXLF1, confirming that the three EBV ORFs are bona fide viral DUBs.

To finally validate our bioinformatics approach, the scoring strategy used to identify BPLF1, BSLF1, and BXLF1 was applied to their homologues encoded by other human herpesviruses. All homologs of BPLF1 and BSLF1 received scores of ≥4, and several scored even higher than the EBV-encoded protein (Table 4). This is in line with the reported DUB activity of several BPLF1 homologues. In agreement with the very low sequence similarity of the BXLF1 homologues expressed in alpha- and gammaherpesvirus these ORFs received very low DUB scores, suggesting that this protein may have different functions in different viruses.

DISCUSSION

In this study we used a bioinformatics approach to identify distant functional homologues of human ubiquitin deconjugases encoded in the EBV genome. This task is complicated by the great genetic variability of viruses, which results in poor sequence conservation even between homologous proteins expressed by different members of the same virus family. Indeed, currently used bioinformatics tools, such as BLAST searches

TABLE 3. ORF annotation and filtering criteria

EBV ORF	DUB score[a]	EBV protein	Homologue			Expression in virus cycle	Location	Function[b]	Filter
			HSV	CMV	KSHV				
BBRF3	9	Glycoprotein M	gM	gM	gM	Late	Envelope	M	(–)
BcLF1	7	Major capsid protein	UL19	UL86	ORF25	Late	Capsid	C	–
BALF5	7	DNA pol catalytic subunit	UL30	UL54	ORF9	Early	Nucleus	R	
BGRF1/BDRF1	7	DNA packaging, Terminase	UL15	UL89	ORF29	Late	Nucleus	P	
BNRF1	6	Major tegument protein			ORF75	Late	Tegument	T	
BPLF1	6	Large tegument protein	UL36	UL48	ORF64	Late	Tegument	T	
BXLF2	5	gp85, gH homologue	UL22	UL75	ORF22	Late	Envelope	M	(–)
ORF35	5	Hypothetical							
ORF88	5	Hypothetical							–
BALF2	5	ssDNA binding protein	UL29	UL57	ORF6	Early	Nucleus	R	
BSLF1	5	Helicase/primase complex	UL52	UL70	ORF56	Early	Nucleus	R	
BILF1	4	gp64, constitutive GPCR				Early	Membrane	M	(–)
BERF3-BERF4	4	EBNA3C				Latent	Nucleus	L	
BaRF1	4	RNase reductase	UL40		ORF60	Early	Nucleus	N	
BRLF1	4	Rta, transactivator			ORF50	I-Early	Nucleus	S	
BXLF1	4	Thymidine kinase	UL23		ORF21	Early	Nucleus	N	

[a] For the details on the scoring, see Table S4 in the supplemental material.
[b] Classification of protein based on function: C, capsid; M, membrane protein; N, nucleotide metabolism; L, latency; P, packaging; R, replication; S, signaling, transactivator, transcription factor; T, tegument.

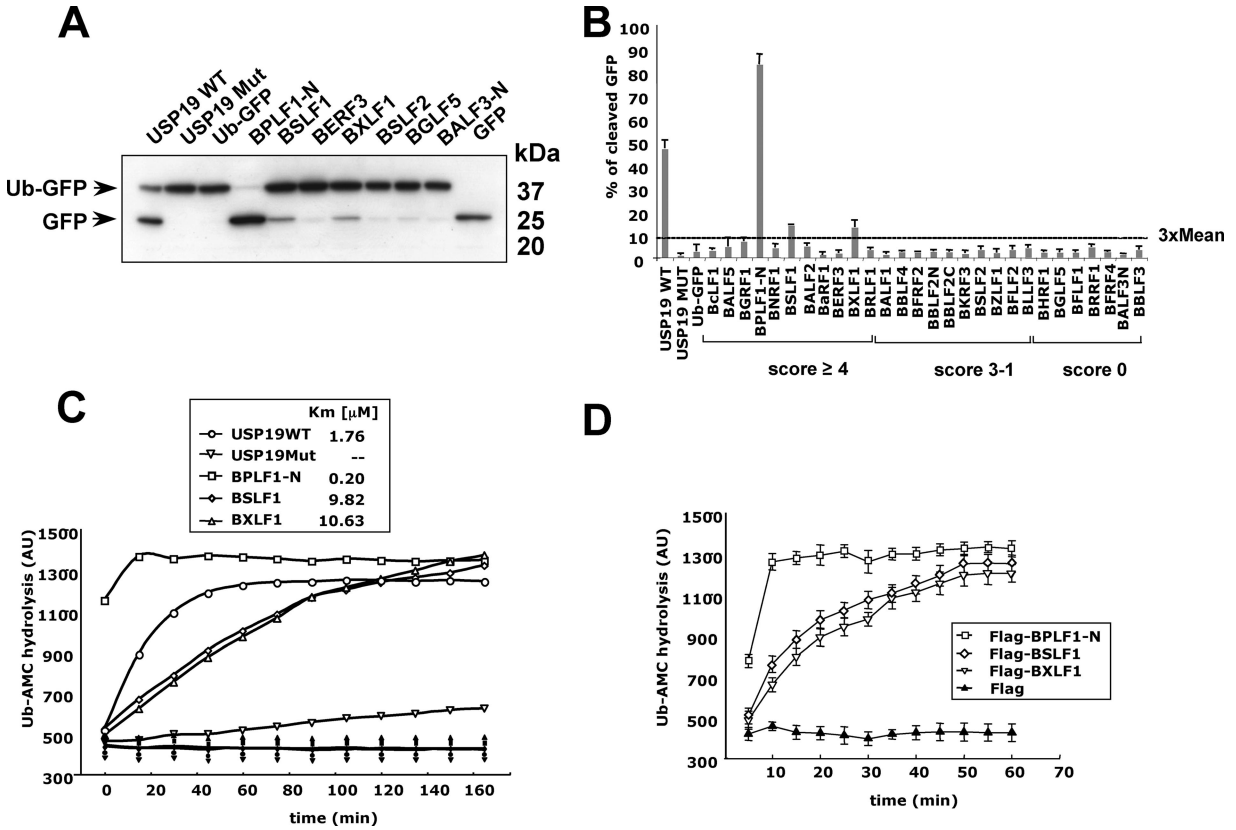

FIG. 3. Functional validation of the candidate DUBs. (A) Representative Western blot illustrating cleavage of the Ub-GFP reporter by a restricted panel of EBV ORFs. BL21 cells were cotransfected with Ub-GFP, and the indicated ORF and protein expression was induced by treatment with IPTG. Cell lysates were fractionated on 4 to 12% sodium dodecyl sulfate-polyacrylamide gel electrophoresis gradient gels, and GFP was detected by Western blotting. Cleavage of the reporter in lysates expressing active DUBs is visualized by appearance of a free GFP band. (B) Enzymatic activity of candidate EBV DUBs (score ≥ 4) and controls (score ≤ 3). The intensity of the bands corresponding to the uncleaved reporter and free GFP was determined by densitometry, and the percent specific cleavage was calculated as follows: intensity of the free GFP band – background/total GFP (uncleaved + cleaved) – background $\times$ 100. A cutoff activity value was calculated as 3 $\times$ the mean percent specific cleavage in cells expressing ORFs with a score of ≤ 3. The mean of three experiments in which all of the ORFs were tested in parallel is shown in the figure. (C) Time course of Ub-AMC hydrolysis. Ub-AMC (1.2 μM) was mixed with 200 nM concentrations of purified GST-USP19wt, GST-USP19mut, GST-BPLF1-N, GST-BSLF1, and GST-BXLF1 in the absence (empty symbols) or presence (filled symbols) of NEM, and the reactions were monitored for 180 min. The release of fluorescent AMC, expressed in arbitrary units (AU), shows the activity of these enzymes to cleave Ub-AMC. The K_m of the reactions was calculated in separate experiments and is indicated in the Figure. (D) Time course of Ub-AMC hydrolysis of BPLF1, BSLF1, and BXLF1 expressed in mammalian cells. The ORFs were cloned in frame in the 3XFlag tag vector and expressed in HEK293 cells. The proteins were immunoprecipitated from the transfected cells using antibodies to the Flag tag, and the cleavage of Ub-AMC was assayed as described for panel C. Equal amounts of proteins were used in all enzymatic assays. The faster kinetics of Ub-AMC cleavage (compare panels C and D) indicates that the enzymatic activity of mammalian expressed BSLF1 and BXLF1 is significantly improved compared to the proteins expressed in bacteria.

or more sophisticated threading programs that use sequence alignment and protein fold recognition algorithms, fail to detect homologies between known viral and cellular DUBs, suggesting that the structural properties of the viral proteases are clearly distinct. This was recently confirmed by the crystal structure of a DUB encoded by the murine gammaherpesvirus M48 that, based on the arrangement of the active-site residues and the architecture of the ubiquitin interacting interface, was classified as the first member of a new class of DUBs (43).

We reasoned that, in spite of strongly divergent sequences, a higher degree of conservation might be expected in regions that are important for enzymatic activity. Thus, although the homology between the catalytically relevant regions of viral and cellular enzymes falls below the statistically significant cutoffs used in conventional searches, distant homologues may be identified using less-stringent search criteria. The human genome encodes for approximately 95 DUBs subdivided in five families (38). Although the sequences of individual DUBs vary widely, the members of each family share a high degree of homology in regions surrounding conserved Cys and His residues that form the catalytic core of the enzymes. We therefore focused on the identification of EBV ORFs containing a region of homology with the C- and H-boxes of each DUB family and scored the candidates based on the degree of homology with the consensus sequences and on the presence of only one or both types of consensus domains. Four different strategies based on sequence alignment, pattern search, HMM motifs, and detection of conserved Cys and His residues in the context of HMM motifs were used to search for putative C- and H-boxes. The use of multiple searches provides a distinct advan-

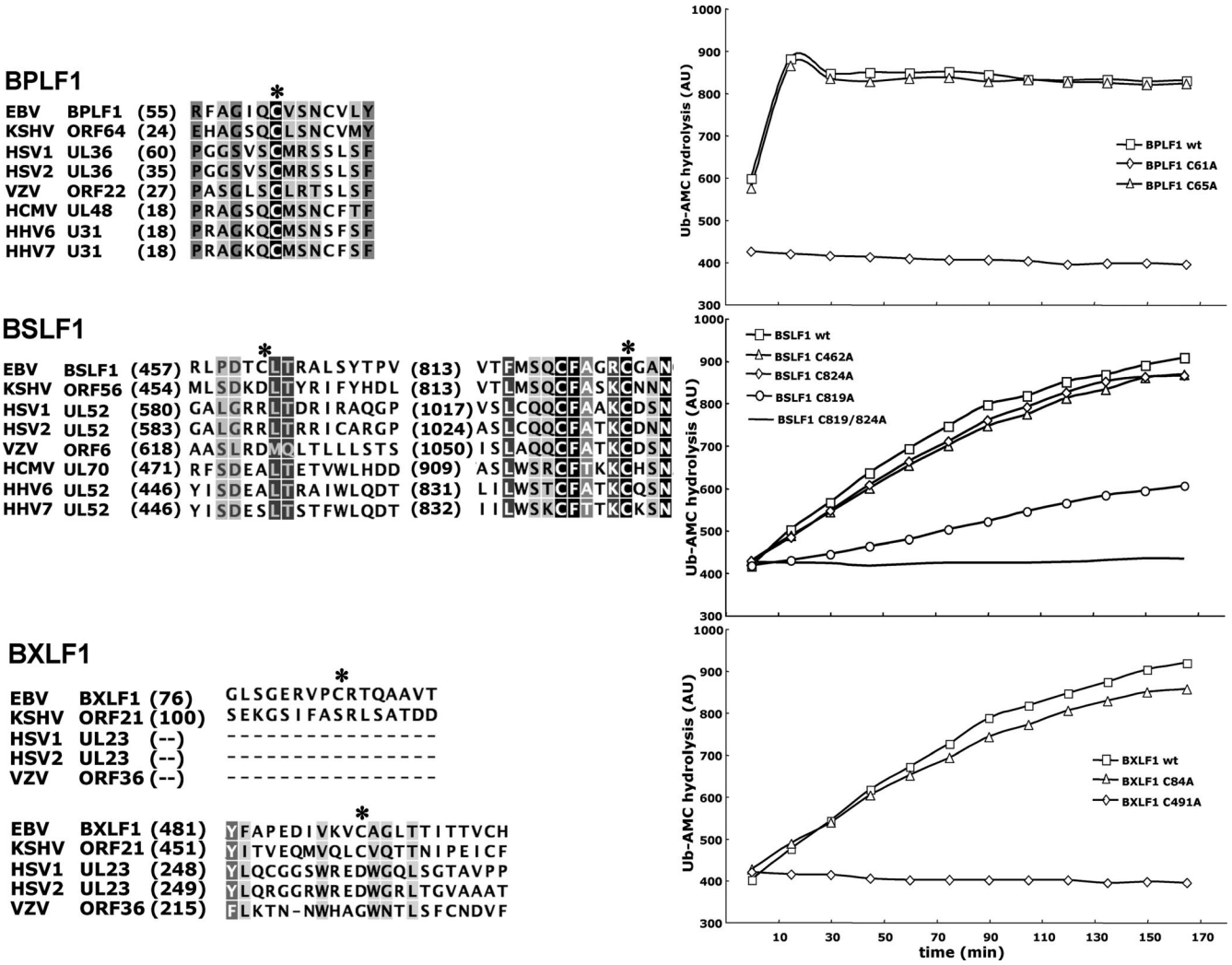

FIG. 4. Identification of the catalytic Cys residues by site-directed mutagenesis. Sequence alignments of the putative catalytic C-boxes in BPLF1, BSLF1, and BXLF1 and their homologs encoded by other HHV members shows conservation of Cys residues that are involved in DUB activity. The conserved residues are shown in white text with a black background, while similar residues in the alignment are shaded in gray. The asterisk above the alignment indicates the Cys residues identified in the bioinformatics search. Mutations were introduced into the predicted catalytic Cys residues, and the ability of the mutants to hydrolyze Ub-AMC was assayed as described in the legend to Fig. 3.

tage since each search is biased by different criteria. Thus, while sequence alignment scores for the presence of a continuous sequence of homologous residues, the pattern search restricts the hits to sequences that share similar residues at critical positions in the motif and HMM gives a global score based on the likelihood that a given residue will be found in each position of the motif. A further refinement of the HMM search was based on the assumption that functionally relevant proteins will be conserved among members of a virus family, and therefore conserved Cys and His residues will be found in the putative catalytic domains. By assigning individual scores to each of these searches and then combining the scores into a global DUB score, we have identified 16 candidates with DUB scores of $\geq$4 out of 106 annotated or predicted ORF in the EBV genome. Five of the candidates were excluded from further analysis because the putative catalytic domains are located within or at the opposite sides for transmembrane domains or because they are either known structural components of the virus capsid or envelope glycoproteins and are therefore unlikely to possess DUB activity.

A previously identified viral DUB encoded by the BPLF1 ORF was found among the high score candidates. BPLF1 is the EBV homologue of UL36, a presumably multifunctional protein of the alphaherpesvirus HSV-1. DUB activity was previously mapped to the N-terminal portion of UL36 by using a functional proteomic approach based on labeling of total cell extracts with and epitope-tagged, Ub-based suicide substrates followed by immunoprecipitation, and identification of the labeled enzyme by mass spectrometry (23). Using a reporter substrate that carries ubiquitin fused to GFP in a conformation that mimics the ubiquitin precursors and, to some extent, a true ubiquitinated substrate, we have now confirmed that the N terminus of BPLF1 is a very potent ubiquitin deconjugase. Interestingly, two additional ORFs in the high-score group, BSLF1 and BXLF1, were also capable of cleaving Ub-GFP at levels significantly above background. The enzymatic activity of

TABLE 4. DUB scores for the herpesvirus homologs of the identified EBV DUBs

ORF	Virus	Search score				Global DUB score[a]
		BLAST	Pattern	HMM	Conserved	
		1	1	2	2	6
ORF64	KSHV	1	1	2	2	6
UL36	HSV-1	2	1	2	2	7
UL36	HSV-2			2	2	4
ORF22	VZV		1	2	2	5
UL48	CMV	3	2	3	3	11
U31	HHV-6	2	1	2	2	7
U31	HHV-7		1	2	2	5
BSLF1	EBV	2		2	1	5
ORF56	KSHV	2	1	1	1	5
UL52	HSV-1	1	1	2	2	6
UL52	HSV-2	1		2	1	4
ORF6	VZV		1	2	2	5
UL70	CMV	2	1	2	2	7
UL52	HHV-6	3		2	1	6
UL52	HHV-7	2	1	2	1	6
BXLF1	EBV	2		2		4
ORF21	KSHV		1			1
UL23	HSV-1					-
UL23	HSV-2		1			1
ORF36	VZV				1	1

[a] For the details on the scoring, see Table S4 in the supplemental material.

the new putative DUBs was in both cases confirmed by the capacity of the purified GST fusion proteins to cleave the fluorogenic substrate Ub-AMC. Furthermore, the catalytic Cys residues were identified in both proteins by mutation analysis, confirming that these EBV ORFs are bona fide DUBs. It is noteworthy that bacterially expressed full-length BSLF1 and BXLF1 exhibited a poor enzymatic activity compared to both the N-terminal portion of BPLF1 and the human DUB USP19 that was included as control. Comparison of the enzymatic activity of purified proteins expressed in mammalian cells suggests that this may be due to the requirement for posttranslational modifications that are not achieved in bacteria. Indeed, only the N terminus of UL36 was identified in the functional screen performed in HSV-1-infected cells, suggesting that the protein may be processed during infection.

The new viral DUBs identified in the present study are expressed in the nucleus of EBV-infected cells during the early phases of the productive virus cycle and, based on their annotated functions, are involved in DNA replication and nucleotide metabolism. It is noteworthy that the efficiency and fidelity of DNA replication is regulated by posttranslational modification of several components of the replication complex, including for example, monoubiquitination, polyubiquitination, and sumoylation of PCNA (36). The BSLF1 gene product shares 23% sequence identity with HSV UL52, the primase component of the trimolecular helicase-primase complex was shown to be essential to HSV replication (12, 13). In EBV the complex is made up of BSLF1, BBLF4 (UL5 homolog), and BBLF2/3 (UL8 homolog) (51), but its activity in viral replication has not been directly confirmed. Similar to UL52, BSLF1 contain several conserved amino acid domains, such as the DxD motif (aa 481 to 498) and a putative zinc finger (Znf; aa 782 to 829) motif at the C-terminal end of protein that are also found in prokaryotic and eukaryotic primases (7, 15, 24). Mutational analysis of the Znf of HSV UL52 showed that this region is required for the virus replication (7, 8, 10). The Znf of BSLF1 partially overlaps with the predicted catalytic C-box.

BXLF1 gene encodes a protein of 607 aa that was annotated as the EBV thymidine kinase (TK) gene due to its capacity to complement TK-negative strains of *E. coli* (30) and partial sequence homology with regions of HSV-1 TK (19). We found that the regions that identify BXLF1 as a putative DUB and the catalytic Cys residue are not conserved in other herpesvirus homologues. Moreover, in contrast to other family members, BXLF1 was shown to localize to the centrosomes, where it encircles the tubulin-rich centrioles in a microtubule-independent manner (20). It remains to be seen whether this atypical localization may reflect a dual enzymatic activity that is not present in the homologues.

In conclusion, we have shown that it is possible to use bioinformatics tools to identify distant homologues of DUBs encoded by viruses. Our strategy of choosing candidates based on a global DUB score obtained by combining the results of multiple low stringency searches identified 16 high scoring ORFs in a database of 106 putative or confirmed EBV ORFs. Enzymatic activity was confirmed for 3 of 11 ORFs tested, whereas ORFs with low score and ORFs lacking putative C- or H-boxes were uniformly negative. Thanks to its relatively good predictive capacity, our approach could provide a valuable complement to the functional screening described by Kattenhorn et al. (23), which, due to the requirement for validation by mass spectroscopy, is strongly biased toward enzymes that are overexpressed in the infected cells. Further studies will be required to assess how the DUB activity of BPLF1, BSLF1, and BXL1 contributes to their role in virus replication and to the remodeling of the cellular environment during productive EBV infection.

ACKNOWLEDGMENTS

We thank Joel Hedlund for help with the sequence clustering procedure.

This study was supported by grants from the Swedish Cancer Society, the Swedish Medical Research Council, and the Karolinska Institutet, Stockholm, Sweden (to M.G.M. and K.L.); by the Carl Trygger Foundation and Linköping University (to B.P.); by Bayerisches Genomeforschungsnetzwork and MRC G0501453 (to J.H.); and by the European Community Integrated Project on Infection and Cancer, project LSHC-CT-2005-018704 (to M.G.M.).

REFERENCES

1. **Altschul, S. F., W. Gish, W. Miller, E. W. Myers, and D. J. Lipman.** 1990. Basic local alignment search tool. J. Mol. Biol. **215:**403–410.
2. **Amerik, A. Y., and M. Hochstrasser.** 2004. Mechanism and function of deubiquitinating enzymes. Biochim. Biophys. Acta **1695:**189–207.
3. **Baer, R., A. T. Bankier, M. D. Biggin, P. L. Deininger, P. J. Farrell, T. J. Gibson, G. Hatfull, G. S. Hudson, S. C. Satchwell, C. Seguin, et al.** 1984. DNA sequence and expression of the B95-8 Epstein-Barr virus genome. Nature **310:**207–211.
4. **Bairoch, A., R. Apweiler, C. H. Wu, W. C. Barker, B. Boeckmann, S. Ferro, E. Gasteiger, H. Huang, R. Lopez, M. Magrane, M. J. Martin, D. A. Natale, C. O'Donovan, N. Redaschi, and L. S. Yeh.** 2005. The universal protein resource (UniProt). Nucleic Acids Res. **33:**D154–D159.
5. **Balakirev, M. Y., M. Jaquinod, A. L. Haas, and J. Chroboczek.** 2002. Deubiquitinating function of adenovirus proteinase. J. Virol. **76:**6323–6331.
6. **Barretto, N., D. Jukneliene, K. Ratia, Z. Chen, A. D. Mesecar, and S. C. Baker.** 2005. The papain-like protease of severe acute respiratory syndrome coronavirus has deubiquitinating activity. J. Virol. **79:**15189–15198.
7. **Biswas, N., and S. K. Weller.** 1999. A mutation in the C-terminal putative Zn^{2+} finger motif of UL52 severely affects the biochemical activities of the HSV-1 helicase-primase subcomplex. J. Biol. Chem. **274:**8068–8076.

8. **Carrington-Lawrence, S. D., and S. K. Weller.** 2003. Recruitment of polymerase to herpes simplex virus type 1 replication foci in cells expressing mutant primase (UL52) proteins. J. Virol. **77:**4237–4247.
9. **Catic, A., S. Misaghi, G. A. Korbel, and H. L. Ploegh.** 2007. ElaD, a deubiquitinating protease expressed by *Escherichia coli*. PLoS ONE **2:**e381.
10. **Chen, Y., S. D. Carrington-Lawrence, P. Bai, and S. K. Weller.** 2005. Mutations in the putative zinc-binding motif of UL52 demonstrate a complex interdependence between the UL5 and UL52 subunits of the human herpes simplex virus type 1 helicase/primase complex. J. Virol. **79:**9088–9096.
11. **Ciechanover, A., A. Orian, and A. L. Schwartz.** 2000. Ubiquitin-mediated proteolysis: biological regulation via destruction. Bioessays **22:**442–451.
12. **Crute, J. J., and I. R. Lehman.** 1991. Herpes simplex virus-1 helicase-primase: physical and catalytic properties. J. Biol. Chem. **266:**4484–4488.
13. **Crute, J. J., T. Tsurumi, L. A. Zhu, S. K. Weller, P. D. Olivo, M. D. Challberg, E. S. Mocarski, and I. R. Lehman.** 1989. Herpes simplex virus 1 helicase-primase: a complex of three herpes-encoded gene products. Proc. Natl. Acad. Sci. USA **86:**2186–2189.
14. **D'Andrea, A., and D. Pellman.** 1998. Deubiquitinating enzymes: a new class of biological regulators. Crit. Rev. Biochem. Mol. Biol. **33:**337–352.
15. **Dracheva, S., E. V. Koonin, and J. J. Crute.** 1995. Identification of the primase active site of the herpes simplex virus type 1 helicase-primase. J. Biol. Chem. **270:**14148–14153.
16. **Drake, J. W.** 2006. Chaos and order in spontaneous mutation. Genetics **173:**1–8.
17. **Eddy, S. R.** 1998. Profile hidden Markov models. Bioinformatics **14:**755–763.
18. **Frias-Staheli, N., N. V. Giannakopoulos, M. Kikkert, S. L. Taylor, A. Bridgen, J. Paragas, J. A. Richt, R. R. Rowland, C. S. Schmaljohn, D. J. Lenschow, E. J. Snijder, A. Garcia-Sastre, and H. W. ten Virgin.** 2007. Ovarian tumor domain-containing viral proteases evade ubiquitin- and ISG15-dependent innate immune responses. Cell Host Microbe **2:**404–416.
19. **Gardberg, A., L. Shuvalova, C. Monnerjahn, M. Konrad, and A. Lavie.** 2003. Structural basis for the dual thymidine and thymidylate kinase activity of herpes thymidine kinases. Structure **11:**1265–1277.
20. **Gill, M. B., J. L. Kutok, and J. D. Fingeroth.** 2007. Epstein-Barr virus thymidine kinase is a centrosomal resident precisely localized to the periphery of centrioles. J. Virol. **81:**6523–6535.
21. **Hershko, A., and A. Ciechanover.** 1998. The ubiquitin system. Annu. Rev. Biochem. **67:**425–479.
22. **Hewitt, E. W., L. Duncan, D. Mufti, J. Baker, P. G. Stevenson, and P. J. Lehner.** 2002. Ubiquitylation of MHC class I by the K3 viral protein signals internalization and TSG101-dependent degradation. EMBO J. **21:**2418–2429.
23. **Kattenhorn, L. M., G. A. Korbel, B. M. Kessler, E. Spooner, and H. L. Ploegh.** 2005. A deubiquitinating enzyme encoded by HSV-1 belongs to a family of cysteine proteases that is conserved across the family *Herpesviridae*. Mol. Cell **19:**547–557.
24. **Klinedinst, D. K., and M. D. Challberg.** 1994. Helicase-primase complex of herpes simplex virus type 1: a mutation in the UL52 subunit abolishes primase activity. J. Virol. **68:**3693–3701.
25. **Kovalenko, A., C. Chable-Bessia, G. Cantarella, A. Israel, D. Wallach, and G. Courtois.** 2003. The tumour suppressor CYLD negatively regulates NF-κB signalling by deubiquitination. Nature **424:**801–805.
26. **Larsen, C. N., J. S. Price, and K. D. Wilkinson.** 1996. Substrate binding and catalysis by ubiquitin C-terminal hydrolases: identification of two active site residues. Biochemistry **35:**6735–6744.
27. **Lee, J. C., and M. E. Peter.** 2003. Regulation of apoptosis by ubiquitination. Immunol. Rev. **193:**39–47.
28. **Lehner, P. J., S. Hoer, R. Dodd, and L. M. Duncan.** 2005. Downregulation of cell surface receptors by the K3 family of viral and cellular ubiquitin E3 ligases. Immunol. Rev. **207:**112–125.
29. **Lindner, H. A., N. Fotouhi-Ardakani, V. Lytvyn, P. Lachance, T. Sulea, and R. Menard.** 2005. The papain-like protease from the severe acute respiratory syndrome coronavirus is a deubiquitinating enzyme. J. Virol. **79:**15199–15208.
30. **Littler, E., J. Zeuthen, A. A. McBride, E. Trost Sorensen, K. L. Powell, J. E. Walsh-Arrand, and J. R. Arrand.** 1986. Identification of an Epstein-Barr virus-coded thymidine kinase. EMBO J. **5:**1959–1966.
31. **Loureiro, J., and H. L. Ploegh.** 2006. Antigen presentation and the ubiquitin-proteasome system in host-pathogen interactions. Adv. Immunol. **92:**225–305.
32. **Lu, G., and E. N. Moriyama.** 2004. Vector NTI, a balanced all-in-one sequence analysis suite. Brief Bioinform. **5:**378–388.
33. **Lynch, O. T., and M. Gadina.** 2004. Ubiquitination for activation: new directions in the NF-κB roadmap. Mol. Interv. **4:**144–146.
34. **Masucci, M. G.** 2004. Epstein-Barr virus oncogenesis and the ubiquitin-proteasome system. Oncogene **23:**2107–2115.
35. **Menard, R., H. E. Khouri, C. Plouffe, R. Dupras, D. Ripoll, T. Vernet, D. C. Tessier, F. Laliberte, D. Y. Thomas, and A. C. Storer.** 1990. A protein engineering study of the role of aspartate 158 in the catalytic mechanism of papain. Biochemistry **29:**6706–6713.
36. **Moldovan, G. L., B. Pfander, and S. Jentsch.** 2007. PCNA, the maestro of the replication fork. Cell **129:**665–679.
37. **Nijman, S. M., T. T. Huang, A. M. Dirac, T. R. Brummelkamp, R. M. Kerkhoven, A. D. D'Andrea, and R. Bernards.** 2005. The deubiquitinating enzyme USP1 regulates the Fanconi anemia pathway. Mol. Cell **17:**331–339.
38. **Nijman, S. M., M. P. Luna-Vargas, A. Velds, T. R. Brummelkamp, A. M. Dirac, T. K. Sixma, and R. Bernards.** 2005. A genomic and functional inventory of deubiquitinating enzymes. Cell **123:**773–786.
39. **Rice, P., I. Longden, and A. Bleasby.** 2000. EMBOSS: the European molecular biology open software suite. Trends Genet. **16:**276–277.
40. **Rytkonen, A., J. Poh, J. Garmendia, C. Boyle, A. Thompson, M. Liu, P. Freemont, J. C. Hinton, and D. W. Holden.** 2007. SseL, a *Salmonella* deubiquitinase required for macrophage killing and virulence. Proc. Natl. Acad. Sci. USA **104:**3502–3507.
41. **Scheffner, M., B. A. Werness, J. M. Huibregtse, A. J. Levine, and P. M. Howley.** 1990. The E6 oncoprotein encoded by human papillomavirus types 16 and 18 promotes the degradation of p53. Cell **63:**1129–1136.
42. **Schlieker, C., G. A. Korbel, L. M. Kattenhorn, and H. L. Ploegh.** 2005. A deubiquitinating activity is conserved in the large tegument protein of the herpesviridae. J. Virol. **79:**15582–15585.
43. **Schlieker, C., W. A. Weihofen, E. Frijns, L. M. Kattenhorn, R. Gaudet, and H. L. Ploegh.** 2007. Structure of a herpesvirus-encoded cysteine protease reveals a unique class of deubiquitinating enzymes. Mol. Cell **25:**677–687.
44. **Schwartz, A. L., and A. Ciechanover.** 1999. The ubiquitin-proteasome pathway and pathogenesis of human diseases. Annu. Rev. Med. **50:**57–74.
45. **Shackelford, J., and J. S. Pagano.** 2004. Tumor viruses and cell signaling pathways: deubiquitination versus ubiquitination. Mol. Cell. Biol. **24:**5089–5093.
46. **Sun, L., and Z. J. Chen.** 2004. The novel functions of ubiquitination in signaling. Curr. Opin. Cell Biol. **16:**119–126.
47. **Thompson, J. D., D. G. Higgins, and T. J. Gibson.** 1994. CLUSTAL W: improving the sensitivity of progressive multiple sequence alignment through sequence weighting, position-specific gap penalties and weight matrix choice. Nucleic Acids Res. **22:**4673–4680.
48. **Uetz, P., Y. A. Dong, C. Zeretzke, C. Atzler, A. Baiker, B. Berger, S. V. Rajagopala, M. Roupelieva, D. Rose, E. Fossum, and J. Haas.** 2006. Herpesviral protein networks and their interaction with the human proteome. Science **311:**239–242.
49. **Verma, R., L. Aravind, R. Oania, W. H. McDonald, J. R. Yates III, E. V. Koonin, and R. J. Deshaies.** 2002. Role of Rpn11 metalloprotease in deubiquitination and degradation by the 26S proteasome. Science **298:**611–615.
50. **Wing, S. S.** 2003. Deubiquitinating enzymes: the importance of driving in reverse along the ubiquitin-proteasome pathway. Int. J. Biochem. Cell. Biol. **35:**590–605.
51. **Yokoyama, N., K. Fujii, M. Hirata, K. Tamai, T. Kiyono, K. Kuzushima, Y. Nishiyama, M. Fujita, and T. Tsurumi.** 1999. Assembly of the Epstein-Barr virus BBLF4, BSLF1 and BBLF2/3 proteins and their interactive properties. J. Gen. Virol. **80**(Pt. 11)**:**2879–2887.
52. **Zhou, H., D. M. Monack, N. Kayagaki, I. Wertz, J. Yin, B. Wolf, and V. M. Dixit.** 2005. *Yersinia* virulence factor YopJ acts as a deubiquitinase to inhibit NF-κB activation. J. Exp. Med. **202:**1327–1332.

II

nature cell biology

A deneddylase encoded by Epstein–Barr virus promotes viral DNA replication by regulating the activity of cullin-RING ligases

Stefano Gastaldello[1], Sebastian Hildebrand[1], Omid Faridani[1], Simone Callegari[1], Mia Palmkvist[1], Claudia Di Guglielmo[1] and Maria G. Masucci[1,2]

The large tegument proteins of herpesviruses encode conserved cysteine proteases of unknown function. Here we show that BPLF1, the Epstein–Barr-virus-encoded member of this protease family, is a deneddylase that regulates virus production by modulating the activity of cullin-RING ligases (CRLs). BPLF1 hydrolyses NEDD8 conjugates *in vitro*, acts as a deneddylase *in vivo*, binds to cullins and stabilizes CRL substrates. Expression of BPLF1 alone or in the context of the productive virus cycle induces accumulation of the licensing factor CDT1 and deregulates S-phase DNA synthesis. Inhibition of BPLF1 during the productive virus cycle prevents cellular DNA re-replication and inhibits virus replication. Viral DNA synthesis is restored by overexpression of CDT1. Homologues encoded by other herpesviruses share the deneddylase activity. Thus, these enzymes are likely to have a key function in the virus life cycle by inducing a replication-permissive S-phase-like cellular environment.

Post-translational modification of proteins by ubiquitin regulates a multitude of cellular processes involving their turnover, activity, interactions and trafficking through cellular compartments[1]. Ubiquitin conjugation is mediated by a cysteine-based enzymatic cascade that comprises an ATP-dependent activating enzyme (E1), a conjugating enzyme (E2) and a substrate-specific ligase (E3) that transfers the modifier to the acceptor protein[2]. The modification is reversed by deconjugases that hydrolyse the covalent bond formed between the modifier and the substrate[3]. Since the discovery of the ubiquitin conjugation system, similar pathways for the conjugation of ubiquitin-like proteins (UbLs), including NEDD8, ISG15, SUMO-1, SUMO-2, SUMO-3 and others, have been identified[4]. Modification by UbLs does not usually result in protein degradation, although important crosstalks have been highlighted by the demonstration that NEDD8 (ref. 5) and SUMO[6,7] regulate the activity of certain E3s. Thus, the best-characterized substrates of NEDD8 conjugation are cullins that function as scaffolds for the assembly of cullin-RING ligases (CRLs)[8]. Neddylation is required for ligase activity and thereby controls the ubiquitylation and kinetics of degradation of CRL substrates[9].

Viruses exploit the ubiquitin and UbL signalling cascades in almost every step of their life cycle[10]. In addition, viruses manipulate innate and adaptive immune responses that are controlled by these modifications, including the production of interferons and immunoregulatory cytokines and the processing of viral proteins into antigenic peptides[11]. Interference strategies are epitomized by the capacity of viral proteins, such as the human papillomavirus E6, to bind cellular E3s and redirect their activity towards substrates whose destruction favours virus replication[12]. Deconjugases, such as the ubiquitin-specific protease USP7-HAUSP, are similarly targeted by herpes simplex virus (HSV) ICP0 (ref. 13) and Epstein–Barr virus (EBV) EBNA-1 (ref. 14) to alter the turnover of cellular regulators of DNA synthesis and apoptosis. Viruses also encode functional homologues of these enzymes that often share little homology with their cellular counterparts and are therefore attractive targets for selective inhibition[15].

EBV is a gammaherpesvirus that immortalizes B lymphocytes and is associated with human malignancies[16]. B-cell immortalization is caused by a latent infection in which viral proteins hijack signalling pathways controlling cell proliferation, differentiation and apoptosis[17]. While this phase of the virus life cycle is relatively well understood, much less is known about virus replication. Virus production is initiated by the immediate-early protein BZLF1, which transactivates viral and cellular promoters, leading to the sequential expression of genes involved in viral DNA synthesis, virus assembly and maturation[18]. In a similar manner to other herpesviruses, the productive cycle of EBV occurs in an S-phase-like cellular environment and activates ATM (ataxia telangiectasia mutated) and Chk2-dependent DNA damage responses[19]. BZLF1 induces this phenotype only in EBV-positive cells, suggesting that other viral proteins are involved.

With the use of a functional screen based on the co-expression of glutathione *S*-transferase (GST)-tagged EBV open reading frames (ORFs) with green fluorescent protein (GFP)-based ubiquitin and UbL reporters

[1]Department of Cell and Molecular Biology, Karolinska Institutet, Box 285, S-17177 Stockholm, Sweden.
[2]Correspondence should be addressed to M.G.M. (e-mail: maria.masucci@ki.se)

Received 7 October 2009; accepted 3 February 2010; published online 28 February 2010; DOI:10.1038/ncb2035

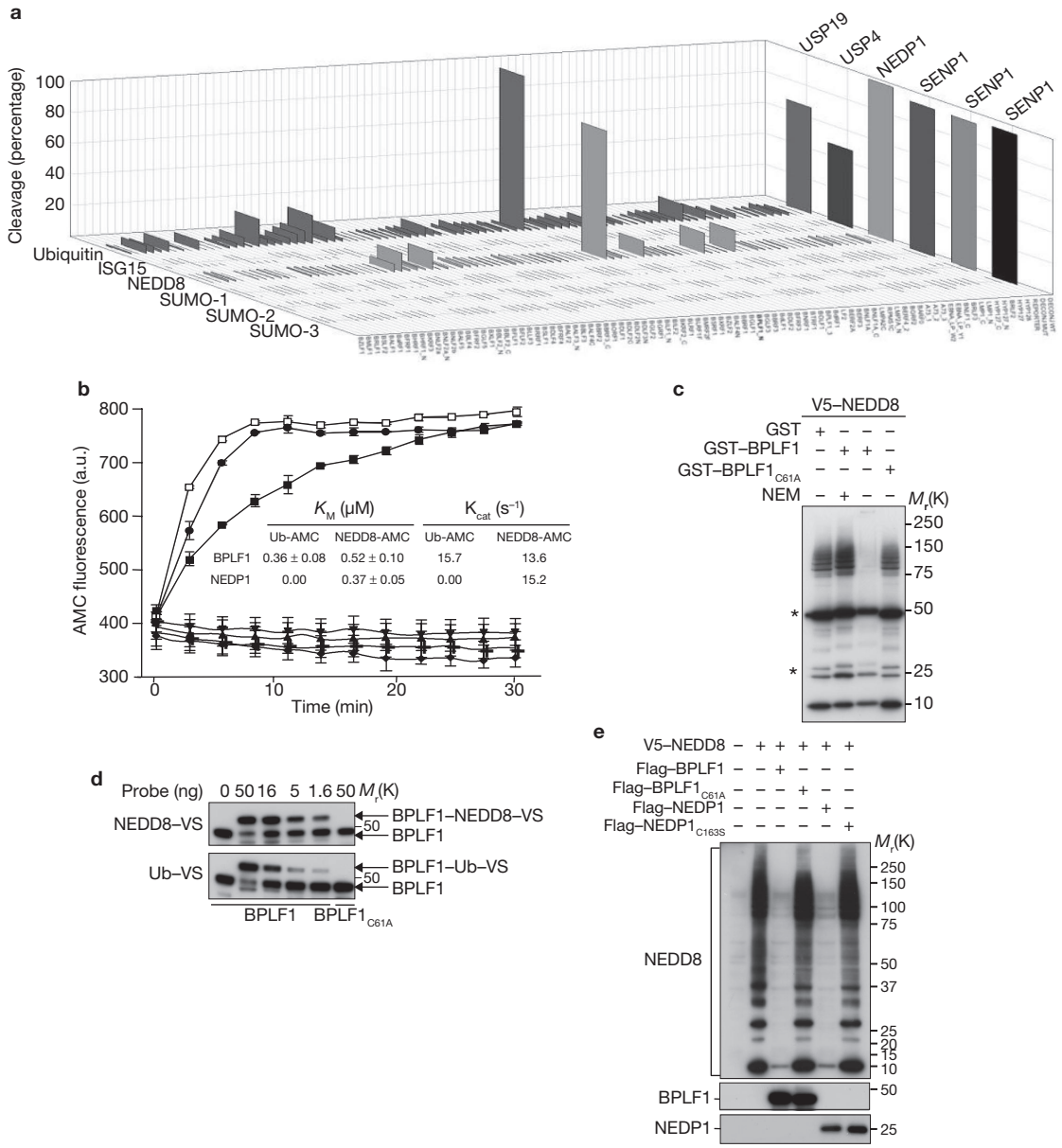

Figure 1 BPLF1 is a NEDD8-specific deconjugase. (**a**) Screen for EBV encoded ubiquitin-specific and UbL-specific deconjugases. A library of 88 EBV ORFs was tested for cleavage of ubiquitin–, ISG15–, NEDD8–, SUMO-1, SUMO-2, or SUMO-3–GFP–S-tag reporters in bacterial assays. Bacterial lysates containing equal GFP fluorescence units were fractionated by SDS–PAGE and western blots were probed with an S-tag-specific antibody. The percentage specific cleavage was calculated as 100 × (intensity of free GFP minus the background)/(total GFP intensity minus background). Specific deconjugases for ubiquitin = USP19, ISG15 = USP4, NEDD8 = NEDP1, SUMO-1, SUMO-2, SUMO-3 = SENP1 were used as positive controls. (**b**) BPLF1 cleaves ubiquitin-AMC (Ub-AMC) and NEDD8-AMC with equal efficiency. The indicated purified proteins (50 nM) were mixed with 1.2 μM ubiquitin-AMC (open symbols) or NEDD8-AMC (filled symbols). Where indicated, the enzymatic reaction was carried out in the presence of 10 mM NEM. The K_m and k_{cat} of the reactions were calculated in two independent experiments by titrating the fluorogenic substrates over a fixed amount of enzyme. Squares, BPLF1; down triangles, $BPLF1_{C61A}$; circles, NEDP1; diamonds, $NEDP1_{C163S}$; plus signs, BPLF1 + NEM; up triangles, NEDP1 + NEM. The mean ± s.d. of two experiments performed in triplicate are shown. (**c**) BPLF1 cleaves NEDD8 conjugates. V5–NEDD8 was expressed in HeLa cells, and conjugates were captured on anti-V5-conjugated Sepharose beads. Equal amounts of beads were mixed with 200 nM of purified GST, GST–BPLF1 or GST–$BPLF1_{C61A}$ and the reaction was run for 1 h at 37 °C. NEDD8 conjugates were detected in western blots probed with the anti-V5 antibody. Only the wild-type BPLF1 hydrolyses NEDD8 conjugates, and the reaction is inhibited by NEM. Immunoglobulin heavy and light chains are indicated by asterisks. (**d**) Eukaryotic expressed BPLF1 retains deneddylase activity. The activity of Flag–BPLF1 or Flag–$BPLF1_{C61A}$ expressed in HeLa cells was assessed by binding of the functional probes ubiquitin-VS and NEDD8-VS. Binding was visualized in western blots probed with the anti-Flag antibody as a band shift of about 10 kDa, corresponding to the size of the probe. (**e**) BPLF1 hydrolyses NEDD8 conjugates *in vivo*. V5–NEDD8 was co-transfected in HeLa cells together with Flag-tagged BPLF1, NEDP1 and the catalytic mutants $BPLF1_{C61A}$ and $NEDP1_{C163S}$. NEDD8 conjugates were detected in western blots with the anti-V5 antibody. BPLF1 and NEDP1 were detected with the anti-Flag antibody. One representative experiment of three is shown. Uncropped images of blots are shown in Supplementary Information, Fig. S6.

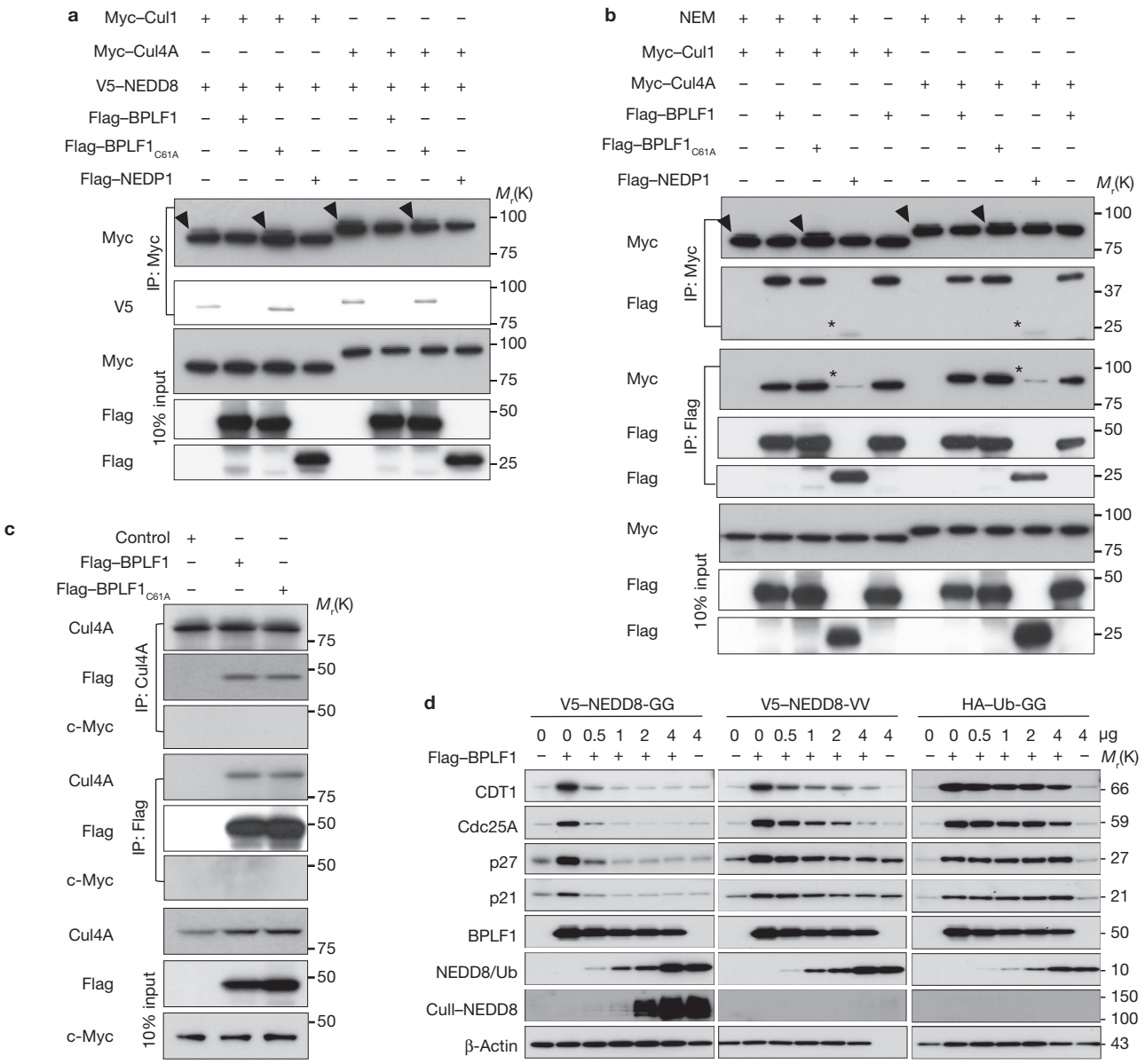

Figure 2 BPLF1 deneddylates cullins and induces the accumulation of CRL substrates. Myc-tagged Cul1 and Cul4A were co-expressed in HeLa cells together with Flag-tagged BPLF1, NEDP1 or BPLF1$_{C61A}$, and co-immunoprecipitations were performed with anti-Myc or anti-Flag antibodies. (**a**) BPLF1 induces cullin deneddylation. Neddylated cullins were detected in blots probed with an anti-Myc antibody as a minor slowly migrating species (upper panel, indicated by arrowheads), and the identity of the bands was confirmed by re-probing with an anti-V5 antibody (lower panel). IP, immunoprecipitation. (**b**) BPLF1 binds to cullins. Cell lysates of HeLa cells co-transfected with Myc-tagged Cul1 or Cul4A and Flag-tagged BPLF1, NEDP1 or BPLF1$_{C61A}$ were immunoprecipitated with anti-Myc (upper panels) or anti-Flag (lower panels) antibodies and western blots were sequentially probed with anti-Myc and anti-Flag antibodies. Both cullins were co-immunoprecipitated by the wild-type and mutant BPLF1, whereas only a weak interaction was detected with NEDP1 (indicated by asterisks). Omission of the cysteine protease inhibitor NEM from the lysis buffer (–) did not affect the efficiency of co-immunoprecipitation of cullin with BPLF1. (**c**) BPLF1 binds to endogenously expressed cullins. Cul4A and BPLF1 were immunoprecipitated from lysates of HeLa cells transfected with Flag alone, Flag–BPLF1 or Flag–BPLF1$_{C61A}$ using specific antibodies, and western blots were sequentially probed with antibodies against Cul4A, Flag and c-Myc. One representative experiment of three is shown. (**d**) Expression of the CRL substrates CDT1, Cdc25A, p27 and p21 was assayed in HeLa cells 48 h after transfection with BPLF1 or a control empty vector. The accumulation of CRL substrates in BPLF1-expressing cells was reversed in a dose-dependent manner by overexpression of NEDD8, whereas a mutant V5–NEDD8-VV, lacking the C-terminal Gly residue required for conjugation, and HA–ubiquitin had minor or no effects. One representative experiment of three is shown. Uncropped images of blots are shown in Supplementary Information, Fig. S6.

we have discovered that the conserved cysteine protease encoded in the amino terminus of major tegument protein BPLF1 is a deneddylase that binds to cullins and regulates the activity of CRLs, leading to deregulation of the cell cycle. Inhibition of BPLF1 during the productive cycle severely diminishes the yield of viral DNA.

RESULTS

The N terminus of BPLF1 encodes a NEDD8-specific deconjugase

In search for EBV-encoded ubiquitin or UbL deconjugases we used a bacterial assay[20] in which plasmids encoding GST-tagged EBV ORFs were co-expressed together with reporter plasmids encoding GFP fused

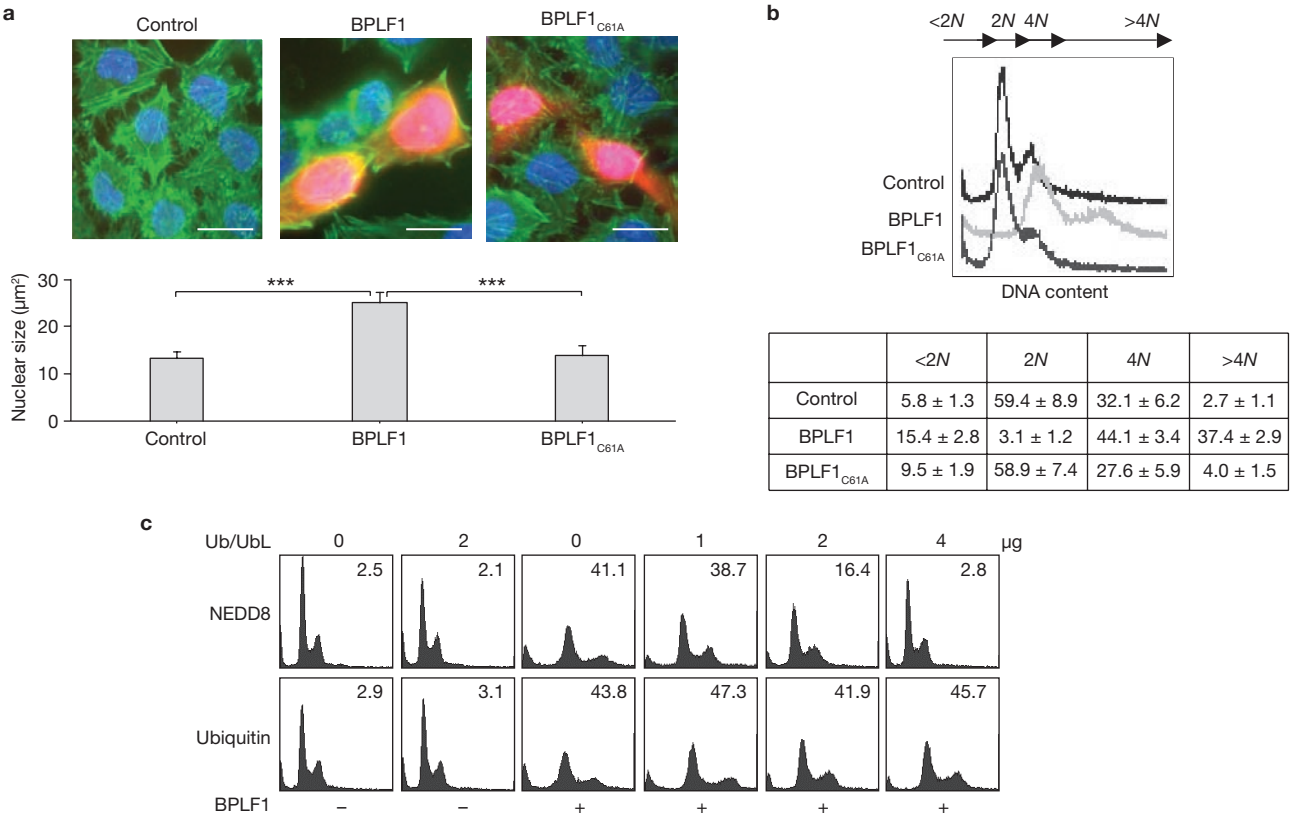

	<2N	2N	4N	>4N
Control	5.8 ± 1.3	59.4 ± 8.9	32.1 ± 6.2	2.7 ± 1.1
BPLF1	15.4 ± 2.8	3.1 ± 1.2	44.1 ± 3.4	37.4 ± 2.9
$BPLF1_{C61A}$	9.5 ± 1.9	58.9 ± 7.4	27.6 ± 5.9	4.0 ± 1.5

Figure 3 Expression of a catalytically active BPLF1 induces accumulation of cells with a DNA content of at least 4*N*. HeLa cells were transfected with Flag–BPLF1 and Flag–$BPLF1_{C61A}$, and subcellular localization and cell cycle profile were assayed after 48 h. (**a**) The subcellular localization of the BPLF1 was detected by immunofluorescence with an anti-Flag antibody (red signal), cytoskeletal actin was revealed by staining with fluorescein isothiocyanate (FITC)-labelled phalloidin (green signal), and cellular nuclei were stained with 4,6-diamidino-2-phenylindole (DAPI). Both the wild-type and catalytic mutant BPLF1 accumulate in the nucleus but only the catalytically active enzyme induces a significant increase in nuclear size. Scale bars, 5 μm. Nuclear size was measured with the ImageJ software in 30 randomly selected nuclei from each experimental condition. One representative experiment of three is shown. Three asterisks, $P = 0.002$. (**b**) The cell cycle profiles of mock-transfected cells (control) and of cells transfected with the wild-type and catalytic mutant BPLF1 were assessed by staining with PI 48 h after transfection. Expression of the catalytically active BPLF1 was accompanied by the accumulation of cells with a DNA content of at least 4*N*. The table shows the percentages of apoptotic cells (less than 2*N*) and cells in G1 (2*N*) and S-G2 (4*N*) and cell with more than 4*N* DNA content (means ± s.d.) in three independent experiments. (**c**) The re-replication phenotype induced by BPLF1 is counteracted in a dose-dependent manner by overexpression of NEDD8. HeLa cells were co-transfected with 2 μg of a plasmid expressing the catalytically active BPLF1 (+) and increasing amounts of plasmids expressing either V5–NEDD8 or HA–ubiquitin. The cell cycle profile was analysed by staining with PI 48 h after transfection. The percentage of cells with DNA content of more than 4*N* is indicated in each panel. Overexpression of NEDD8 or ubiquitin alone had no effect on the cell cycle profile. One representative experiment of three is shown.

to either ubiquitin, ISG15, NEDD8, SUMO-1, SUMO-2 or SUMO-3. Cleavage of the reporters was assessed in western blots by the appearance of free GFP (Supplementary Information, Fig. S1). Representative assays in which the ORF library was tested against each reporter alongside appropriate controls are shown in Fig. 1a. Ubiquitin–GFP and NEDD8–GFP were cleaved almost completely by a construct encoding the N-terminal 325 amino-acid residues of the major tegument protein BPLF1 (hereafter termed BPLF1). Additional ORFs showed inefficient cleavage of these reporters, and none cleaved the ISG15, SUMO-1, SUMO-2 and SUMO-3 reporters.

The N terminus of BPLF1 encodes the EBV homologue of a conserved herpesvirus cysteine protease[21]. Because other members of this family had been shown to act preferentially as ubiquitin-specific proteases, we first examined whether BPLF1 is a true deneddylase. The activity of purified GST–BPLF1 against the fluorogenic substrates ubiquitin-AMC (where AMC is 7-amino-4-methylcoumarin) and NEDD8-AMC was tested alongside a mutant in which the catalytic Cys 61 was replaced by Ala ($BPLF1_{C61A}$), the NEDD8-specific protease NEDP1 (ref. 22) and its catalytic mutant $NEDP1_{C163S}$. Ubiquitin-AMC and NEDD8-AMC were hydrolysed by BPLF1, whereas NEDP1 hydrolysed only NEDD8-AMC, as expected. BPLF1 and NEDP1 showed comparable K_m and k_{cat} values for NEDD8-AMC, suggesting similar affinities for the substrate (Fig. 1b). Hydrolysis was abrogated by the cysteine protease inhibitor *N*-ethylmaleimide (NEM) and by mutation of the catalytic cysteine. To test whether BPLF1 can hydrolyse true NEDD8 conjugates, a V5-tagged NEDD8 was expressed in HeLa cells and conjugates were captured on anti-V5-Sepharose beads. Equal amounts of beads were incubated with purified GST–BPLF1 in the presence or absence of NEM or, as controls, with purified GST and GST–$BPLF1_{C61A}$ (Fig. 1c). Only wild-type BPLF1 hydrolysed the NEDD8 conjugates as detected in western blots probed with the anti-V5 antibody. As expected, ubiquitin conjugates were also cleaved (Supplementary Information, Fig. S2).

Having confirmed the capacity of recombinant BPLF1 to act as a deneddylase *in vitro* we examined whether the activity is retained by

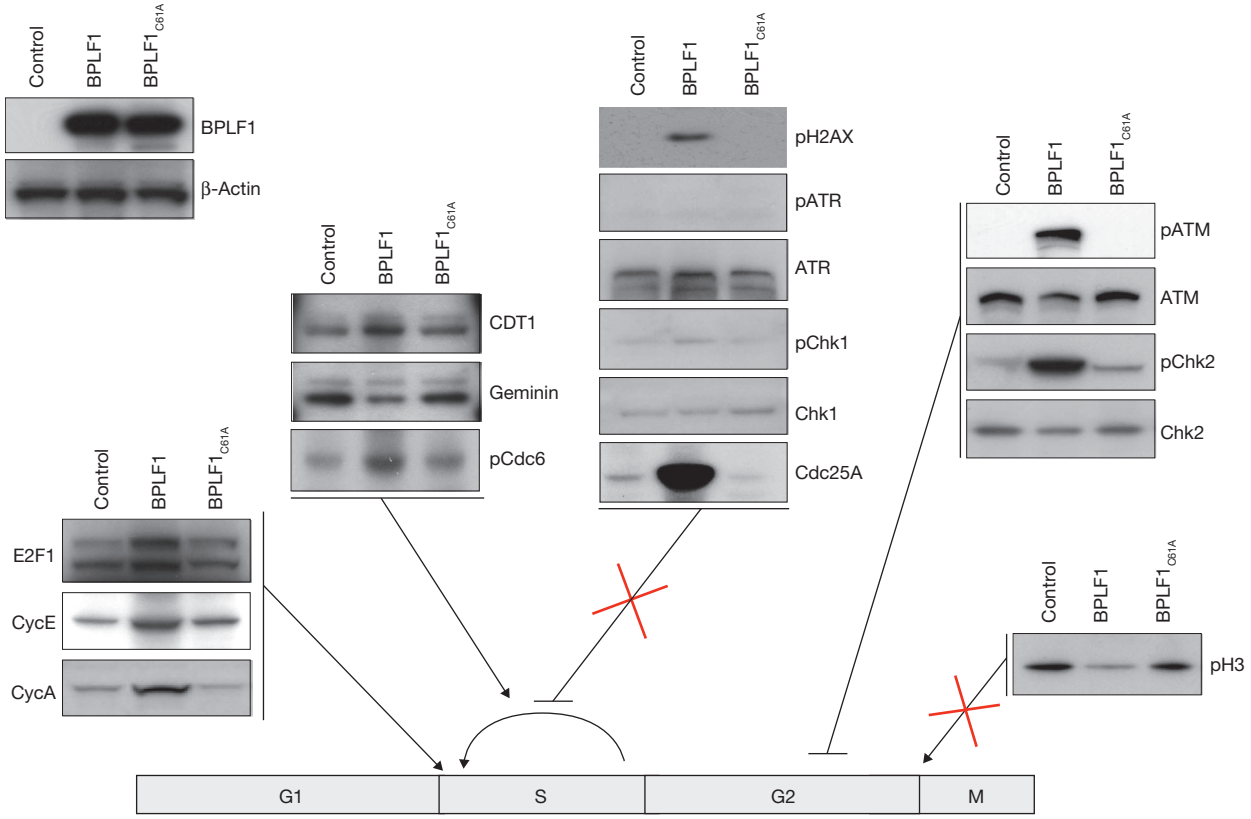

Figure 4 Cell cycle deregulation in cells expressing BPLF1. Total cell lysates from HeLa cells transfected with empty vector (control), BPLF1 or $BPLF1_{C61A}$ were fractionated by SDS–PAGE and western blots were probed sequentially with the indicated antibodies. Expression of the catalytically active BPLF1 was associated with an accumulation of E2F1, cyclin E and cyclin A, indicating entry into S phase; increased levels of pCdc6 and CDT1 and decreased levels of the CDT1 inhibitor geminin suggesting re-licensing of replication origins; failure to activate the ATR kinase and its downstream target Chk1 and accumulation of Cdc25A suggesting failure to activate the intera-S-phase checkpoint; accumulation of pATM, pChk2 and phosphorylated H2AX (pH2AX) indicating induction of DNA damage and activation of the G2 checkpoint; failure to accumulate phosphohistone H3 (pH3) indicating that the cells are not progressing into mitosis. Results from one representative experiment of three are shown. Uncropped images of blots are shown in Supplementary Information, Fig. S6.

eukaryotic-expressed BPLF1. Lysates of HeLa cells expressing Flag–BPLF1 and Flag–$BPLF1_{C61A}$ were labelled with the functional probes ubiquitin-VS and NEDD8-VS (where VS is 3-vinyl-(methyl)-sulphone), which form covalent adducts with the catalytic cysteine residue[23]. As illustrated in Fig. 1d, in which activity is revealed by a shift of the specific band corresponding to the size of the probe, BPLF1 bound ubiquitin and NEDD8 with comparable efficiency over a wide range of concentrations, whereas binding was abolished in the catalytic mutant. We finally tested whether BPLF1 acts as a deneddylase *in vivo*. Flag-tagged BPLF1, NEDP1 and their catalytic mutants were co-transfected in HeLa cells together with V5–NEDD8, and the presence of conjugates was assayed in western blots with the anti-V5 antibody (Fig. 1e). A comparable decrease in NEDD8 adducts was observed in cells expressing BPLF1 and NEDP1, whereas the catalytic mutants had no effect. Taken together, these data demonstrate that the N terminus of the EBV major tegument protein BPLF1 encodes a cysteine protease with specificity for NEDD8 conjugates *in vitro* and *in vivo*.

BPLF1 binds to cullins and inhibits the activity of CRLs

Cullins are the best-characterized substrates of NEDD8 conjugation. We therefore examined whether BPLF1 acts as a cullin deneddylase. Myc-tagged versions of two representative members of this family, Cul1 and Cul4A, were co-transfected in HeLa cells together with V5–NEDD8 and Flag–BPLF1, Flag–$BPLF1_{C61A}$ or Flag–NEDP1. Cell lysates were immunoprecipitated with an anti-Myc antibody, and western blots were probed sequentially with anti-Myc and anti-V5 antibodies (Fig. 2a). Slowly migrating species corresponding to neddylated cullins, confirmed by reactivity with the anti-V5 antibody (Fig. 2a, lower panel), were detected when the proteins were expressed alone or together with $BPLF1_{C61A}$, whereas the neddylated species disappeared in the presence of BPLF1 and NEDP1.

To investigate whether the enzymes interact with their substrates, lysates of HeLa cells co-transfected with Myc-tagged cullins and Flag-tagged enzymes were immunoprecipitated with the anti-Myc or anti-Flag antibodies. Sequential probing of western blots revealed a strong interaction of BPLF1 with both cullins, whereas NEDP1 interacted only very weakly (minor co-precipitated species are indicated by asterisks in Fig. 2b). The interaction of BPLF1 with cullins was independent of its catalytic activity and was not affected by the omission of NEM from the lysis buffer, suggesting that it does not involve binding to NEDD8. To test whether BPLF1 also interacts with endogenously expressed cullins, Cul4A was immunoprecipitated from lysates of HeLa cells transfected with Flag-vector, Flag–BPLF1 and Flag–$BPLF1_{C61A}$, and western blots were sequentially probed with anti-Flag, anti-Cul4A and, as control,

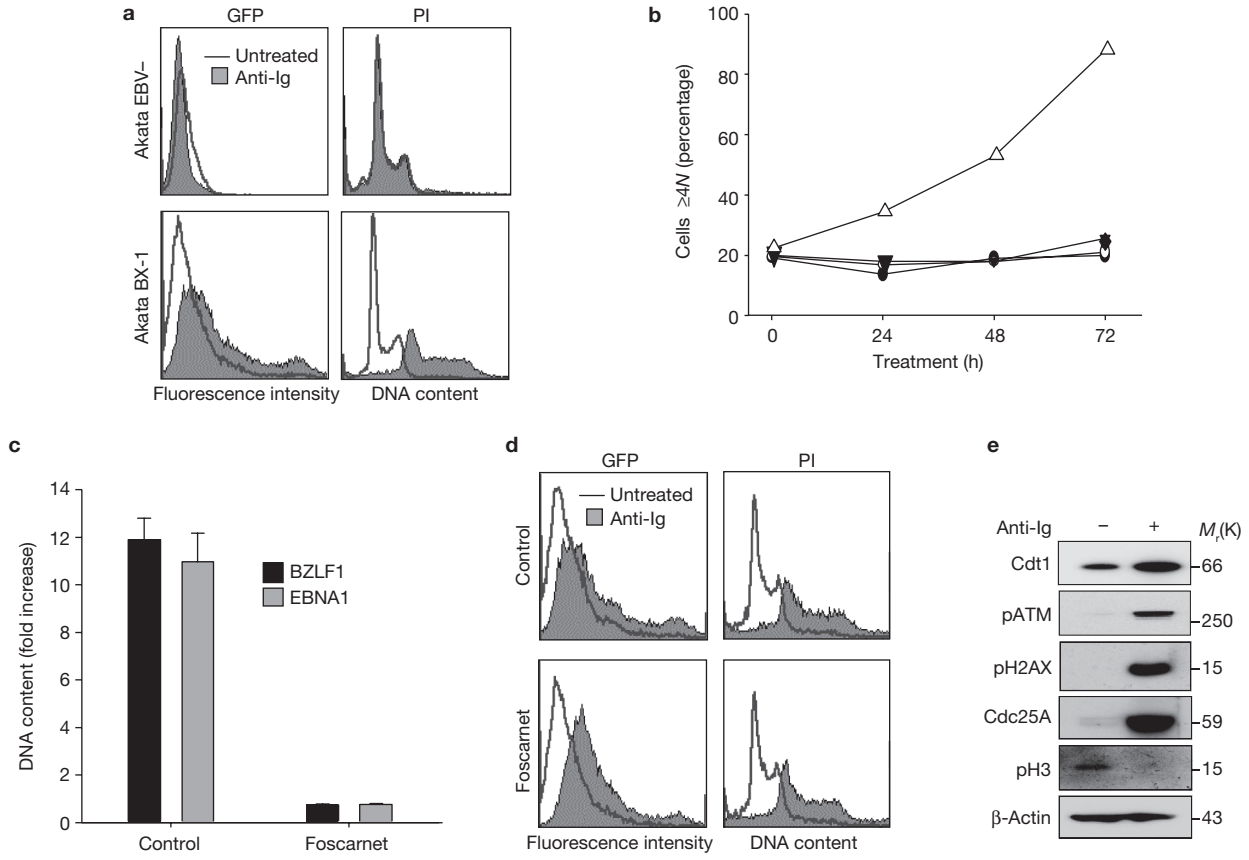

Figure 5 Activation of the EBV productive cycle is associated with cellular DNA re-replication. The productive virus cycle was induced in Akata-Bx1 cells by treatment with anti-human IgG antibodies and revealed by GFP fluorescence. (**a**) Activation of the productive cycle induces the accumulation of cells with a DNA content of 4*N* or more. DNA content was analysed by staining with PI in EBV-negative Akata and Akata-Bx1 cells treated with the anti-IgG antibody for 72 h. (**b**) Time-dependent accumulation of cells with a DNA content of 4*N* or more: the percentage of cells with this DNA content was measured over time in Akata cells (circles) and Akata-Bx1 cells (triangles) either untreated (filled symbols) or treated with anti-IgG antibodies (open symbols). Almost all live Akata-Bx1 cells showed a DNA content of 4*N* or more within 72 h of treatment. One representative experiment of three is shown. (**c**) Inhibition of EBV DNA replication by treatment with the viral polymerase inhibitor Foscarnet. EBV DNA content was assessed by qPCR in Akata-Bx1 cells treated for 72 h with anti-IgG alone (control) or in the presence of 50 μM Foscarnet. A more than tenfold increase in viral DNA was detected by qPCR specific for unique sequences in the genes encoding BZLF1 and EBNA-1 in the control anti-IgG-treated Akata-Bx1 calls, whereas viral DNA replication was abolished in the presence of Foscarnet. Results are shown as means and s.d. for two experiments performed in triplicate. (**d**) Treatment with Foscarnet does not affect the accumulation of cells with a DNA content of 4*N* or more. DNA content was assessed by staining with PI in Akata-Bx1 cells treated with anti-IgG for 72 h in the presence or absence of 50 μM Foscarnet. One out of two representative experiments is shown. (**e**) Induction of the productive virus cycle is associated with cellular S-phase defects. Cell lysates of untreated Akata-Bx1 cells and cells treated with anti-IgG for 72 h were fractionated by SDS–PAGE, and western blots were probed sequentially with the indicated antibodies. Uncropped images of blots are shown in Supplementary Information, Fig. S6.

anti-Myc antibodies (Fig. 2c). Both the active and catalytic mutant BPLF1 were detected in the immunoprecipitates, whereas c-Myc was not, confirming the specificity of the interaction.

Because neddylation activates CRLs we then asked whether BPLF1 modulates the activity of CRLs *in vivo*. Flag–BPLF1 and Flag–BPLF1$_{C61A}$ were transfected in HeLa cells and the expression of CDT1 (CRL4-DDB1^{CDT2} and CRL1^{Skp2} substrate[24]), Cdc25A (CRL1$^{\beta TrCP}$ substrate[25]), p21 and p27 (CRL1^{Skp2} substrates[26]) was assayed in western blots. Strong accumulation was observed in cells expressing the active enzyme (Fig. 2d) but not in those expressing the catalytic mutant (Supplementary Information, Fig. S3). This was reversed in a dose-dependent manner by co-expression of V5–NEDD8, in parallel with reconstitution of cullin neddylation (Fig. 2d). A V5–NEDD8-VV mutant that lacks the carboxy-terminal Gly residue required for conjugation had some effect only at the highest plasmid concentrations when faint cullin–NEDD8 bands were also detected, whereas haemagglutinin (HA)-tagged ubiquitin had no effect.

BPLF1 deregulates S-phase DNA synthesis

The binding to cullins and selective inhibition by overexpression of NEDD8 are consistent with the possibility that BPLF1 may act as a deneddylase *in vivo*. This was investigated by expressing BPLF1 in a range of cell types. The wild-type and mutant BPLF1 showed a predominant nuclear localization in transfected HeLa cells (Fig. 3a) and in other cell lines tested, including HEK293 and Chinese hamster ovary (not shown). The active enzyme induced a marked increase in the size of the nucleus (Fig. 3a, lower panel) and, on prolonged expression, extensive cell death. To explore the cause of nuclear enlargement, the cell cycle profile and DNA content were assessed by staining with propidium iodide (PI; Fig. 3b). Expression of BPLF1 was associated with a decrease in the

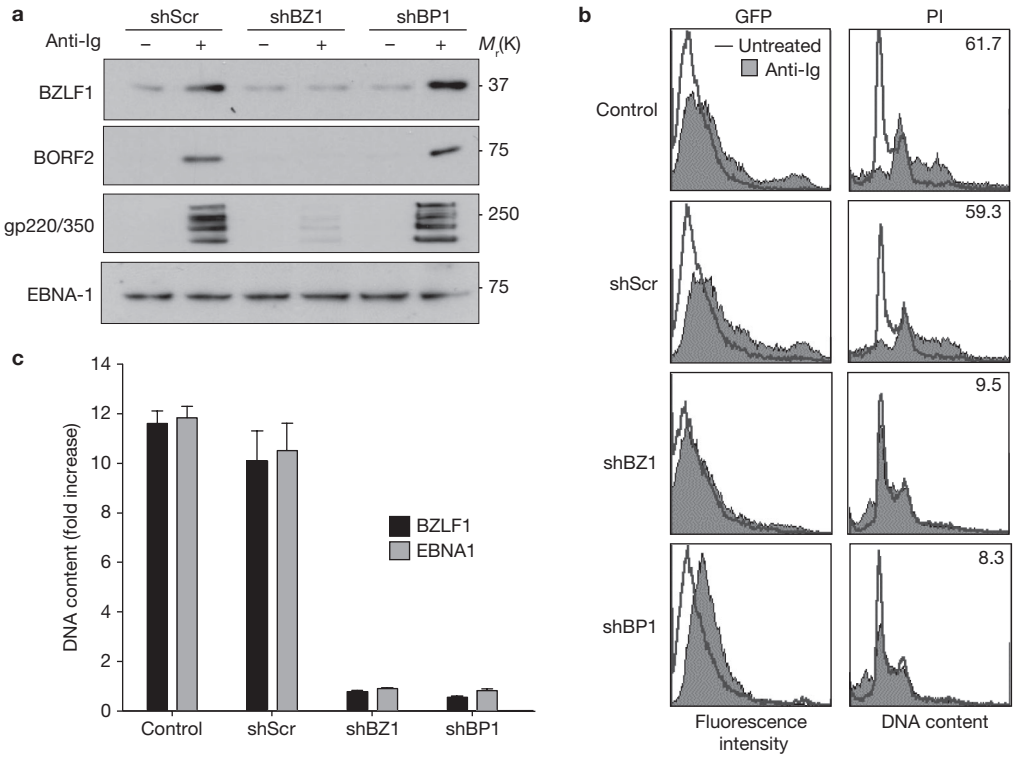

Figure 6 Expression of BPLF1 is required for efficient EBV DNA replication. Akata-Bx1 cells were infected with recombinant lentivirus expressing a scrambled shRNA (shScr) or shRNAs specific for the EBV immediate-early protein BZLF1 (shBZ1) or BPLF1 (shBP1). After 48 h, half of the infected cells were treated with anti-IgG antibodies to induce the productive cycle. (**a**) Total cell lysates were fractionated by SDS–PAGE, and western blots were probed with antibodies specific for the EBV transactivator BZLF1, the early antigen BORF2 (ribonucleotide diphosphate reductase involved in viral DNA replication) and late antigen gp220/350 (viral envelope glycoprotein). Antibodies against the EBV latent antigen EBNA-1 and against actin (not shown) were used as loading controls. Expression of early and late products of the EBV replicative cycle was inhibited by shRNA knockdown of BZLF1, whereas knockdown of BPLF1 had no effect. One representative experiment of three is shown. (**b**) Expression of BPLF1 is required for cellular DNA re-replication in cells entering the productive virus cycle. The efficiency of entry into the productive cycle (GFP fluorescence) and DNA content (staining with PI) were monitored in Akata-Bx1 cells and in Akata-Bx1 cells infected with the indicated recombinant lentiviruses. BZLF1 knockdown prevented both entry into the productive virus cycle and accumulation of cells with a DNA content of 4*N* or more, whereas BPLF1 knockdown selectively abolished cellular DNA re-replication. The percentage of cells with a DNA content of more than 4*N* is indicated in each panel. (**c**) qPCR analysis of EBV DNA content was performed in anti-IgG-treated Akata-Bx1 cells infected with the indicated recombinant lentiviruses. Comparable inhibition of EBV DNA replication was achieved by knockdown of BZLF1 and BPLF1. Results are shown as means and s.d. for three experiments each performed in triplicate. Uncropped images of blots are shown in Supplementary Information, Fig. S6.

number of cells in G1 stage and an increase in cells with a DNA content of 4*N* or more. More than 80% of the transfected cells showed a DNA content of 4*N* or more within 48 h, and the remaining cells showed signs of apoptosis (DNA content less than 2*N*; Fig. 3b, lower panel). Almost all the BPLF1-expressing cells were dead within 4–5 days after transfection. This phenotype was reversed in a dose-dependent manner by overexpression of NEDD8 but not by overexpression of ubiquitin (Fig. 3c).

The accumulation of cells with a DNA content of 4*N* or more suggests that BPLF1 may cause deregulation of the S phase and re-replication of cellular DNA. Consistent with this possibility, expression of the active enzyme was associated with accumulation of the $CRL1^{Skp2}$ substrate E2F1 (ref. 27) and its downstream targets cyclin E and cyclin A (Fig. 4). Furthermore, phosphorylated Cdc6 and CDT1 were increased, whereas the CDT1 inhibitor geminin was decreased, suggesting enhanced licensing of DNA replication origins. DNA re-replication induces DNA damage and elicits DNA-damage responses that halt progression of the cell cycle[28]. DNA damage was revealed by the accumulation of phosphorylated histone H2AX. However, the ATR (ataxia telangiectasia and rad-3-related) kinase and its downstream target Chk1 were not phosphorylated, and Cdc25A, which is targeted for degradation after phosphorylation by Chk1 (ref. 25), was strongly stabilized, suggesting failure of the intra-S-phase checkpoint[29]. Enhanced phosphorylation of ATM and its downstream targets Chk2 indicated activation of the G2 checkpoint[30], whereas the failure to accumulate phosphohistone H3 confirmed that BPLF1-expressing cells did not undergo transition into mitosis[31]. Taken together, these findings indicate that BPLF1 induces DNA re-replication, which correlates with the stabilization of several CRL substrates that regulate DNA synthesis and cell cycle progression.

BPLF1 is required for efficient EBV DNA replication

The contribution of the cellular DNA replication machinery to herpesvirus replication is poorly understood. To assess whether the pseudo-S-phase induced by BPLF1 has any function, we used the Akata-Bx1 cell line, which carries a recombinant EBV in which the thymidine kinase gene has been replaced with GFP[32]. The productive virus cycle is induced in Akata-Bx1 cells by the crosslinking of surface immunoglobulins, which mimics the physiological trigger of EBV replication occurring *in vivo*[33].

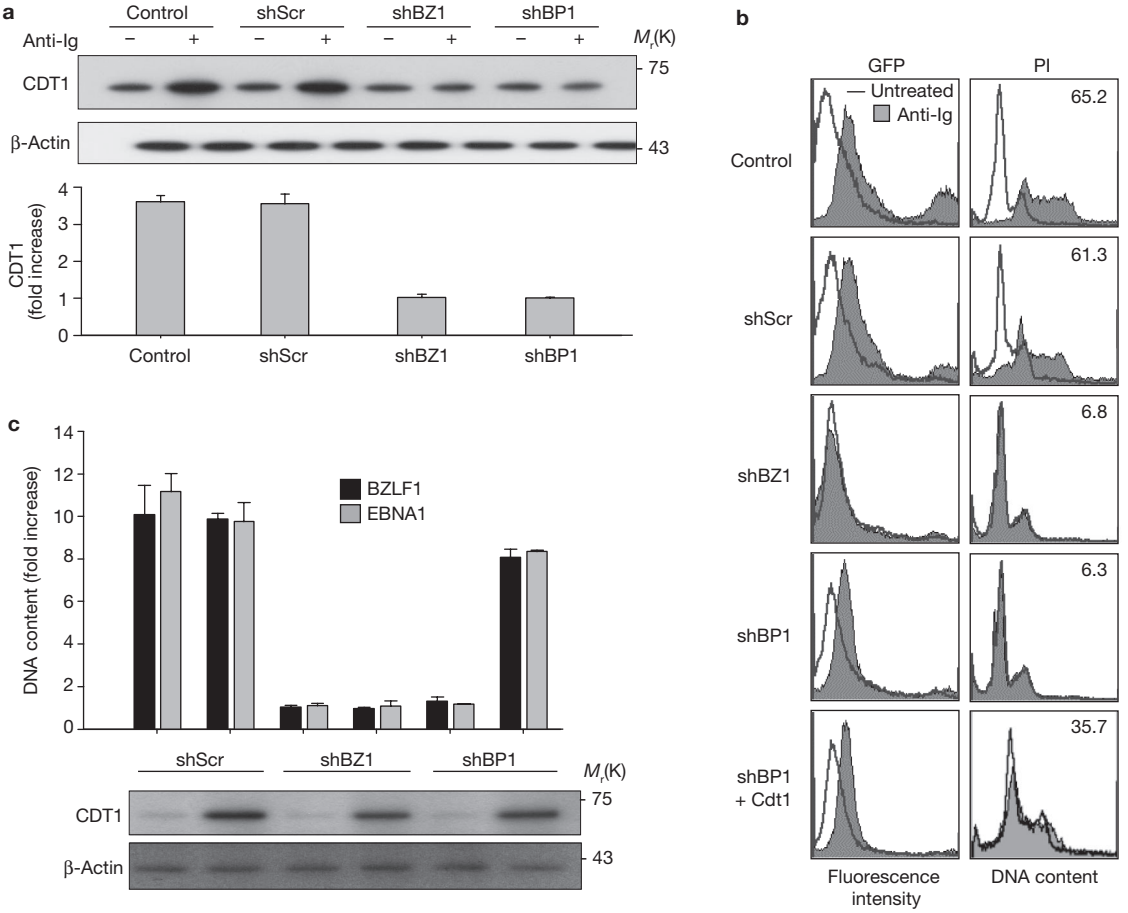

Figure 7 Overexpression of CDT1 promotes EBV DNA replication. (**a**) BPLF1 knockdown prevents the accumulation of the licensing factor CDT1 in cells entering the productive virus cycle. Expression of CDT1 was investigated in western blots of control and anti-IgG-treated Akata-Bx1 cells infected with the indicated recombinant lentiviruses. CDT1 did not accumulate when entry into the productive virus cycle was inhibited by BZLF1 knockdown, and similar inhibition was achieved by knockdown of BPLF1. CDT1 levels were quantified by densitometry of western blots from three independent experiments; the histogram shows fold increases in CDT1 (means and s.d.). (**b**) CDT1 overexpression reconstitutes cellular DNA re-replication in BPLF1 knockdown cells. Induction of productive virus cycle (GFP fluorescence) and DNA content (staining with PI) were monitored in anti-IgG-treated Akata-Bx1 cells with or without infection with the indicated lentiviruses. Cells transduced with the shBP1 lentivirus were transfected with a CDT1 expression vector, and expression of the transfected gene was confirmed by western blots. (**c**) overexpression of CDT1 reconstitutes EBV DNA replication. The amount of viral DNA was quantified in control and anti-IgG-treated Akata-Bx1 cells by qPCR with primers specific for BZLF1 and EBNA-1. Overexpression of CDT1 (lower panel) did not affect EBV DNA replication in cells transduced with the control scrambled shRNA lentivirus and did not promote virus replication in the absence of BZLF1, whereas viral DNA replication was reconstituted by overexpression of CDT1 in cells transduced with the shBP1 lentivirus. The fold increases in DNA content are shown as means and s.d. for two experiments performed in triplicate. Uncropped images of blots are shown in Supplementary Information, Fig. S6.

We first examined whether the productive virus cycle is associated with cellular DNA re-replication. EBV-negative Akata and Akata-Bx1 cells were treated with anti-IgG, followed by monitoring of virus reactivation and cell cycle distribution by GFP fluorescence and staining with PI. Treatment with anti-IgG did not affect the cell cycle in Akata cells, whereas EBV reactivation was accompanied by a marked increase in the number of cells with a DNA content of 4*N* or more in Akata-Bx1 cells (Fig. 5a), reaching more than 80% of the live cell population within 72 h (Fig. 5b). To exclude a possible contribution of newly synthesized viral DNA, the anti-IgG treatment was repeated in the presence of the herpesvirus DNA polymerase inhibitor Foscarnet[34]. Treatment with Foscarnet abolished EBV DNA replication (Fig. 5c) but did not affect the re-replication of cellular DNA (Fig. 5d). Furthermore, induction of the productive virus cycle was accompanied by the accumulation of CDT1, pATM, pH 2AX and Cdc25A and a failure to accumulate phosphohistone H3 (Fig. 5e).

Although BPLF1 is a virion component, expression of the messenger RNA was detected by quantitative polymerase chain reactions (qPCRs) specific for the N-terminal and C-terminal domains of the transcript within few hours after triggering by anti-IgG (Supplementary Information, Fig. S4). This kinetics of expression is reminiscent of that of early genes that are induced by BZLF1 and mediate replication of the EBV genome[35]. To test whether BPLF1 regulates EBV replication, its expression was inhibited by transducing anti-IgG-treated Akata-Bx1 cells with recombinant lentiviruses expressing specific short hairpin RNAs (shRNAs) (shBP1) and, as controls, shRNAs to BZLF1 (shBZ1) or a scrambled shRNA (Supplementary Information, Fig. S5). The scrambled shRNA did not affect EBV reactivation as detected by expression of the immediate-early protein BZLF1, the early protein BORF2 and the late proteins gp220–350, whereas full inhibition was achieved by BZLF1 knockdown, as expected (Fig. 6a).

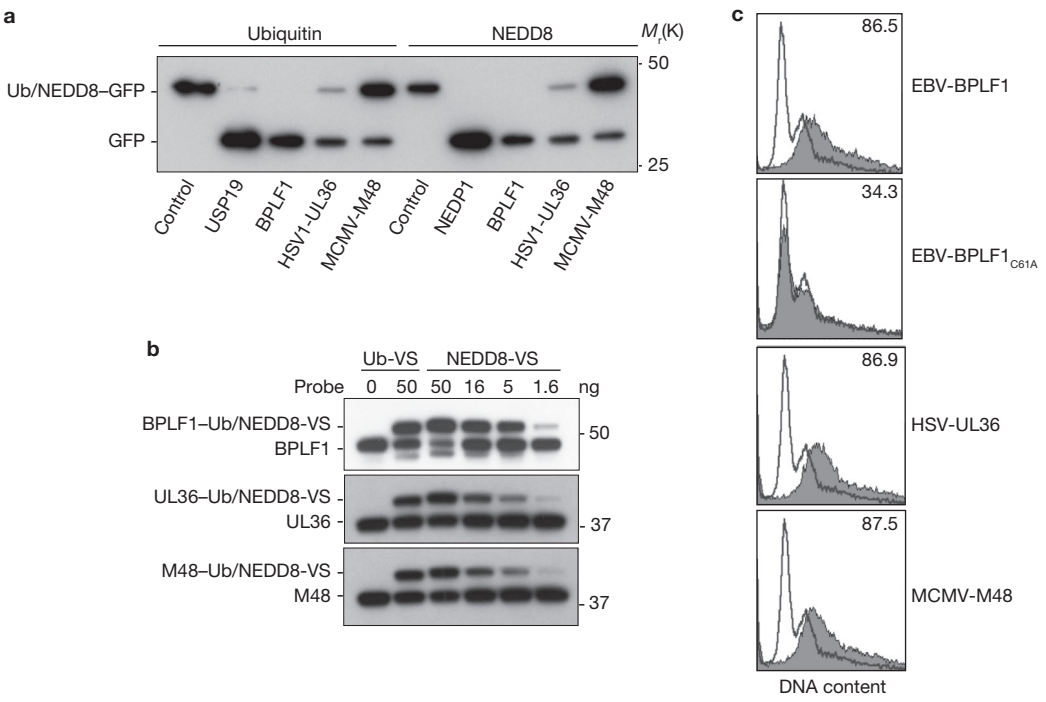

Figure 8 Deneddylase activity is shared by BPLF1 homologues encoded by other herpesviruses. (**a**) GST-fusion chimaeras of the N-terminal EBV-BPLF1 (amino-acid residues 1–325), HSV-UL36 (residues 1–290) and MCMV-M48 (residues 1–315) were tested for cleavage of the ubiquitin–GFP and ubiquitin-NEDD8 reporters as described in the legend to Fig. 1a. One representative experiment of three is shown. (**b**) Eukaryotic expressed proteins retain deneddylase activity. Flag-tagged BPLF1, HSV-UL36 and MCMV-M48 were expressed in HeLa cells, and enzymatic activity was assayed by labelling with ubiquitin-VS and increasing amounts of NEDD8-VS. Binding of the probes was detected in western blots probed with the anti-Flag antibody. (**c**) The cell cycle profile of HeLa cells transfected with wild-type and catalytic mutant BPLF1, HSV-UL36 or MCMV-M48 was assessed by staining with PI 48 h after transfection. Expression of the active enzymes induced a comparable accumulation of cells with a DNA content of 4*N* or more. The percentage of cells with a DNA content of 4*N* or more is indicated in each panel. One representative experiment of three is shown. Uncropped images of blots are shown in Supplementary Information, Fig. S6.

The expression of viral proteins was not affected by BPLF1 knockdown (Fig. 6a). However, the accumulation of cells with a DNA content of 4*N* or more was abrogated (Fig. 6b), which was correlated with an almost complete inhibition of virus DNA replication (Fig. 6c). Thus, BPLF1 seems to act downstream of BZLF1 to promote efficient replication of the EBV genome.

EBV replication is dependent on overexpression of CDT1

We then sought to identify which among the cellular products regulated by BPLF1 is required for EBV DNA replication. Because overexpression of CDT1 causes cellular DNA re-replication[36], we tested whether BPLF1 is required for the accumulation of CDT1 in cells entering the productive virus cycle. Transduction of anti-IgG-treated Akata-Bx1 cells with the shBZ1 lentivirus abolished the accumulation of CDT1; a comparable inhibition was observed with the shBP1 lentivirus, confirming that BPLF1 regulates the abundance of this CRL substrate during productive infection (Fig. 7a). Overexpression of CDT1 partly reconstituted the cellular DNA re-replication phenotype induced by BPLF1 knockdown (Fig. 7b). Most significantly, although overexpression of CDT1 did not affect EBV DNA replication either alone or in the absence of BZLF1 (Fig. 7c), it reconstituted virus production in BPLF1 knockdown cells. Taken together, these data demonstrate that stabilization of CDT1 is critical for the induction of an S-phase-like environment that is permissive of virus replication.

Deneddylase activity of BPLF1 homologues

We finally tested whether the deneddylase activity and induction of cellular DNA re-replication are conserved among BPLF1 homologues encoded by other herpesviruses. GST fusions of the N termini of HSV-UL36 and MCMV-M48 were assayed for cleavage of the ubiquitin/UbL–GFP reporters in bacteria co-expression assays. The ubiquitin and NEDD8 reporters were cleaved with comparable efficiency (Fig. 8a). Furthermore, Flag-tagged viral proteins retained the capacity to bind NEDD8-VS when expressed in HeLa cells (Fig. 8b), and overexpression was associated with an accumulation of cells with a DNA content of 4*N* or more, comparable to that achieved by overexpression of BPLF1 (Fig. 8c). Thus, both deneddylase activity and S-phase deregulation seem to be conserved in this family of viral enzymes.

DISCUSSION

Pathogenic viruses and intracellular bacteria have evolved elaborate strategies for manipulating the ubiquitin and UbL signalling machineries, including the production of functional homologues of cellular enzymes. Here we discovered that a conserved cysteine protease encoded in the N terminus of the major tegument protein of *herpesviridae* acts *in vivo* as a NEDD8-specific protease that binds to cullins and regulates the turnover of CRL substrates. Expression of this viral deneddylase is associated with deregulation of the cell cycle and with the establishment of an S-phase-like environment that is required for efficient replication of the viral genome.

On the basis of *in vitro* assays performed with fluorogenic substrates, branched peptides and functional probes, it was suggested that UL36, the HSV1-encoded founding member of this family of viral enzymes, and other homologues including BPLF1, preferentially cleave ubiquitin adducts[21]. Our data confirm the capacity of EBV-BPLF1, HSV-UL36 and MCMV-M48 to cleave ubiquitin conjugates but demonstrate that they cleave NEDD8 adducts with comparable efficiency (Fig. 8). Most significantly, we have shown that BPLF1 is capable of hydrolysing true NEDD8 conjugates *in vitro* and in transfected cells (Fig. 1). Given the high degree of homology between ubiquitin and NEDD8 this dual specificity is not surprising and is indeed shared by many ubiquitin-specific proteases[3]. It is noteworthy that the exquisite specificity of NEDP1 for NEDD8 adducts was attributed to the presence of bulky residues in the catalytic cleft that restrict the access of ubiquitin[37]. The large Arg 72 residue in the C terminus of ubiquitin is replaced by Ala in NEDD8, which may allow accommodation of the slender C terminus into a broader range of catalytic clefts. On the basis of the crystal structure of MCMV-M48 crosslinked to ubiquitin-vinylmethyl ester (VME) it was proposed that a hydrogen bond between Arg 72 and Thr 80 in MCMV-M48 may be crucial for the binding of ubiquitin, and lack of this interaction was implicated in the failure to bind NEDD8-VME[38]. We have used a different NEDD8 probe, namely NEDD8-VS. Conceivably, the presence of a glycine-VS reactive group, rather than glycine-VME, could explain the different reactivity of MCMV-M48. Indeed, previous reports have documented differences in the crosslinking efficiency of various ubiquitin functional probes, including failure of ubiquitin-VME to recognize the ubiquitin protease OTUB1 (ref. 39).

Although the double specificity of BPLF1 for both ubiquitin and NEDD8 was documented in a range of *in vitro* assays, several lines of evidence suggest that the deneddylase activity may have a dominant function *in vivo*. BPLF1 binds to and deneddylates cullins and induces the stabilization of several CRL substrates. The capacity to interact tightly with cullins is a unique feature of BPLF1 and, together with its nuclear localization, suggests that the enzyme may specifically target this group of NEDD8 substrates. The finding that stabilization of CRL substrates, such as CDT1, Cdc25A, p21 and p27, was efficiently counteracted by overexpression of NEDD8 but not that of NEDD8-VV or ubiquitin further supports the key role of cullin deneddylation. Although both ubiquitin and NEDD8 are abundantly expressed in cells, the effect of NEDD8 overexpression indicates that the neddylation cycle may be tightly regulated and may be critically dependent on local concentrations of the modifier. Most significantly, the phenotype of BPLF1 overexpression is consistent with the selective stabilization of CRL substrates that control DNA replication and cell cycle progression. A very similar phenotype is induced in cells treated with MLN4924, a potent inhibitor of the NEDD8-activating enzyme that inactivates the conjugation cascade[40]. A surprising difference between the effect of BPLF1 and MLN4924 is the failure to activate ATR and Chk1 in BPLF1-expressing cells. The mechanisms of this selectivity are unclear but may reflect the capacity of the viral enzyme to interact preferentially with a distinct subset of NEDD8 substrates *in vivo*. Thus, although a contributory effect of deubiquitylation is possible, our findings strongly indicate that the deneddylase activity and the specific targeting to cullins are decisive for the effect of BPLF1 in transfected cells and during EBV reactivation.

The strict human tropism of EBV does not allow a direct assessment of the contribution of BPLF1 to viral infection *in vivo*. However, evidence from animal herpesviruses confirms that the enzymatic activity of this protein family is important in viral pathogenesis by regulating the yield of infectious virus. Thus, mutations of the catalytic cysteine residue in ORF64 of murine gammaherpesvirus-68 and pUL36 of pseudorabies virus (suid herpesvirus 1) yielded viruses that replicate less efficiently *in vitro* and are less pathogenic *in vivo*[41,42], whereas a mutation that inactivates the homologue encoded by Marek's disease virus was shown to diminish replication *in vivo* and severely limit the oncogenic potential of the virus[43]. Our finding that BPLF1, and by inference other homologues, regulates the efficiency of virus replication by contributing to the establishment of an S-phase-like environment provides a new insight into the still poorly understood process of herpesvirus replication. Although increasing evidence implicates viral proteins in the deregulation of the host cell cycle that accompanies viral DNA synthesis, the mechanisms and possible contribution of cellular factors remain largely unknown[44]. Notably, although all the components of the DNA polymerases of herpesviruses are known, the reconstituted enzymes are poorly active *in vitro*, suggesting that cellular processivity factors may be missing[45]. Our finding that BPLF1 promotes EBV DNA replication by stabilizing CDT1 points to this and possibly other components of the cellular DNA-replication licensing machinery as likely candidates. □

METHODS

Methods and any associated references are available in the online version of the paper at http://www.nature.com/naturecellbiology/

Note: Supplementary Information is available on the Nature Cell Biology website.

ACKNOWLEDGEMENTS

We thank Ron T. Hay, Frauke Melchior, Zhen-Quian-Pan, Dong-Er Zhang, Chiba Chikatumi and Jürgen Haas for providing plasmids, antibodies and technical advice. This study was supported by grants awarded by the Swedish Cancer Society, the Swedish Medical Research Council, the Karolinska Institutet, Stockholm, Sweden, and by the European Community Integrated Project INCA, contract no. LSHC-CT-2005-018704, and Network of Excellence RUBICON, contract no. LSG-CT-2005-018683. S.H. is supported by a fellowship from the European Community Marie Curie Early Training Network UbiRegulators contract no. MRTN-CT-2006-034555.

AUTHOR CONTRIBUTIONS

S.G. and M.G.M. designed the experiments; O.F. produced the recombinant lentiviruses; S.H., M.P and C.D.G. performed analysis; S.C. performed bioinformatics analysis; S.G. and M.G.M. wrote the manuscript.

COMPETING FINANCIAL INTERESTS

The authors declare no competing financial interests.

Published online at http://www.nature.com/naturecellbiology
Reprints and permissions information is available online at http://npg.nature.com/reprintsandpermissions/

1. Glickman, M. H. & Ciechanover, A. The ubiquitin–proteasome proteolytic pathway: destruction for the sake of construction. *Physiol. Rev.* **82,** 373–428 (2002).
2. Ciechanover, A., Orian, A. & Schwartz, A. L. The ubiquitin-mediated proteolytic pathway: mode of action and clinical implications. *J Cell Biochem Suppl* **34,** 40–51 (2000).
3. Reyes-Turcu, F. E., Ventii, K. H. & Wilkinson, K. D. Regulation and cellular roles of ubiquitin-specific deubiquitinating enzymes. *Annu. Rev. Biochem.* **78,** 363–397 (2009).
4. Kerscher, O., Felberbaum, R. & Hochstrasser, M. Modification of proteins by ubiquitin and ubiquitin-like proteins. *Annu. Rev. Cell Dev. Biol.* **22,** 159–180 (2006).
5. Chiba, T. & Tanaka, K. Cullin-based ubiquitin ligase and its control by NEDD8-conjugating system. *Curr. Protein Pept. Sci.* **5,** 177–184 (2004).
6. Tatham, M. H. *et al.* RNF4 is a poly-SUMO-specific E3 ubiquitin ligase required for arsenic-induced PML degradation. *Nature Cell Biol.* **10,** 538–546 (2008).
7. Lallemand-Breitenbach, V. *et al.* Arsenic degrades PML or PML-RARα through a SUMO-triggered RNF4/ubiquitin-mediated pathway. *Nature Cell Biol.* **10,** 547–555 (2008).
8. Duda, D. M. *et al.* Structural insights into NEDD8 activation of cullin-RING ligases: conformational control of conjugation. *Cell* **134,** 995–1006 (2008).
9. Pan, Z. Q., Kentsis, A., Dias, D. C., Yamoah, K. & Wu, K. Nedd8 on cullin: building an expressway to protein destruction. *Oncogene* **23,** 1985–1997 (2004).

10. Isaacson, M. K. & Ploegh, H. L. Ubiquitination, ubiquitin-like modifiers, and deubiquitination in viral infection. *Cell Host Microbe* **5,** 559–570 (2009).
11. Loureiro, J. & Ploegh, H. L. Antigen presentation and the ubiquitin–proteasome system in host–pathogen interactions. *Adv. Immunol.* **92,** 225–305 (2006).
12. Scheffner, M., Huibregtse, J. M., Vierstra, R. D. & Howley, P. M. The HPV-16 E6 and E6-AP complex functions as a ubiquitin-protein ligase in the ubiquitination of p53. *Cell* **75,** 495–505 (1993).
13. Boutell, C., Canning, M., Orr, A. & Everett, R. D. Reciprocal activities between herpes simplex virus type 1 regulatory protein ICP0, a ubiquitin E3 ligase, and ubiquitin-specific protease USP7. *J. Virol.* **79,** 12342–12354 (2005).
14. Saridakis, V. *et al.* Structure of the p53 binding domain of HAUSP/USP7 bound to Epstein–Barr nuclear antigen 1 implications for EBV-mediated immortalization. *Mol. Cell* **18,** 25–36 (2005).
15. Randow, F. & Lehner, P. J. Viral avoidance and exploitation of the ubiquitin system. *Nature Cell Biol.* **11,** 527–534 (2009).
16. Young, L. S. & Rickinson, A. B. Epstein–Barr virus: 40 years on. *Nature Rev. Cancer* **4,** 757–768 (2004).
17. Bishop, G. A. & Busch, L. K. Molecular mechanisms of B-lymphocyte transformation by Epstein–Barr virus. *Microbes Infect.* **4,** 853–857 (2002).
18. Tsurumi, T., Fujita, M. & Kudoh, A. Latent and lytic Epstein–Barr virus replication strategies. *Rev. Med. Virol.* **15,** 3–15 (2005).
19. Kudoh, A. *et al.* Epstein–Barr virus lytic replication elicits ATM checkpoint signal transduction while providing an S-phase-like cellular environment. *J. Biol. Chem.* **280,** 8156–8163 (2005).
20. Sompallae, R. *et al.* Epstein–Barr virus encodes three bona fide ubiquitin-specific proteases. *J. Virol.* **82,** 10477–10486 (2008).
21. Kattenhorn, L. M., Korbel, G. A., Kessler, B. M., Spooner, E. & Ploegh, H. L. A deubiquitinating enzyme encoded by HSV-1 belongs to a family of cysteine proteases that is conserved across the family Herpesviridae. *Mol. Cell* **19,** 547–557 (2005).
22. Mendoza, H. M. *et al.* NEDP1, a highly conserved cysteine protease that deNEDDylates Cullins. *J. Biol. Chem.* **278,** 25637–25643 (2003).
23. Borodovsky, A. *et al.* A novel active site-directed probe specific for deubiquitylating enzymes reveals proteasome association of USP14. *EMBO J.* **20,** 5187–5196 (2001).
24. Nishitani, H. *et al.* Two E3 ubiquitin ligases, SCF-Skp2 and DDB1-Cul4, target human Cdt1 for proteolysis. *EMBO J.* **25,** 1126–1136 (2006).
25. Busino, L. *et al.* Degradation of Cdc25A by β-TrCP during S phase and in response to DNA damage. *Nature* **426,** 87–91 (2003).
26. Auld, C. A., Fernandes, K. M. & Morrison, R. F. Skp2-mediated $p27^{Kip1}$ degradation during S/G2 phase progression of adipocyte hyperplasia. *J. Cell Physiol.* **211,** 101–111 (2007).
27. Ohta, T. & Xiong, Y. Phosphorylation- and Skp1-independent *in vitro* ubiquitination of E2F1 by multiple ROC-cullin ligases. *Cancer Res.* **61,** 1347–1353 (2001).
28. Cook, J. G. Replication licensing and the DNA damage checkpoint. *Front. Biosci.* **14,** 5013–5030 (2009).
29. Wilsker, D. & Bunz, F. Chk1 phosphorylation during mitosis: a new role for a master regulator. *Cell Cycle* **8,** 1161–1163 (2009).
30. Chen, Y. & Poon, R. Y. The multiple checkpoint functions of CHK1 and CHK2 in maintenance of genome stability. *Front. Biosci.* **13,** 5016–5029 (2008).
31. Hans, F. & Dimitrov, S. Histone H3 phosphorylation and cell division. *Oncogene* **20,** 3021–3027 (2001).
32. Guerreiro-Cacais, A. O., Uzunel, M., Levitskaya, J. & Levitsky, V. Inhibition of heavy chain and β2-microglobulin synthesis as a mechanism of major histocompatibility complex class I downregulation during Epstein–Barr virus replication. *J. Virol.* **81,** 1390–1400 (2007).
33. Daibata, M., Humphreys, R. E., Takada, K. & Sairenji, T. Activation of latent EBV via anti-IgG-triggered, second messenger pathways in the Burkitt's lymphoma cell line Akata. *J. Immunol.* **144,** 4788–4793 (1990).
34. Chrisp, P. & Clissold, S. P. Foscarnet. A review of its antiviral activity, pharmacokinetic properties and therapeutic use in immunocompromised patients with cytomegalovirus retinitis. *Drugs* **41,** 104–129 (1991).
35. Yuan, J., Cahir-McFarland, E., Zhao, B. & Kieff, E. Virus and cell RNAs expressed during Epstein–Barr virus replication. *J. Virol.* **80,** 2548–2565 (2006).
36. Kim, Y. & Kipreos, E. T. Cdt1 degradation to prevent DNA re-replication: conserved and non-conserved pathways. *Cell Div.* **2,** 18 (2007).
37. Shen, L. N. *et al.* Structural basis of NEDD8 ubiquitin discrimination by the deNEDDylating enzyme NEDP1. *EMBO J.* **24,** 1341–1351 (2005).
38. Schlieker, C. *et al.* Structure of a herpesvirus-encoded cysteine protease reveals a unique class of deubiquitinating enzymes. *Mol. Cell* **25,** 677–687 (2007).
39. Edelmann, M. J. *et al.* Structural basis and specificity of human otubain 1-mediated deubiquitination. *Biochem. J.* **418,** 379–390 (2009).
40. Soucy, T. A. *et al.* An inhibitor of NEDD8-activating enzyme as a new approach to treat cancer. *Nature* **458,** 732–736 (2009).
41. Gredmark-Russ, S. *et al.* A gammaherpesvirus ubiquitin-specific protease is involved in the establishment of murine gammaherpesvirus 68 infection. *J. Virol.* **83,** 10644–10652 (2009).
42. Bottcher, S. *et al.* Mutagenesis of the active-site cysteine in the ubiquitin-specific protease contained in large tegument protein pUL36 of pseudorabies virus impairs viral replication *in vitro* and neuroinvasion *in vivo*. *J. Virol.* **82,** 6009–6016 (2008).
43. Jarosinski, K., Kattenhorn, L., Kaufer, B., Ploegh, H. & Osterrieder, N. A herpesvirus ubiquitin-specific protease is critical for efficient T cell lymphoma formation. *Proc. Natl Acad. Sci. USA* **104,** 20025–20030 (2007).
44. Davy, C. & Doorbar, J. G2/M cell cycle arrest in the life cycle of viruses. *Virology* **368,** 219–226 (2007).
45. Boehmer, P. E. & Lehman, I. R. Herpes simplex virus DNA replication. *Annu. Rev. Biochem.* **66,** 347–384 (1997).

DOI: 10.1038/ncb2035

METHODS

Antibodies. The following antibodies were used: anti-S-tag (71549-3, 1:6000, Novagen, Darmstadt, Germany); anti-V5 (R960-25, 1:2500, Invitrogen, Carlsbad, CA); anti-β-actin and anti-Flag (AC-15 1:5000, F-3165 1:8000, Sigma, St Louis, MO); anti-p27/Kip1 and anti-human IgG (M7203 1:1000, A0423 1:50, DAKO, Denmark); anti-p21/Cip1/WAF1 (610233 1:1000, BD Biosciences); anti EBV EA-R (BORF2, sc-56979 1:1000), BZLF1 (sc-53094 1:1000), ATR (sc-28091 1:1000), E2F-1 (sc-251 1:1000), geminin (sc-13015 1:1000), cyclin-E (sc-20684 1:1000), cyclin-A (sc-751 1:1000), cyclin-B1 (sc-245 1:1000), Cdt1 (sc-28262 1:1000), p53 (sc-126 1:1000), c-Myc (sc-40 1:3000), Cdc25A (sc-7157 1:1000), phospho-Cdc6-S54 (sc-12970-R 1:1000) from Santa Cruz Biotechnogy, Santa Cruz CA; anti-retinoblastoma (Rb) (SA-124 1:1000, Enzo, Life Sciences, PA); anti-phospho-Chk2-T68, phospho-Chk1-S345 1:1000, phospho-ATR-S428, anti-phospho-H3-S10 1:1000 all from Cell Signalling, Danvers, MA; anti-phospho-ATM-S1981 (NB100-306 1:1000, Novus Biologicals, Littleton, CO); anti-ATM and anti-Cullin4A (ab-34897 1:1000, ab-2618 1:3000, AbCam, Cambridge, MA); anti-phospho-H2AX-S139 1:1000 (Millipore Corporation, Billerica, MA); anti-EBV gp220/350 1:100 and EBNA1 (OT1-X 1:1000) (gifts of Jaap M. Middeldorp, CCA-VUMC, Amsterdam, The Netherlands).

Plasmids. The GST–BPLF1 (amino-acid residues 1–325) and ubiquitin–GFP plasmids were described previously[20]. The coding sequences of NEDD8, ISG15, SUMO-1, SUMO-2 and SUMO-3 were cloned in frame with GFP into the *Bgl*II and *Xho*I sites of the GFP–S-tag-pACYCDuet-1 plasmid (Novagen). Bacterial and eukaryotic expression plasmids encoding residues 1–290 of HSV1-UL36 and residues 1–315 of MCMV-M48 were cloned in the pDEST-GST Flag-tag vectors.

Immunoblots. The cells were lysed in buffer (25 mM Tris-HCl pH 7.6, 50 mM NaCl, 1 mM EDTA, 0.5% Nonidet P40, 0.1% SDS, 0.5% sodium deoxycholate) containing protease inhibitors (Complete Mini Protease Inhibitor Cocktail tablets; Roche) and 10 mM NEM (Sigma), and protein concentration was measured with a Protein Assay kit (Bio-Rad Laboratories). Equal amounts of proteins were fractionated in a polyacrylamide Bis-Tris 4–12% gradient or in polyacrylamide Tris-acetate 7% linear precast gels (Invitrogen). After transfer to poly(vinylidene difluoride) membranes (Millipore), the filters were blocked in PBS saline buffer containing 5% non-fat milk and 0.1% Tween 20 and incubated with primary antibodies either for 1 h at 24°C or overnight at 4 °C followed by incubation for 1 h with the appropriate horseradish peroxidase-conjugated secondary antibodies. The complexes were revealed by chemiluminescence (ECL; GE Healthcare).

RT-PCR and qPCR. Complementary DNA was synthesized from 1 μg of total RNA in 20 μl of buffer containing 200 ng of Random Primers (48190-011; Invitrogen) and 0.5 mM dNTP. After heating at 65 °C for 5 min, 4 μl of 5 × first-strand buffer, 2 μl of 100 mM dithiothreitol and 1 μl of RNasin Ribonuclease Inhibitor (40 U μl^{-1}, 9PIN211; Promega) were added, followed by incubation at 37 °C for 2 min and the addition of 200 U of Moloney-murine-leukaemia virus reverse transcriptase (28025-013; Invitrogen). Annealing was performed at 37 °C for 50 min followed by 15 min at 70 °C. cDNA (0.5 μg) was used as a template for PCR amplifications in 5 μl of 10 × PCR buffer (200 mM Tris-HClpH 8.4, 500 mM KCl, 50 mM $MgCl_2$), 4 μl of 2.5 mM dNTP mix, 2 μl of primers (100 μM), 0.3 μl of *Taq* DNA polymerase (10342; Invitrogen), made up to 50 μl with water. Amplification was performed for 30 cycles of denaturation for 1 min at 95 °C, annealing for 1 min at 64 °C, and extension for 80 s at 74 °C, with final extension for 10 min at 74 °C. The products were run on a 1.2% agarose gel and detected by staining with ethidium bromide. The primers were designed with the free software at http://frodo.wi.mit.edu/. qPCR reactions were performed with 100 ng of DNA or cDNA, using the KAPA SYBR FAST qPCR Kit (KK4604; KAPA Biosystems) with the following cycling conditions: denaturation at 95 °C for 10 min, followed by 40 cycles of 95 °C for 15 s, 60 °C for 1 min, 95 °C for 15 s, 60 °C for 20 s and 95 °C for 15 s, and a final extension for 10 min at 72 °C. Melting curves between 65 and 90 °C, 1 °C s^{-1} transition, were incorporated. All qPCR was performed in an AbiPrism 7000 Sequence detection system.

Recombinant lentiviruses. The hairpins sh-Scramble (5′-AGGTAGTGTA-ATCGCCTTG-3′), sh-BZLF1_1 (5′-GACCAAGCTACCAGAGTCTAT-3′), sh-BZLF1_2 (5′-CTGCCTATCATGTTTCAACCGC-3′), sh-BPLF1_1 (5′-ATGTCAGAGTCAGCACCTATG-3′), sh-BPLF1_2 (5′-ACGGCGAATAAT-ACCGTATAAC-3′), sh-BPLF1_3 (5′-GCCATCATCATCGAGACAGA-3′) and sh-BPLF1_4 (5′-GGCCCAGTTCATCCTCTACAT-3′) were cloned in the *Age*I and *Eco*RI sites of the pLKO.1 plasmid[46]. Recombinant plasmids were co-transfected with the packaging plasmids psPAX2 and pMD2.G (Addgene; EPFL) in HEK293T cells by precipitation with calcium phosphate, and supernatant containing viral particles was collected after 48 h. Virus titres were measured with a QuickTiter lentivirus titre kit (Cell Biolabs Inc.).

Screen for EBV deconjugases. The deconjugase activity of an EBV ORF library cloned in the pDEST–GST vector was assayed by co-expression with ubiquitin/UbL–GFP reporters in competent BL21 bacteria as described[20]. GST fusions of the ubiquitin-specific deconjugase USP19 (ref. 47), the ISG15 deconjugase USP4 (ref. 48), the NEDD8 deconjugase NEDP1 (ref. 22) and the SUMO-1, SUMO-2 and SUMO-3 deconjugase SENP1 (ref. 49) were used as positive controls. Exponentially growing bacteria were induced for 5 h at 30 °C with 0.5 mM isopropyl β-D-thiogalactoside and then lysed by sonication in PBS supplemented with protease inhibitors. After normalization for GFP content the lysates were fractionated by SDS–PAGE and cleavage of the reporters was assessed in western blots with anti-S-tag antibody. The intensity of the GFP bands was quantified by densitometry and the percentage cleavage was calculated as the ratio between the intensity of the free GFP band and the total GFP. Each screen was repeated at least twice.

Deconjugase activity assays. GST fusions of BPLF1, a catalytically inactive $BPLF1_{C61A}$ mutant, NEDP1 and the catalytic mutant $NEDP1_{C163S}$ were affinity-purified and protein concentrations were determined. Hydrolysis of the fluorogenic substrates ubiquitin-AMC and NEDD8-AMC (Enzo) was assayed at 30 °C in 100 μl of buffer (50 mM Tris-Cl pH 7.5, 150 mM NaCl, 2 mM EDTA, 2 mM dithiothreitol) containing 50 nM enzyme. K_m and k_{cat} were calculated by titrating the substrate at concentration ranging between 0 and 20 μM. The enzymatic activity was blocked by addition of 10 mM NEM. NEDD8 conjugates were purified from lysates of HeLa cells transfected with a V5–NEDD8 plasmid by adsorption on anti-V5-conjugated Sepharose beads. Equal amounts of beads were incubated with 200 nM enzymes for 1 h at 37 °C, and western blots were probed with anti-V5 antibodies. The enzymatic activity of eukaryotic expressed BPLF1 was assayed by labelling lysates of transfected HeLa cells with the ubiquitin-VS and NEDD8-VS functional probes (Boston Biochem) as described[23]. Cell lysate (5 μg) was incubated for 1 h at 37 °C with increasing concentration of the probe. Unmodified and ubiquitin/NEDD8-VS crosslinked species were detected in western blots by using the anti-Flag antibody. *In vivo* deneddylase activity was assayed in HeLa cells co-transfected with V5–NEDD8 and Flag-tagged BPLF1, NEDP1, $BPLF1_{C61A}$ and $NEDP1_{C163S}$. The transfected cells were harvested after 48 h, and NEDD8 conjugates were detected in western blots by using the anti-V5 antibody.

Cullin neddylation and co-immunoprecipitation assays. The coding sequences of human cullin-1 and cullin-4A were subcloned in the *Bam*H1 and *Not*1 sites of the pcDNA4/Myc vector (Invitrogen). Cullin deneddylation was assayed in HeLa cells co-transfected with the Myc-tagged cullins, V5–NEDD8 and Flag–BPLF1, Flag–$BPLF1_{C61A}$ or Flag–NEDP1. Cell lysates prepared 48 h after transfection were fractionated by SDS–PAGE, and western blots were probed sequentially with the anti-Myc and V5 antibodies. For co-immunoprecipitation, aliquots of the cell lysates were incubated either for 1 h with the anti-Myc antibody followed by Protein-G-coupled Sepharose beads (GE Healthcare) or for 2 h with anti-Flag agarose affinity gel (A-2220; Sigma) followed by elution with a 3 × Flag peptide (F-4799; Sigma). Western blots were probed sequentially with the anti-Myc and anti-Flag antibodies. Interaction with endogenous cullins was assayed by immunoprecipitation of cell lysates of HeLa cells transfected with empty vector, Flag–BPLF1 and Flag–$BPLF1_{C61A}$ with anti-Flag and anti-Cull4A antibodies.

Immunofluorescence and cell cycle analysis. The subcellular localization of Flag–BPLF1 and Flag–$BPLF1_{C61A}$ was investigated by immunofluorescence. HeLa cells were grown on coverslips and transfected with the jetPEI Kit (Polyplus Transfection). After 48 h the monolayers were fixed with 4% paraformaldehyde and permeabilized for 20 min with 0.5% v/v Triton X-100 in PBS. Staining with the anti-Flag antibody (dilution 1:5,000 in PBS containing 0.5% BSA) was performed for 2 h at room temperature followed by incubation for 1 h with tetramethylrhodamine β-isothiocyanate-conjugated anti-mouse immunoglobulin antibodies (1:200 dilution; R0270; Dako). Cytoskeletal actin was stained with FITC-labelled phal-

loidin (1:100 dilution; P-5252; Sigma). The slides were mounted with Vectashield containing DAPI (H-1200; Vector Laboratories) and images were captured with a Leica DM RXA fluorescent microscope and analysed with the Improvision OpenLab 3.1.4 software (http://www.improvision.com). Nuclear size was measured with the ImageJ software (http://rsbweb.nih.gov). For staining with PI, the cells were fixed for 1 h in cold 70% ethanol and stained for 45 min in ice-cold staining solution (50 mg ml^{-1} PI, 25 mg ml^{-1} RNase A, 1 mg ml^{-1} sodium citrate, 0.3% Nonidet P40). DNA content was measured by fluorescence-activated cell sorting (FACS) with a FACSCalibur (Becton Dickinson) and analysed with CellQuestPro software. Where indicated, the cells were co-transfected with 2 μg of the BPLF1 plasmid and increasing amounts of either the HA–ubiquitin or the V5–NEDD8 plasmids for 48 h before being stained with PI.

Induction of the EBV productive cycle and quantification of viral DNA. The productive virus cycle was induced in the Akata Bx-1 cell line that carries a recombinant EBV in which the thymidine kinase gene is replaced by a cytomegalovirus (CMV) immediate-early promoter-driven GFP, by incubating cell pellets for 1 h at 37 °C with polyclonal rabbit anti-human IgG[32]. EBV DNA content was assayed by qPCR with probes specific for unique regions in the genes encoding BZLF1 and EBNA1 and the KAPA SYBR FAST qPCR Kit (KK4604; KAPA Biosystems). Where indicated, EBV DNA replication was inhibited by the addition of 50 μM Foscarnet, a herpesvirus DNA polymerase inhibitor[50]. Akata-Bx1 cells were infected with recombinant lentiviruses for 72 h at a multiplicity of infection of 2.55×10^{10} in the presence of 8 mg ml^{-1} Polybrene (AL-118; Sigma). Where indicated, cells infected for 24 h were treated with anti-human IgG antibody for 48 h before FACS and western blot analysis. A human CDT1 expression plasmid was purchased from OriGene Technologies (SC122393). Expression was assayed in cells transfected with the Cell Line Nucleofector Kit V (AMAXA; Lonza Group) using a specific antibody.

46. Moffat, J. *et al.* A lentiviral RNAi library for human and mouse genes applied to an arrayed viral high-content screen. *Cell* **124,** 1283–1298 (2006).
47. Hassink, G. C. *et al.* The ER-resident ubiquitin-specific protease 19 participates in the UPR and rescues ERAD substrates. *EMBO Rep.* **10,** 755–761 (2009).
48. Zhao, B., Schlesiger, C., Masucci, M. G. & Lindsten, K. The ubiquitin specific protease 4 (Usp4) is a new player in the Wnt signalling pathway. *J. Cell. Mol. Med.* **13,** 1886–1895 (2009).
49. Duda, D. M. *et al.* Structure of a SUMO-binding-motif mimic bound to Smt3p–Ubc9p: conservation of a non-covalent ubiquitin-like protein-E2 complex as a platform for selective interactions within a SUMO pathway. *J. Mol. Biol.* **369,** 619–630 (2007).
50. Yao, G. Q., Grill, S., Egan, W. & Cheng, Y. C. Potent inhibition of Epstein–Barr virus by phosphorothioate oligodeoxynucleotides without sequence specification. *Antimicrob. Agents Chemother.* **37,** 1420–1425 (1993).

nature cell biology

DOI: 10.1038/ncb2035

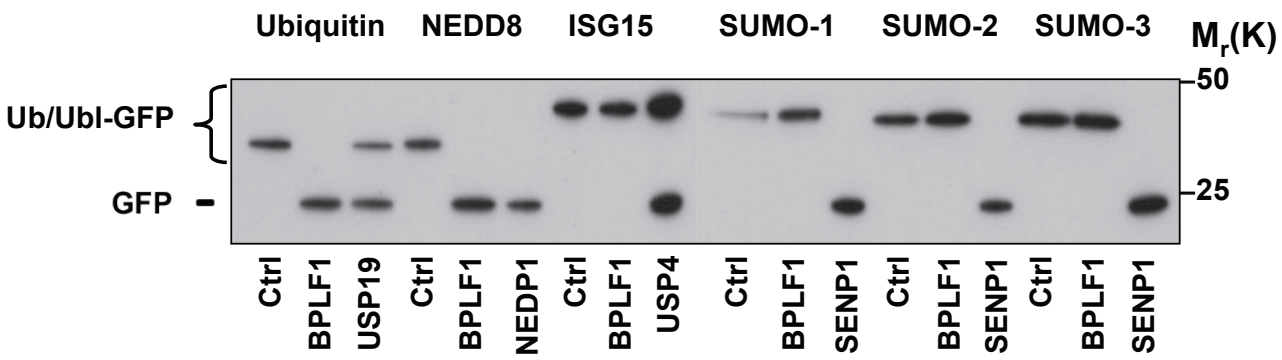

Figure S1 Western blot analysis of bacteria co-expression assays where GST-BPLF1 was testes for cleavage of the Ub- and UbL-GFP reporters alongside the empty GST vector and the appropriate positive controls (USP19, NEDP1, USP4 and SENP1). Cleavage of the reporter is visualized by the appearance of a free GFP band (GFP) detected by antibodies to the C-terminal S-tag.

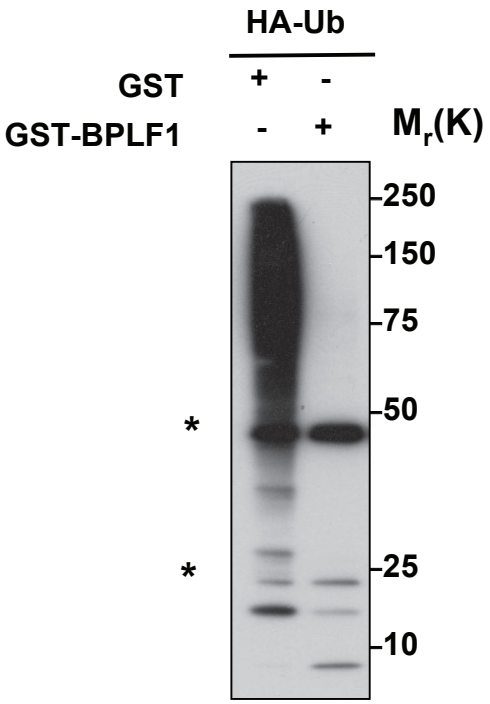

Figure S2 BPLF1 cleaves ubiquitin conjugates. HA-ubiquitin was expressed in HeLa cells and conjugates were captured on anti-HA conjugated sepharose beads. Equal amounts of beads were mixed with 200 nM of purified GST- or GST-BPLF1 and the reaction was run for 1h at 37°C. Ubiquitin conjugates were visualized in Western blots probed with the HA antibody. Immunoglobulin heavy and light chains are indicated by asterisks.

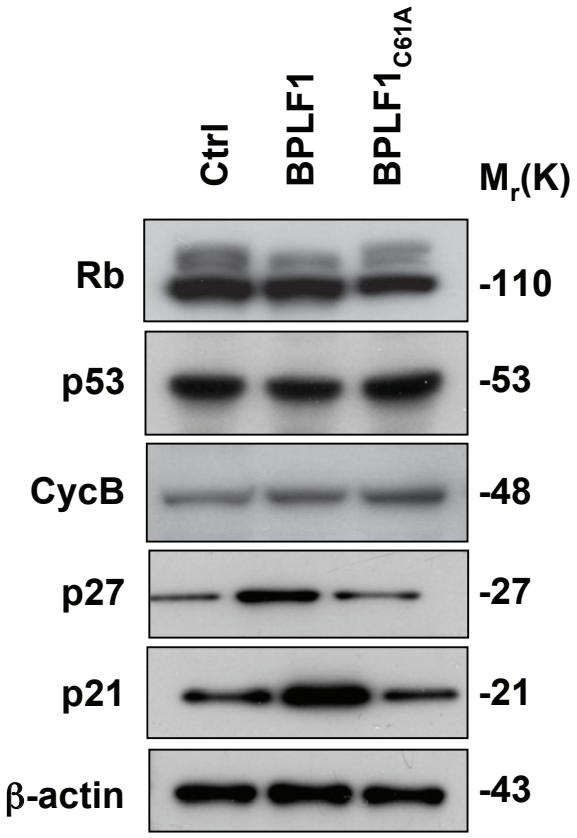

Figure S3 A catalytically active BPLF1 selectively induces the accumulation of CRL substrates. The expression levels of Rb (MDM2 substrate), p53 (MDM2 substrate), CycB (APC/C substrate), p27 and p21 ($CRL1^{Skp2}$ substrates) were assayed in HeLa cells 48h after transfection with the wild type BPLF1, the catalytic mutant $BPLF1_{C61A}$ or a control empty vector. Expression of the catalytically active BPLF1 was associated with accumulation of CRL substrates p21 and p27 while the expression levels of Rb, p53 and CycB were not affected. The result of one representative experiments out of three are shown in the figure.

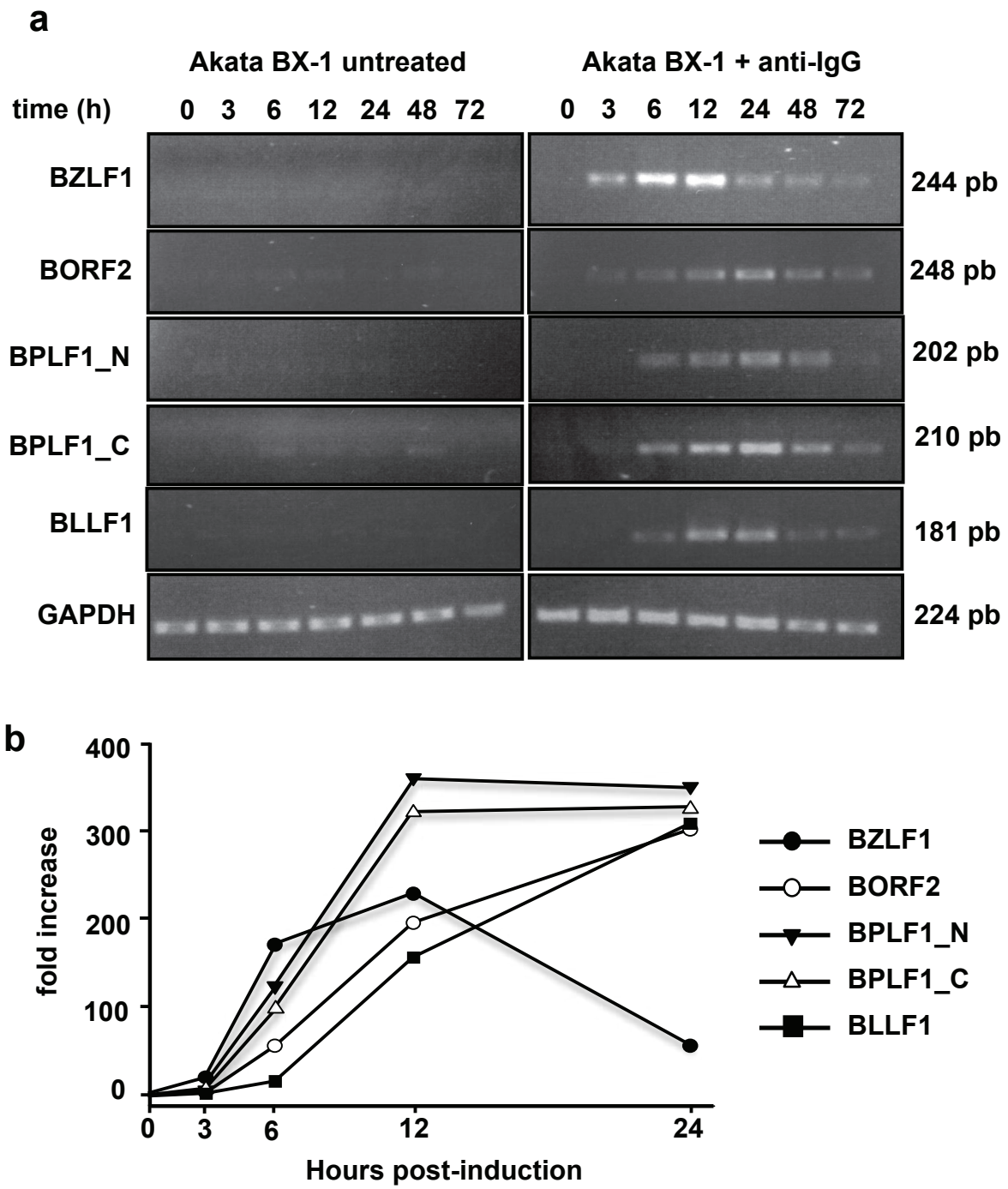

Figure S4 Time kinetics of EBV gene expressed in untreated and anti-IgG treated Akata-Bx1. Total RNA were extracted at the indicate time and cDNA were synthesized as described in materials and methods. Quantitative PCR were preformed on cDNA templates with the specific primers, and GAPDH was used as standard control for the normalization. The products were run in 1.5% agarose gel and the fold increase is plotted on the graphic.

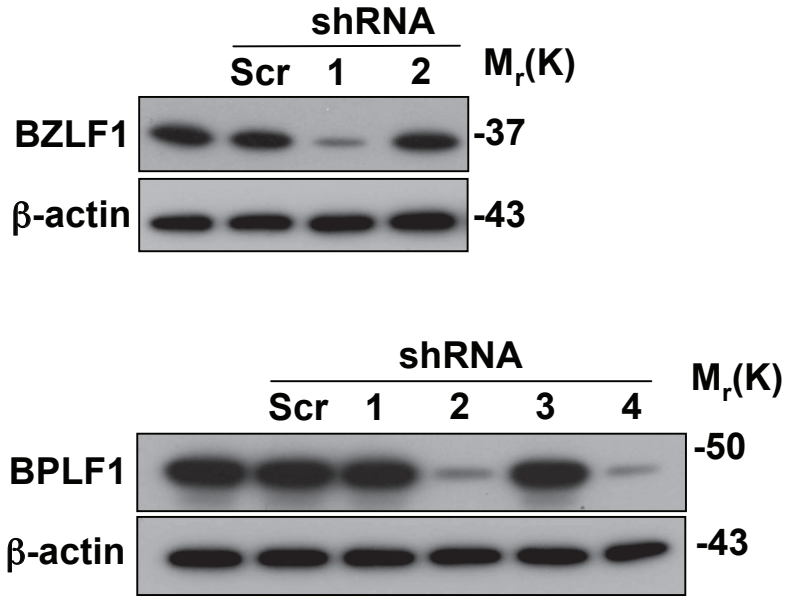

Figure S5 Characterization of shRNA lentiviruses. The empty pLKO.1 vector and recombinant plasmids expressing a scrambled shRNA or shRNAs specific for the EBV BZLF1 and BPLF1 genes were co-transfected in HeLa cells together with plasmids expressing BZLF1 or Flag-BPLF1 at 9:1 molar ratio and expression of the viral proteins was assayed after 72 h in Western blots probed with the anti-BZLF1 or anti-Flag antibodies. The shBZ1-1 and shBP1-2 and -4 hairpins that induced >90% silencing of the target mRNAs were used for production of recombinant lentiviruses.

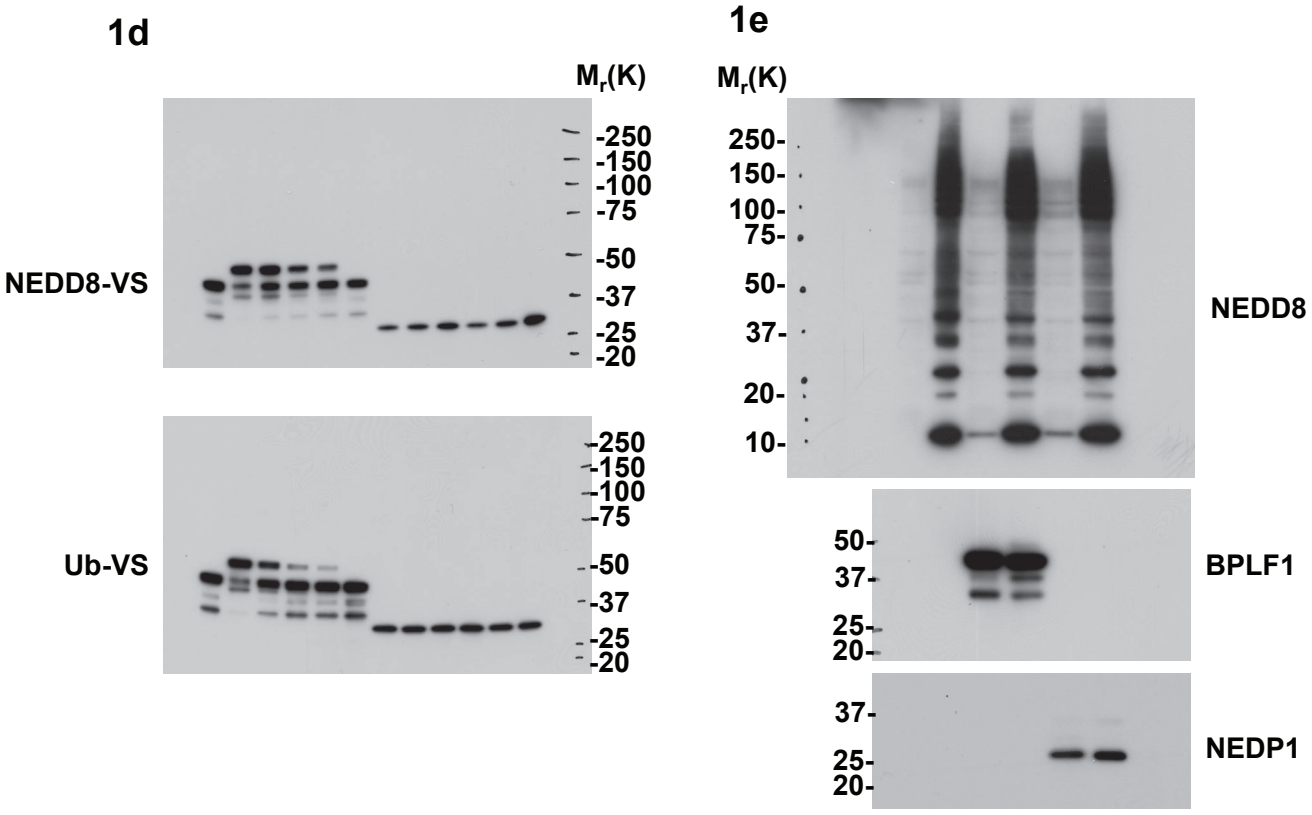

Figure S6 Full scans for figures 1d and 1e. The rectangles correspond to the crops

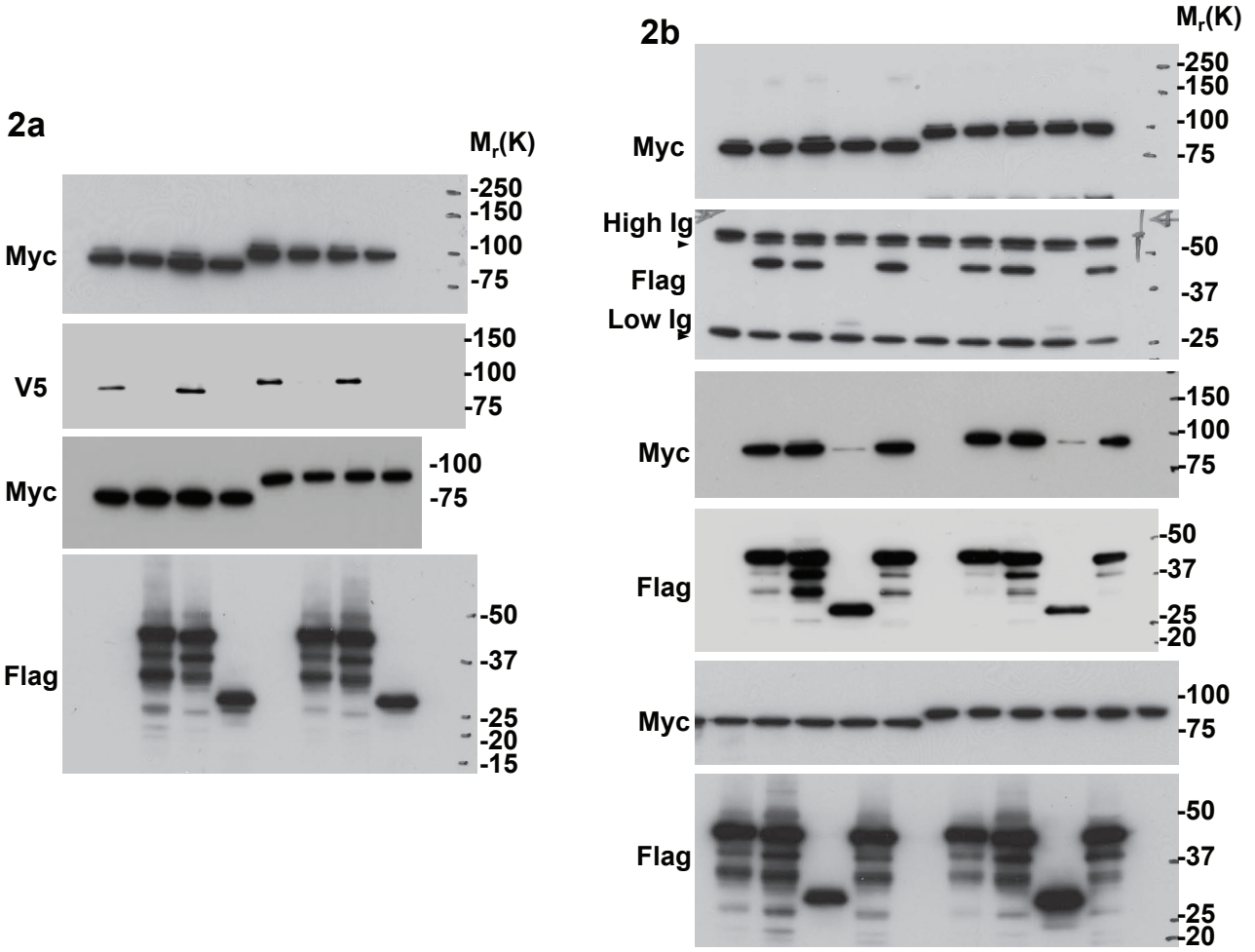

Figure S6 continued Full scans for figures 2a and 2b. The rectangles correspond to the crops

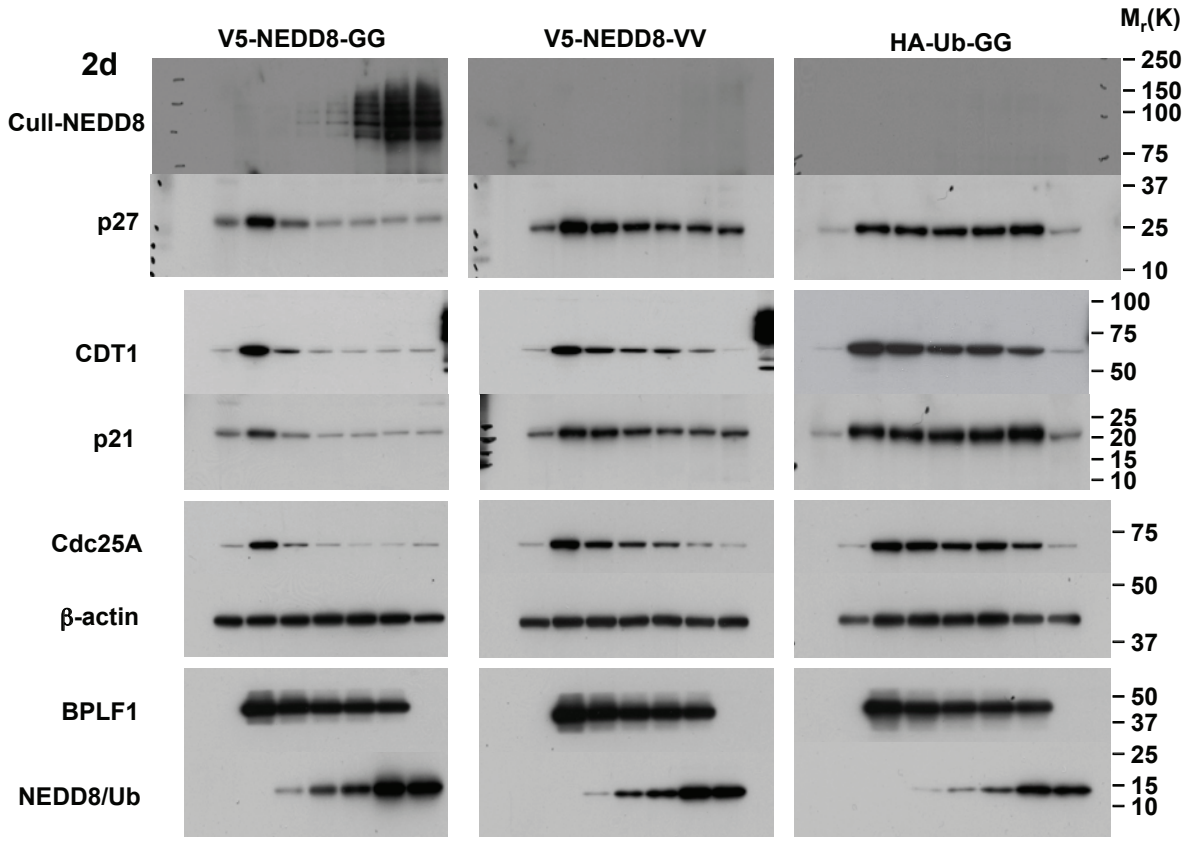

Figure S6 continued Full scans for figure 2d. The rectangles correspond to the crops

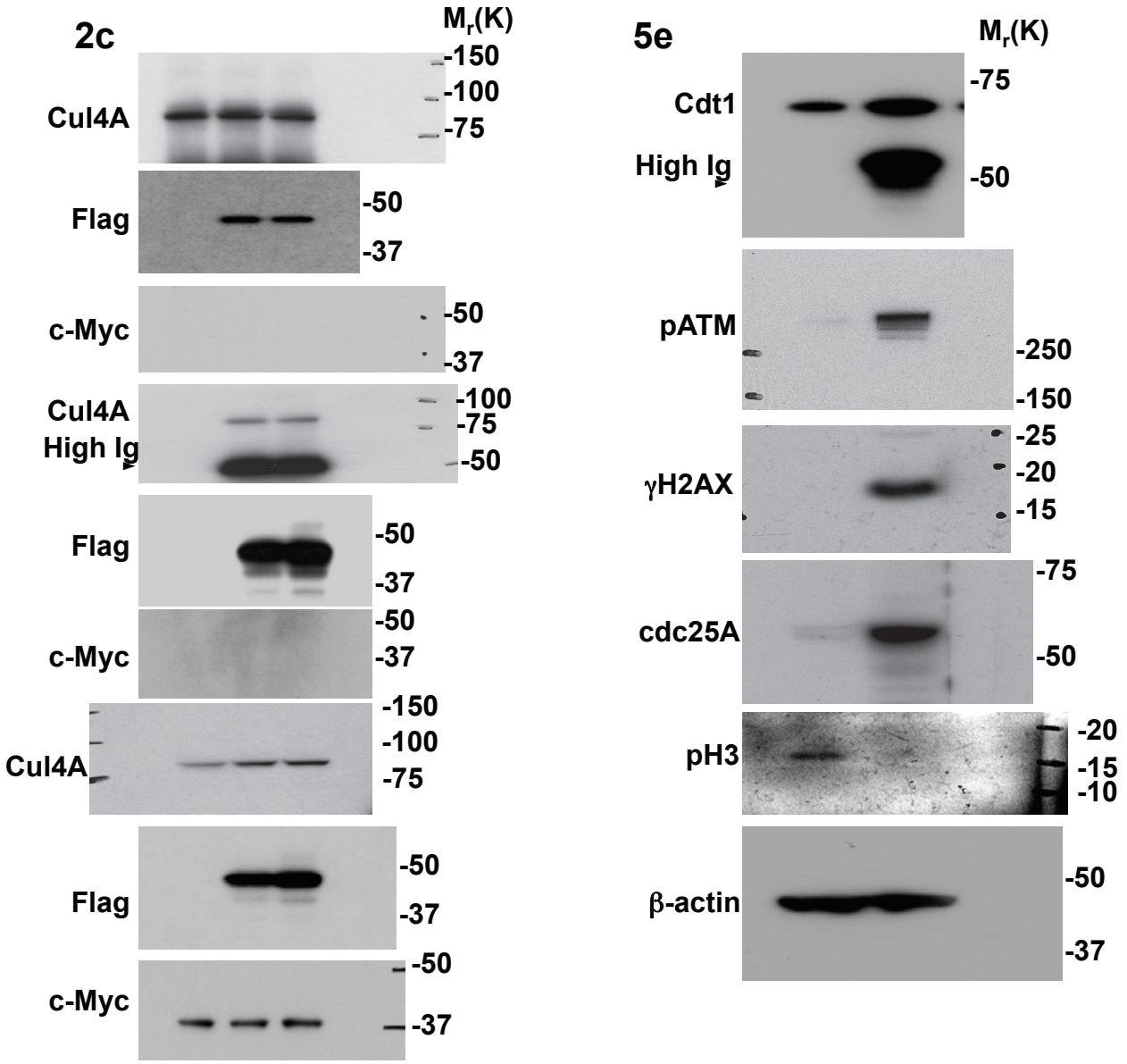

Figure S6 continued Full scans for figures 2c and 5e. The rectangles correspond to the crops

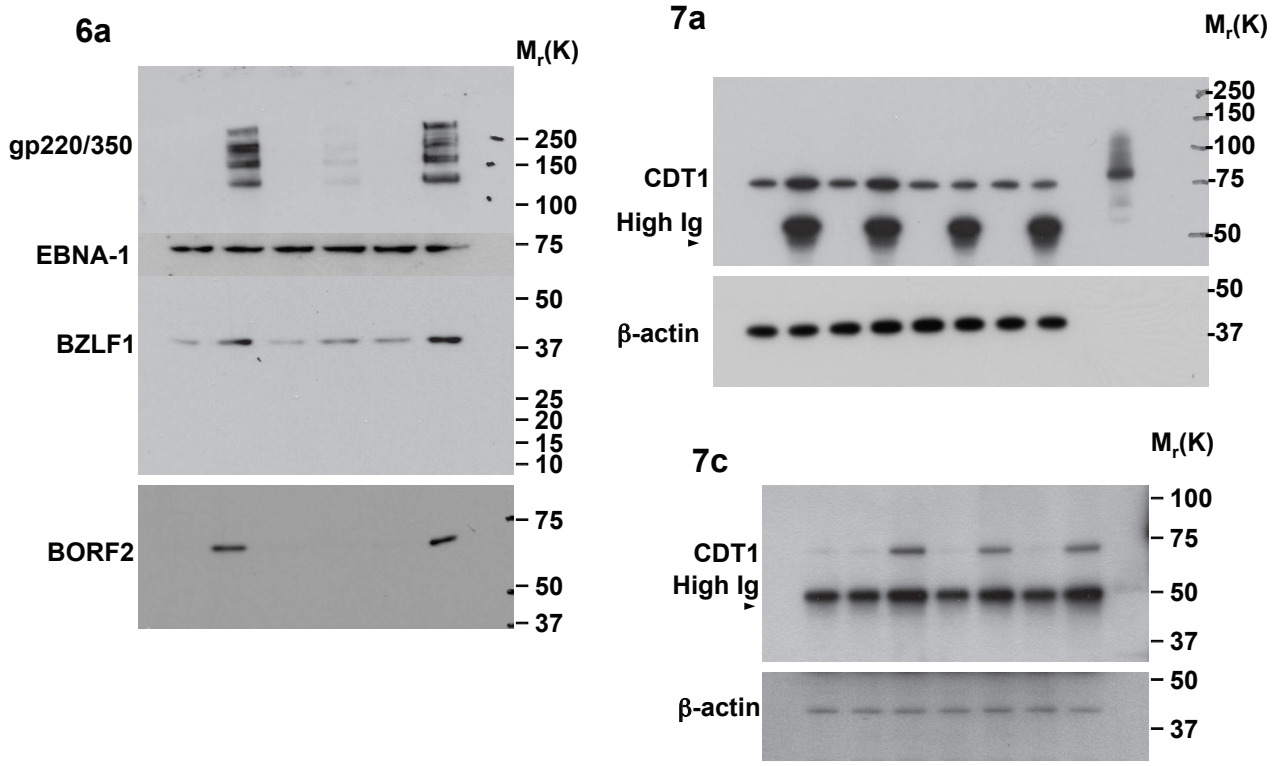

Figure S6 continued Full scans for figure 6a, 7a and 7c. The rectangles correspond to the crops

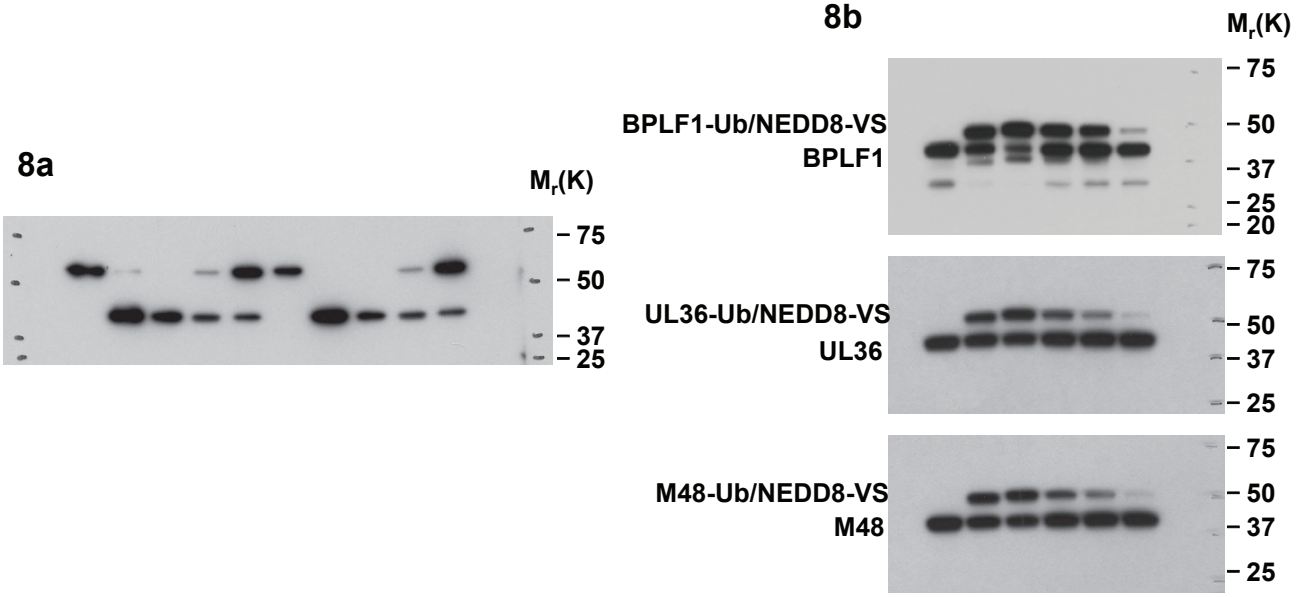

Figure S6 continued Full scans for figures 8a and 8b. The rectangles correspond to the crops